WL-TR-96-4013

LARGE AREA COMPOSITE INSPECTION SYSTEM LACIS-D

FRANK KARPALA, PhD
OMER HAGENIERS, PhD

CANADIAN COMMERCIAL CORPORATION
50 O'CONNOR STREET, 11TH FLOOR
OTTAWA, ONTARIO, CANADA K1A-OS6

AUGUST 1995

FINAL REPORT FOR PERIOD SEPTEMBER 1993 to AUGUST 1995

MATERIALS DIRECTORATE
WRIGHT LABORATORY
AIR FORCE MATERIEL COMMAND
WRIGHT PATTERSON AFB OH 45433- 7734

NOTICE

WHEN GOVERNMENT DRAWINGS, SPECIFICATIONS, OR OTHER DATA ARE USED FOR ANY PURPOSE OTHER THAN IN CONNECTION WITH A DEFINITELY GOVERNMENT-RELATED PROCUREMENT, THE UNITED STATES GOVERNMENT INCURS NO RESPONSIBILITY OR ANY OBLIGATION WHATSOEVER. THE FACT THAT THE GOVERNMENT MAY HAVE FORMULATED OR IN ANY WAY SUPPLIED THE SAID DRAWINGS, SPECIFICATIONS, OR OTHER DATA, IS NOT TO BE REGARDED BY IMPLICATION OR OTHERWISE IN ANY MANNER CONSTRUED, AS LICENSING THE HOLDER OR ANY OTHER PERSON OR CORPORATION, OR AS CONVEYING ANY RIGHTS OR PERMISSION TO MANUFACTURE, USE, OR SELL ANY PATENTED INVENTION THAT MAY IN ANY WAY BE RELATED THERETO.

THIS REPORT IS RELEASABLE TO THE NATIONAL TECHNICAL INFORMATION SERVICE (NTIS). AT NTIS, IT WILL BE AVAILABLE TO THE GENERAL PUBLIC, INCLUDING FOREIGN NATIONS.

THIS TECHNICAL REPORT HAS BEEN REVIEWED AND IS APPROVED FOR PUBLICATION.

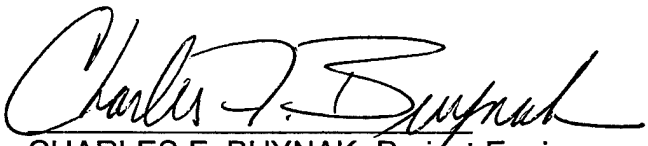

CHARLES F. BUYNAK, Project Engineer
Nondestructive Evaluation Branch
Metals and Ceramics Division

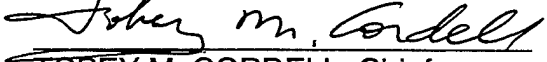

TOBEY M. CORDELL, Chief
Nondestructive Evaluation Branch
Metals and Ceramics Division

WALTER M. GRIFFITH, Asst. Chief
Metals, Ceramics & Nondestructive
Evaluation Division
Materials Directorate

IF YOUR ADDRESS HAS CHANGED, IF YOU WISH TO BE REMOVED FROM OUR MAILING LIST, OR IF THE ADDRESSEE IS NO LONGER EMPLOYED BY YOUR ORGANIZATION, PLEASE NOTIFY, WL/MLLP, WRIGHT-PATTERSON AFB OH 45433-7817 TO HELP US MAINTAIN A CURRENT MAILING LIST.

COPIES OF THIS REPORT SHOUL.D NOT BE RETURNED UNLESS RETURN IS REQUIRED BY SECURITY CONSIDERATIONS, CONTRACTUAL OBLIGATIONS, OR NOTICE ON A SPECIFIC DOCUMENT.

REPORT DOCUMENTATION PAGE

FORM APPROVED
OMB NO. 0704-0188

1. AGENCY USE ONLY (Leave blank)	2. REPORT DATE	3. REPORT TYPE AND DATES COVERED
	August 1995	Final Report 9/93 - 8/95

4. TITLE AND SUBTITLE
Large Area Composite Inspection System LACIS-D

5. FUNDING NUMBERS
C -F33615-93-C-5365
PE -63112F
PR -3153
TA -00
WU -13

6. AUTHOR(S)
Frank Karpala, Omer Hageniers

7. PERFORMING ORGANIZATION NAMES(S) AND ADDRESS(ES)
Canadian Commercial Corporation
50 O'Connor Street, 11th Floor
Ottawa, Ontario, Canada K1A-OS6

8. PERFORMING ORGANIZATION REPORT NUMBER

9. SPONSORING/MONITORING AGENCY NAMES(ES) AND ADDRESS(ES)
Materials Directorate (POC: Charles F. Buynak, WL/MLLP-
Wright Laboratory phone: 937-255-9807)
Materiel Command
Wright-Patterson AFB, Ohio 45433- 7734

10. SPONSORING/MONITORING AGENCY REPORT NUMBER
WL-TR-96-4013

11. SUPPLEMENTARY NOTES

12a. DISTRIBUTION/AVAILABILITY STATEMENT
Approved for public release; distribution is unlimited.

12b. DISTRIBUTION CODE
A

13. ABSTRACT (Maximum 200 words)
The purpose of this program was to conduct the advanced development, integration, modification, and demonstration of a large area nondestructive inspection technique for the rapid detection and quantification of material properties and defects in large fiber-reinforced composite aircaft compoents.

14. SUBJECT TERMS
composites, retro-reflection, visual inspection, nondestructive evaluation, highlighter, d. sight, dais, delamination, corrosion, disbond

15. NUMBER OF PAGES
104

16. PRICE CODE

17. SECURITY CLASSIFICATION OF REPORT	18. SECURITY CLASSIFICATION OF THIS PAGE	19. SECURITY CLASSIFICATION OF ABSTRACT	20. LIMITATION OF ABSTRACT
Unclassified	Unclassified	Unclassified	SAR

TABLE OF CONTENTS

1 INTRODUCTION 1
1.1 *D SIGHT* Principles 2

2 COMPOSITE PROPERTIES 3
2.1 Identify Geometry 3
2.2 Identify Materials 4
2.3 Identify Damage Types 4
2.3.1 Impacts 4
2.3.2 Disbonds 6
2.3.3 Delaminations 6
2.3.4 Summary of Defect Geometry 7

3 SPECIMEN DAMAGE INTRODUCTION AND EVALUATION 9
3.1 Introduction 9
3.2 Materials 10
3.2.1 Material Specifications for Hercules AS4/3501-6 10
3.2.2 Material Specifications for Cytec IM7/5250-4 11
3.3 Design of Hat-Stiffened Composite Panel 12
3.4 Specimens in Test Plan 13
3.5 Surface Preparation 14
3.5.1 Sanding 14
3.5.2 Painting 15
3.6 NDI of Specimens Prior to Damage Introduction 15
3.7 Delamination and Disbond Damage 16
3.7.1 Delamination and Disbond Damage Introduction Techniques 16
3.7.2 Delamination Damage Sites 17
3.7.3 Post Damage Summary of Panel No.857 18
3.7.4 Post Damage Summary of Panel No. 862 24
3.8 Impact Damage 26
3.8.1 Equipment and Damage Types 26
3.8.2 Summary and Analysis of Impact Damage 28
3.8.3 Impact Indent Relaxation 33
3.9 Radome 35
3.10 F-16 Horizontal Stabilizer 36
3.10.1 Predamage Inspection and Damage Introduction 36
3.10.2 Postdamage Assessment 40
3.10.3 Discussion of Results 41
3.11 Conclusions 43
3.11.1 Delaminations and Disbonds 43
3.11.2 Impact Damage 43
3.11.3 Impact Dent Relaxation 43

4 HIGHLIGHTER SELECTION 44
4.1 Introduction 44
4.2 Highlighters 44
4.2.1 Desirable Properties 44
4.2.2 Commercial Types 45
4.3 Highlight Quality 46
4.4 Application Methods 49
4.5 Recommendations 50

5 HARDWARE DEVELOPMENT 51
5.1 Sensor Optimization 51
5.1.1 DAIS-500 Deficiencies 51
5.1.2 Optimization Criteria 52
5.1.3 Design of Experiments 52
5.1.4 Optimization Sample Set 53
5.1.5 Experimental Results 57
5.2 Hardware Description 60
5.2.1 Host Controller 60
5.2.2 Pendant Controller 61
5.2.3 DAIS-500 Sensor 61
5.2.4 Printer 62

6 SOFTWARE DEVELOPMENT 64
6.1 General 64
6.2 DAIS File Structure 65
6.3 Description of Program Modules 66
6.3.1 Inspection Plan Module 66
6.3.2 Install/Calibrate Module 68
6.3.3 Acquisition Module 69
6.3.4 Analysis Module 71
6.3.5 Repair Module 75

7 FIELD TRIAL SUMMARY 77

8 CONCLUSIONS 79

9 RECOMMENDATIONS 80

10 REFERENCES 81

11 PUBLICATIONS 81

12 APPENDIX: TRIP REPORTS 82
12.1 Northrup-Grumman/JSTARS 82
12.2 Tinker AFB (OC-ALC) 84
12.3 Kelly AFB (SA-ALC) 87
12.4 Hill AFB (OO-ALC) 87
12.5 Whiteman AFB 89
12.6 McClellan AFB (SM-ALC) 91

LIST OF FIGURES

Figure		Page
1	Locations of Damage Situation Types	17
2	Machining Operations Required for Damage Introduction	18
3	Delamination and Disbond Damage Site Map, Panel No. 857	19
4	Postdamage C-Scan, Panel No. 857	20
5	Mosaic of Perspectively Corrected *D SIGHT* Images of Panel No. 857 Using a Simulated DAIS-500 Setup	21
6	DAIS-500 Image of Panel No. 857 Showing Delamination and Disbond Damage for Numbered Site Locations in **Figure 3**.	22
7	Another view of Panel No. 857 Showing Delamination and Disbond Damage for Numbered Site Locations in **Figure 3**.	22
8	Delamination and Disbond Damage Site Map, Panel No. 862	24
9	Impact Damage Situation Types	26
10	Typical Impact Damage Site Map, Panel 856	27
11	DAIS-500 Image of Impact Damage Indications for Section of Panel	28
12	Site type sensitivity to impact damage as measured by impact energy required to generate *D SIGHT* detectable damage	31
13	Radome under point source lighting with suspected indications marked by an arrow	35
14	Radome under broad source lighting with suspected indications marked by an arrow	35
15	C-scan of F-16 Horizontal Stabilizer as Received	37
16	F-16 Damage Site Map and X-ray Inspection Zones	39
17	C-Scan of the F-16 Stabilizer after Damage Introduction	40
18	DORRI Reflectivity vs. Time for Different Highlighters	48
19	Dimensions of Edge Delaminations	54
20	Dimensions of Artificial Delaminations on Three Composite Sheets	55
21	CMM profiles of specimen 234A	56
22	Original DAIS-500 configuration	58
23	DAIS-500 with broad light source	58
24	35 mm lens, camera at 22.5 deg., camera to surface = 68 in. retro to surface = 30 in.	58
25	25 mm lens at 22.5 deg., camera to surface = 58 in., retro to surface = 22 in.	58
26	25 mm lens at 27 deg., camera to surface = 52 in., retro to surface = 22 in.	58
27	Left side, carbon fiber sheet, same setup as **Figure 26**	59
28	Right side, carbon fiber sheet, same setup as **Figure 26**	59
29	Honeycomb delamination, same setup as **Figure 26**	59
30	Honeycomb delamination with simulated sheet metal delamination on right side, 1" diameter, 1 mil high	59
31	All edge delamination samples. Left to right, sample 1, sample 2, 848-1, 848-2, 848-4, and 484-6	59
32	Specimen 234A using new camera	59
33	DAIS Hardware Configuration and Connections	60
34	Pendant and Computer Host	62
35	DAIS-500 Prototype Sensor	62

Figure Page

36 DAIS-500 Sensor Drawing 63
37 Example Turtle Diagram with Sensor Placements 64
38 Relationship of DAIS Modules and System Files 65
39 Image Acquisition Display Window 69
40 Analysis Dialog Box for Viewing and Marking Defects 73
41 Delamination indication (circled) 89
42 Small Impact Indications (circled) 89
43 Example Inspection Plan for Lower Left Wing of B-2 90
44 A-10A Inspection Area 92
45 A-10A Inspection with DAIS-500 92
46 Radome Inspection with DAIS 500 93

LIST OF TABLES

Table Page

1 LACIS-D Applications by Aircraft 5
2 Dimensional Characterization of Defect Types 7
3 Material Specifications for Hercules AS4/3501-6 11
4 Material Specifications for Cytec IM7/5250-4 12
5 Stiffened Panel Configurations 13
6 Test Matrix 14
7 Test Matrix and Inspection Results, Panel No. 857 23
8 Test Matrix and Inspection Results, Panel No. 862 25
9 Test Matrix and Inspection Results, Panel 856. [D=detected, N=not detected] 29
10 Number of impact events per site type and number of sites detected using various NDI methods 30
11 Impact Indent Depth Reduction Measurements 34
12 Description of F-16 Site Type Locations 38
13 Test Matrix and Inspection Results of Damage 42
14 Commercial Highlighters 45
15 Physical Highlighter Properties 46
16 Rating of Highlighters 49
17 Highlighter Application Methods 50
18 Sample Parts for Optimization 53
19 Inspection Plan Menu Items 66
20 Install/Calibrate Menu Items 68
21 Acquisition Menu Items 70
22 Analysis Menu Items 72
23 Image Print Menu Items 74
24 Repair Planning Menu Items 75

ABBREVIATIONS

ASNT	American Society for Nondestructive Testing
ASTM	American Society for Testing and Materials
BVID	Barely Visible Impact Damage
CCD	Charge Coupled Device
CMM	Coordinate Measuring Machine
D/A	Digital to Analog
DAIS	*D SIGHT* Aircraft Inspection System
DND	Department of National Defence of Canada
DOI	Distinctness of Image
DPI	Dots Per Inch
D SIGHT	Diffracto Sight
FAA	Federal Aviation Administration
FOV	Field of View
I/O	Input/Output
JSTARS	Joint Surveillance Target and Attack Radar System
LCD	Liquid Crystal Display
MB	Megabyte
MHz	Megahertz
MAUS	Mobile Automated Ultrasonic Scanner
NDI/NDT	Nondestructive Inspection/Nondestructive Testing
NRC/IAR	National Research Council Canada/Institute for Aerospace Research
PC	Personal Compter
PEP	Personal Expandable Platform
RAF	Royal Air Force
RAM	Random Access Memory
TCA	Transport Canada Aviation
TDC	Transportation Development Centre
TFT	Thin Film Transistor
USAF	United States Air Force
VAC	Volts Alternating Current
VDC	Volts Direct Current
VGA	Video Graphics Adapter
WL	Wright Laboratory
WL/MLLP	Wright Laboratory/Materials Directorate - Nondestructive Evaluation Branch
WPAFB	Wright Patterson Air Force Base
ϕ	diameter

ACKNOWLEDGEMENTS

The authors are grateful to Wright Patterson Air Force Base, Wright Laboratory (WL) and the Canadian Department of National Defence (DND) for their support in funding this project. The authors also wish to acknowledge the funding assistance of the National Research Council Canada, Institute for Aerospace Research (NRC/IAR) under a collaborative research agreement. Special thanks go to Charlie Buynak of WL/MLLP for his efficient coordination of this project as project manager and to Bob Hastings of DND, DRDA-6, for his enthusiastic support and assistance.

We are especially thankful to Jerzy Komorowski and his research team from NRC/IAR for their technical skill and enthusiasm involving the fabrication and testing of the composite panels and their assistance at most of the field trials.

Research Team:

Diffracto Ltd.

Dr. Omer Hageniers, Project Manager
Dr. Frank Karpala, Researcher
William James, Researcher
Marc Noël, Researcher
Eldon Cooper, Researcher
Rodger Reynolds, Researcher
Don Clarke, Senior Technician

NRC/IAR

Jerzy Komorowski, Project Leader, Senior Research Officer
Ronald Gould, Technical Officer
Anton Marincak, Technical Officer

EXECUTIVE SUMMARY

The purpose of this program was to conduct the advanced development, integration, modification, and demonstration of a large area nondestructive inspection technique for the rapid detection and quantification of material properties and defects in large fiber-reinforced composite aircraft components.

To accomplish this objective, a patented optical technique called *D SIGHT*™ was used to develop a sensor and inspection system with the ability to evaluate the integrity of large areas of composite structures, store inspection information, and perform these functions quickly and with high defect sensitivity. Additional considerations related to portability, efficient information recording and retrieval, and equipment ruggedness were also addressed.

The program consisted of five main areas as follows:

- identification and characterization of composite materials and defect types
- fabrication, damage introduction, and NDI of composite structures using *D SIGHT* and other NDI technologies for collaboration purposes
- optimization, design, and build of a prototype sensor and inspection system
- software development for data acquisition, data storage and retrieval, and recording of analysis results
- field demonstration of inspection system at several ALC locations.

Results from each of these areas indicate that a successful inspection method to detect subsurface damage can be developed from the optical *D SIGHT* technology. The resulting system, called DAIS (*D SIGHT* Aircraft Inspection System), has high sensitivity to impact damage and can also be used to detect delamination/disbond defects. The system is portable, inspects large areas quickly, and has a user friendly computer interface to manage the vast quantity of data.

1 INTRODUCTION

The USAF has a wide variety of aircraft in its inventory ranging from those that structurally are completely metallic to those that are completely composite, and quite naturally intermediate types where both metallic and composite structures are present.

USAF aircraft in service today have a variety of materials including high strength steels, aluminum, exotic metallic alloys and composite materials. Many of these materials are subjected to wear, fatigue, and other forms of in-service damage. For many structural parts, nondestructive testing (NDT) is used to evaluate the structures for potentially dangerous defects that are not obvious on the surface of the structure. Visual, eddy current, ultrasonic, radiographic, magnetic particle, and penetrant testing have been the mainstays of inspection for metallic structures for the past 50 years. Some of these methods are also used for the inspection of composite structural elements.

Fiber reinforced composite structure has been used on commercial and military aircraft for over 30 years. Fiberglass structure was the main composite used until the early 1980s. Though early aircraft had just a few pounds of the material, aircraft designed in the late 1960s had as much as 15,000 pounds of fiberglass structure. Research on the use of advanced composite materials was done in the mid 1970s leading to graphite and Kevlar materials being incorporated into aircraft structures in the early 1980s. Typically, fairings and cowlings, landing gear doors, movable control surfaces, and wing fixed trailing edge surfaces are made of advanced composite materials. These structures are referred to as secondary structures. The loss of one of these surfaces in flight while serious in nature would not endanger the survival of the aircraft.

By the mid 1980s, composite materials were being used on primary structure. Current designs by several airframe manufacturers include use of composite materials for primary structure of vertical and horizontal stabilizers. One recently designed commercial aircraft has 34,000 pounds of composite structure with about 9,000 pounds of that being carbon/epoxy material.

In-service damage of composite structure can occur from a number of sources: impact, lighting strikes, fire, etc. In some cases small amounts of damage may lead to major part failures due to high loads, fatigue, and wind erosion.

The primary inspection method for composite structure as well as for the rest of the aircraft is visual inspection. In some areas where structure experiences high loads such as around actuators or attach fittings, special detailed nondestructive tests may be specified. In most other areas the concern is for damage caused by impact, lightning strike, and fire or heat damage, all of which can be initially detected visually. Once an area has been identified visually, a nondestructive test can then be carried out to determine the extent of damage. Visual signs of impact damage include cracked, crazed and chipped paint, cracked or fractured plies, and partial or total loss of plies. In addition to the above indications, lightning strikes and fire damage can give blistered, scorched or discolored paint, and exposed frayed fibers.

Visual inspection relies on adequate lighting, good access and a clean area to inspect. A flashlight, mirror, and 10X magnifying lens are required for many inspections. In some instances, fiber borescopes or miniature cameras called video probes can provide close visual inspection in areas

difficult to access for direct visual inspection.

Current NDT inspections on composites involve traditional ultrasonic inspection, ultrasonic bond testing, and radiography. No one method provides the best inspection for all types of defects. The different methods complement each other on the type of information they provide. These are also the methods used for production inspection of advanced composite parts. For in-service inspection the methods are tailored for inspection of relatively small areas with the access constraints encountered on an assembled aircraft.

Visual inspection has limitations in sensitivity of detection that can lead to the development of serious levels of structural damage before a decision to carry out sophisticated NDT is made. The role of *D SIGHT* as an aid to visual inspection is to enhance those defects whose presence is manifested by a localized change in surface shape. This enhancement process is both dramatic and readily detectable by the human eye even in a large area of view.

The purpose of this report is to document the development of a large area *D SIGHT* aircraft inspection system for inspecting composite surfaces for impact damage, delaminations, and disbonds. The major activities reported relate to laboratory experimentation for detection sensitivity, hardware optimization and development, software development, and experience at ALC facilities using the prototype equipment to determine both operational characteristics and user feed back.

1.1 *D SIGHT* Principles

D SIGHT uses a CCD camera, a white light source mounted slightly below the camera lens, and a retroreflective screen. The retroreflective screen is a critical optical element in *D SIGHT* returning light falling on its surface in the same direction as the incident light. The light returned by the retroreflector is slightly dispersed due to the physical and optical characteristics of the micro-beads, but returns most of the light along the incident direction toward the light source, and back through the reflective surface.

When the surface is illuminated by the light source, local curvature variations on the surface act to focus or disperse the light onto the retroreflective screen. The pattern or primary image of curvature variations of the surface on the retroreflector is unique for that surface; defining distinct patterns of directional light just in the right position for surface backlighting. By viewing the surface slightly off-axis from the primary light source and because the light returned is slightly dispersed by the retroreflector, the unique pattern from the retroreflector is seen through the surface, near the local curvature distortions, as bright and dark gray scale variations. Higher curvature variations which focus or defocus the light more intensely will have greater image contrast so that the degree of surface deformation can be inferred from the contrast in the *D SIGHT* image. To operate properly, the surface must be reflective. When it is not, a thin liquid film, called a highlighter, may be applied to the surface to increase its reflectivity.

Various parameters in this basic configuration can be changed to produce different signatures of the defect indications. Some of these parameters include camera grazing angle, camera distance to surface, retroreflective screen distance, light source properties, surface properties, etc. Determining an optimal set of parameters ensures maximum signal-to-noise and defect sensitivity.

2 COMPOSITE PROPERTIES

2.1 Identify Geometry

The geometry of the components to be inspected on aircraft has two major influences on the design of the *D SIGHT* inspection head. These influences are the area of the inspection carried out by the sensor in a single placement and the radius of curvature of the surface.

The area covered in a single sensor head placement must balance the speed of inspection, the surface damage resolution, the size of the sensor head and the ease of use of the equipment. The minimum radius of curvature of the surface of components being inspected is important because it influences the design of the interface between the sensor and surface for ambient light sealing. Also, on curved surfaces, the amount of surface that can be inspected rapidly becomes smaller because the light striking the surface becomes diverged after reflection from the surface, requiring an even larger retro-screen to catch it for return to the surface. Physical constraints of course limit the size of the retro-screen.

The USAF has a very large inventory of aircraft types as shown in **Table 1**. The table is by no means complete but attempts to encompass the aircraft representing the largest components of the USAF inventory.

Of the aircraft listed, only three have primary structure made of composites, namely the B-2, F-117 and F-22. These aircraft are therefore those of primary long term interest from the large area composite NDI point of view. Unfortunately these aircraft, representing the leading edge of aircraft technology were not available to this program, both due to their classified nature and the limited number of these aircraft in existence.

Many other aircraft have secondary structure that is made of composite materials and is important to the safe operation of the aircraft. It is expected that inspection of these components will provide the bulk of the opportunities for problem identification and demonstration of NDI performance. Furthermore, while these surfaces are not as large as the primary structure aircraft surfaces they can still be substantial in size. An example is a C-17 wing flap seen at McDonnell Douglas in Long Beach, CA., which was 10 ft long by 6 ft wide by 12 in thick. There are of course several panels of this size in the complete C-17 wing flap system.

In general, composite component sizes range from the extremely large B-2 Bomber wings >5000 ft^2 to very small hatch covers, approximately 1 ft^2. The majority of the surfaces to be inspected are flat to mildly convex curvatures. A lower limit to curvature for the *D SIGHT* system has been set at a 10 in radius.

An important consideration that came out of a previous contract with DND in areas of impact damage detection relates to the potential for interference between the sensor and other parts of the aircraft. The sensor optical requirements limit the design to a box configuration that is approximately as high as it is wide. This necessity for height can cause difficulties for example in the area of wing tanks, pylons, antennas, etc. The result of allowing for such aircraft accessory interference is that the sensor head size can become limited because of such considerations. It

is also important to note that the physical sensor construction will also limit the ability to inspect completely into corners as formed by wing attachment points for example. In addition, the side wall of the sensor will require some physical space as will the light sealing mechanism on the side wall leading to inaccessible areas within the inspection zone. Many of these considerations are of course aircraft type unique and, therefore, lead to a trade-off between universal applicability and sensor size (i.e., area covered per inspection).

2.2 Identify Materials

There are a large number of composite materials in use and under development for future use. The goal here is to identify those that are of major interest, i.e., those in use in the largest number of applications and components. In discussions with Mr. Ted Reinhart of the Air Force Materials Laboratory, WPAFB, he states that the most widely used composites are AS4/3501-6 and T300/5208 in 8 to 250 ply quasi-isotropic layups.

The primary interest in this program is solid composite structures rather than those structures made up in the form of honeycombs, etc. This is based on the fact that the use of honeycomb structures in future aircraft designs is not as likely, while solid composites appear to be the choice for the future. However, based on the significant number of honeycomb structures in current use, they will be given consideration in the project.

The most commonly used solid composite structures are Graphite/Epoxy, Graphite/BMI, and Kevlar/Epoxy. These will all be studied in this contract. Additionally looking to the future a Graphite/Thermoplastic composite will be studied. The materials selected and the types of layups, number of plies used in the study phase, will be specified in the appropriate tasks.

2.3 Identify Damage Types

There are three types of composite structure defects to be detected: impacts, disbonds and delaminations.

2.3.1 Impacts

Impacts on the surface of a composite structure lead to internal damage (delaminations) of the structure which can lead to catastrophic failure of the structure when it is subsequently loaded. The nature of composite structures is such that internal damage can be caused by an impact that leaves no visible (to the unaided eye) mark on the surface. A previous study sponsored by the Canadian Department of National Defense under contract #W2207-1-AF07/01-SV was carried out to study the ability of *D SIGHT* to detect impact damage on CF-18 composite structures (AS4/3501-6).

An extensive sample study was carried out using various ply layups with AS4/3501-6, IM6/5245C, AS4/PEEK and KEVLAR 49/985. These were impacted at various energy levels with four types of impactor shapes. The results of the study for the materials studied, clearly established the detectability thresholds for impact damage using *D SIGHT* .

Table 1: LACIS-D Applications by Aircraft

Aircraft	Commercial Base	USAF ALC	Structural Composites	Ancillary Composites	Honeycomb Structures
Bombers					
B1B Lancer	---	OC-ALC			
B2	---	OC-ALC	X	X	X
B52 Stratofortress	---	OC-ALC			
Fighters/Attack					
A-37 Dragonfly	---	SA-ALC			
A-7 Corsair II	---	OC-ALC			
A-10 Thunderbolt II	---	SM-ALC			
F-111 Raven	---	SM-ALC			
F-117 Night Hawk	---	SM-ALC	X		
F4 Phantom	---	OO-ALC			
RF-4C Phantom	---	OO-ALC			
F-15 Eagle	---	WR-ALC		X	X
F-16 Falcon	---	OO-ALC		X	X
F-22 Rapier	---	SM-ALC	X		
Transports					
C-130 Hercules	---	WR-ALC			
C-135/KC-135 Stratotanker	B-707	OC-ALC/SM-ALC			
C-137/C-18	B-707	OC-ALC			
C-141 Startifter	---	WR-ALC			
C-5 Galaxy	---	SA-ALC			
C-9 Nightingale	DC-9	SA-ALC			
C10/KC-10 Extender	DC-10	OC-ALC			
C-12 Huron	Beech 200	SM-ALC			
C-17	---	SA-ALC		X	X
C-20 Gulfstream III	Gulfstream				
C-21	Learjet 35A				
C-22	B-727	OC-ALC			
C-23 Sherpa	Shorts SC-7				
C-25	B-747				
C-26 Metro	Metro				
C-27	G222				
Electronic Warfare					
E-3 Sentry	B-707	OC-ALC	X		
E-4	B-747	OC-ALC		X	X
E-8 J-Stars	B-707				
E-9	Dash 8				
Trainers					
T-37	---	SA-ALC			
T-38 Talon	---	SA-ALC			
T-41 Mescalero	Cessna 172	SA-ALC			
T-43	B-737	SA-ALC			
T-1 Jayhawk	Beechjet 400				
Helicopters					
H-53	---	WR-ALC			
H-60 Pave Hawk	---				
H-1 Iroquis	---	WR-ALC			

WR-ALC - Warner Robins Air Logistic Center, Robins AFB, GA
SA-ALC - San Antonio Air Logistic Center, Kelly AFB, TX
SM-ALC - Sacramento Air Logistic Center, McClellan AFB, CA
OC-ALC - Oklahoma City Air Logistic Center, Tinker AFB, OK
OO-ALC - Ogden Air Logistic Center, Ogden AFB, UT

The important goal in this study is to extend the impact detection work done previously to additional materials and impact conditions.

2.3.2 Disbonds

Disbonds are subsurface regions of the composite structure that have separated at a joint or splice at a surface where two separate structures have been joined (as opposed to delaminations which are separations between plies of the composite structure). The materials may be dissimilar, i.e., a composite skin bonded to a metal structure (honeycomb) or they may be of a similar material, glued after curing or combined during curing.

Disbonds can result from poor glue application or poor glue curing at the time of part manufacture. Disbonds can also occur due to overloading of the structure, either mechanically or thermally (fire or lightning).

Disbonds can be viewed at the exterior surface of a structure by *D SIGHT* because their presence causes the surface to bulge up due to a release of load across the bond line.

The characteristics of disbonds manifested at the structure surface are a large area, low amplitude surface bulge with a positive deflection above the surface. This surface effect is quite different from that observed in impact damage where the surface effect is very localized and of low amplitude with a negative deflection into the surface. It is postulated based on our past experience that disbonds of interest have approximately a 0.01 in. positive deflection with a 2 to 5 in. diameter.

A particularly significant type of disbond relates to honeycomb structures with thin composite skins. In this case the disbond will cover several cells of the honeycomb structure that is disbonded. While these will be given only limited study in this project, they remain of interest because such a large number of honeycomb structures are in use on aircraft at this time and for the foreseeable future.

The design of honeycomb structures with thin composite skins is such that once the glue interface is broken, the composite skin is free to move away from the honeycomb structure. In this case, we have the advantage of knowing how far below the composite material surface, the disbond is located, i.e., the thickness of the composite skin. Based on a nominal honeycomb cell size of 0.25 inch and a somewhat arbitrary requirement that a disbond be 5 cells or so across, then the minimum disbond diameter, ϕ, becomes 1.25 inches with an amplitude similar to that of the solid composite disbond of 0.01 inch.

2.3.3 Delaminations

Delaminations occur between the plies in composite structures. Of particular difficulty is the fact that the delaminations can occur at any depth within the surface, i.e., between laminations 1 and 2 or far away from the structural surface being viewed, for example between layers 29 and 30 in a 30 layer structure.

The occurrence of a delamination in a composite structure will allow both free surfaces to bulge slightly. We detect this bulging using *D SIGHT* but the bulging effect will be larger on the surface

which is closest to the delamination.

There is an additional type of delamination which can occur at the free edge of a composite panel, appropriately named on edge delamination. This type of delamination occurs predominantly from composite panel handling, when the panel is struck by an object at the free edge. This type of delamination is crescent shaped and should be easier to detect because only the edge zones of the panel need to be inspected.

It is anticipated that, based on damage assumptions in the Damage Tolerance Design Guide [1], the size of delaminations to be detected will be approximately 2 inches in diameter. Edge delaminations are expected to be smaller in diameter at approximately ½ inch. The profile height of these delaminations from lab specimens is typically 0.005 inch and 0.002 inch, respectively.

2.3.4 Summary of Defect Geometry

It is important to note that the defect geometries shown in **Table 2** are estimated to be the minimum level requiring detection based on the information available [1]. Two factors remain to be established via experimental work consisting of damaged specimens and field work: first, is more sensitivity to physical surface shape required to detect all impact damage, disbonds and delamination of interest and second, does the surface condition (i.e., surface roughness noise) of the aircraft components allow *D SIGHT* to reliably detect surface shapes as defined above.

Table 2: Dimensional Characterization of Defect Types

Defect Type	Height/depth	Size	Radius of Curvature
Impact Signature	0.008" D	0.3" ϕ	0.71 in^{-1}
Disbond	0.010" H	2" ϕ	0.02 in^{-1}
Honeycomb Disbond	0.010" H	1.25" ϕ	0.05 in^{-1}
Delamination	0.005" H	2" ϕ	0.01 in^{-1}
Edge Delamination	0.002" H	½" ϕ	0.06 in^{-1}

If it is assumed that composite defects such as delaminations and disbonds can be represented as spherical sections, their curvatures may be calculated as follows: given a defect with a height of h mm and a diameter of d mm, the curvature of the defects surface is

$$\frac{8 \times h}{(4 \times h^2) + (d^2)} \ mm^{-1}$$

As an example, a delamination with a 25.4 mm (1 in.) diameter and 0.05 mm (0.002 in.) height would have a curvature of 0.00062 mm^{-1} (0.016 in^{-1}).

D SIGHT's sensitivity to small curvatures is improved by changing the hardware parameters. As shown below, each change brings with it a disadvantage.

To Improve Sensitivity	Disadvantage
Increase distance between surface and screen	Increases screen size and overall package size
Increase camera magnification	Decreases field of view
Reduce reflection grazing angle	Increases the magnification differences within the image
Decrease the light source size	Increases sensitivity to surface noise

As can be seen from the above comments relative to surface curvature (surface curvature is what creates the *D SIGHT* image contrast effect), impact signatures are relatively easy to detect because they have a high curvature, while the other defect types have low radii of curvature. The sensor design challenge is to optimize for these defects while maintaining sensitivity to impact signatures.

3 SPECIMEN DAMAGE INTRODUCTION AND EVALUATION

3.1 Introduction

Composite structures are susceptible to in-service damage in many forms. The primary service-induced damage of concern is low velocity impact damage by a hard object. This could occur during ground handling or during service. The nature of the damage is dependent on the residual impactor shape and on many other geometric and material parameters. When an impact causes an indentation of greater than 0.1 inch on the surface, it is referred to as a visible impact damage. This is generally expected to be detected by a visual inspection, leading to a subsequent inspection by ultrasonic equipment to obtain information on the extent of accompanying internal damage. Residual impact indentations below 0.1 inch, although barely visible or invisible, may also be accompanied by considerable internal damage. In both cases, the residual compressive strength of the laminate could be severely degraded. This is the situation that currently causes considerable concern in the design, fabrication and service of composite structures in aircraft. It is imperative to develop a cost effective technique for detecting non or barely visible damage on composite structures.

Graphite reinforced resins are finding increasing applications in airframes of military and civilian aircraft. These materials offer high specific strength and stiffness properties and very good fatigue resistance. Unfortunately, the materials are sensitive to low energy impact damage from such common occurrences as hailstones, stones thrown off the runway or tools dropped by maintenance personnel. These impacts may result in significant levels of internal damage while surface damage may be barely or nonvisible.

Operational experience with composite structures indicates that 81% of all damage is due to impact while lightning strikes (10%), overheating (7%) and delamination (2%) constitute the reminder of damage types [2].

Regular in-service inspections of aircraft with scanning devices are not practical if only due to cost and time required for such inspections. Current practices rely on visual detection of impact damage. The United States Air Force (USAF) Damage Tolerance Design Guide for composites requires that composite aircraft structure be able to carry ultimate load with impact damage resulting in 0.1 inch (2.5 mm) deep indentation. Thus 0.1 inch is regarded as the visibility threshold. Other organizations have established lower thresholds typically 0.05 inch (1.25 mm), while Aérospatiale has certified the ATR-72 composite wing box using 0.3 mm (0.012 inch) as the visibility threshold (close visual inspection with 50% probability of detection). These attempts to lower the threshold are driven by the desire to design lighter structures with higher allowable strain levels.

Recent research by NRC/IAR and Aérospatiale has shown that significant reductions in impact dent depths can be expected due to relaxation, cyclic loading, moisture and temperature effects (up to 45%). Thus, if visual inspections are to be used, the allowable design strain levels should be lowered even further. A cost effective method for rapid regular inspection of composite structures with a capability better than close visual inspection could result in lighter composite structures and

enhanced safety of operation of current designs.

Preliminary observations using artificially delaminated specimens indicated that DAIS might also be capable of detecting this type of defect. While delaminations not related to impact are significantly less common, it was thought that establishing the *D SIGHT* capabilities in detecting this damage type was none the less important. Thus, impact damage and delaminations are two types of damage which were used under this project. A careful set of experiments were conducted to evaluate the sensitivity of *D SIGHT* by the introduction of damage to the fabricated composite structures followed by nondestructive inspections (NDI) of the specimens and finally a correlation evaluation between *D SIGHT* inspection and other NDI methods. Much of the material presented in this chapter is borrowed from the NRC/IAR task reports [3, 4] summarizing their findings for this contract.

3.2 Materials

The Structures, Materials and Propulsion Laboratory of NRC/IAR and DND/USAF agreed that the two composite material systems to be used in this study were Hercules AS4/3501-6 and Cytec IM7/5250.

3.2.1 Material Specifications for Hercules AS4/3501-6

The prepreg material was unidirectional carbon fibres preimpregnated with epoxy resin, Hercules 3501-6. The carbon fibres were Hercules Corp. Magnamite continuous type AS4. This material has been widely used in the aerospace industry for over 15 years and is the material being used on Canadian CF-18 fighter aircraft. To support the Canadian Department of National Defence, several research projects using this material are being carried out in the Structures, Materials and Propulsion Laboratory and a large in-house data base for this material has been established.

To ensure the materials to be used in this project are consistent and meet the requirements, materials were procured from Hercules Corp. to the Structures, Materials and Propulsion Laboratory's specifications, **Table 3**. The AS4/3501-6 is a high service temperature (-59 to 150°C) thermoset composite material having physical and mechanical properties as presented in **Table 3**. The prepreg material was from a single batch and was delivered in good condition packed in dry ice. The supplier also provided information on defects in each roll of material, including locations and length of defect and any defects were clearly marked on one end of each roll.

Table 3: Material Specifications for Hercules AS4/3501-6

Physical Properties	
Resin content, percent weight	35 ± 3
Volatiles content, percent weight	1 max
Flow, percent weight	16 ± 5
Gel time	9 ± 4 min.
Fiber areal weight	4.4 oz/yd^2
Cured thickness (Nominal)	5.2 mils
Width	12 in.
Out time at room temperature	10 days min.
Shelf life at 0°F (-18°C)	12 months

Mechanical Properties	
0° tensile strength at 77°F (25°C)	310 ksi
0° tensile modulus at 77°F (25°C)	21.5 msi
0° compression strength at 77°F (25°C)	230 ksi
0° compression modulus at 77°F (25°C)	20.0 msi
0° flexural strength at 77°F (25°C)	260 ksi
0° flexural modulus at 77°F (25°C)	18.5 msi
Short beam shear strength at 77°F (25°C)	18.5 ksi

3.2.2 Material Specifications for Cytec IM7/5250-4

The other composite material system selected for this study was unidirectional carbon fibres preimpregnated with bismaleimide resin, Cytec's Rigidite 5250-4 and the carbon fibres were Hercules Corp. Magnamite continuous type IM7. Material was procured from Cytec Engineering Materials Inc. to the Structures, Materials and Propulsion Laboratory material specifications. According to the manufacturer, IM7/5250-4 is a high service temperature (-59 to 204 C) and high strength fibre material. Typical physical and mechanical properties of this material are presented in **Table 4**. This material system was relatively new on the market and has been reported to have been used in the construction of new generation fighter aircraft such as the F-22. Since this material has potential for high temperature application, an in-house material characterization was carried out to generate a data base and also to develop processing techniques and handling experience. The prepreg material was from a single batch (lot number) and was delivered in good condition packed in dry ice. The supplier also provided information on defects in each roll of material, including locations and lengths of defects which were clearly marked on one end of each roll.

Table 4: Material Specifications for Cytec IM7/5250-4

Physical Properties	
Resin content, percent weight	31
Volatiles content, percent weight	2.1 max
Flow, percent weight	16 ± 5
Gel time	9 ± 4 min.
Fiber areal weight	4.3 oz/yd^2
Cured thickness (Nominal)	5.0 mils
Width	12 in.
Out time at room temperature	10 days min.
Shelf life at 0°F (-18°C)	12 months

MechanicalProperties	
0° tensile strength at 77°F (25°C)	380 ksi
0° tensile modulus at 77°F (25°C)	23.5 msi
0° compression strength at 77°F (25°C)	264 ksi
0° compression modulus at 77°F (25°C)	22.9 msi
In-plane shear strength at 77°F (25°C)	14.9 ksi
In-plane shear modulus at 77°F (25°C)	0.86 msi
Short beam shear strength at 77°F (25°C)	20.0 ksi

3.3 Design of Hat-Stiffened Composite Panel

General guidelines for the design of composite panels have been developed from many research efforts. An important consideration is that the design of the ply orientation and the number of plies depend on load magnitude and modes. These guidelines are summarized below:

a) the outer plies should be 45° for all elements of the structure to carry the shear loads;

b) at least one 0° ply (parallel to the load) should be adjacent to the outer 45° plies, where it is applicable;

c) it is more efficient to place the 90° plies next to the 0° plies (these 90° plies greatly improve the junctures between elements by providing resistance to out of plane displacements, thus both buckling and post buckled strengths are increased);

d) the 0° plies located in the cap and skin would improve the structural efficiency, but the number of these 0° plies should be carefully calculated for the particular load;

e) the webs should be as near perpendicular to the skin as possible in order to reduce peeling

stresses in the flange-skin interface; and

f) in order to minimize distortion, the plies should be oriented symmetrically about the midplane of the various elements.

From the above guidelines, two stiffened panels with different configurations were designed, see **Table 5**. Configuration 1 was designed as a lightly loaded fairing type structure while configuration 2 was a heavily loaded wing skin type structure.

Table 5: Stiffened Panel Configurations

Configuration		Plies	Stacking Sequence	Laminate Thickness (in.)	
				IM7/5250-4	AS4/3501-6
1	Skin	12	$(45/0/ 45/90)_s$	0.060	0.0624
	Cap	26	$(45/0_4/90/0_3/ 45/0)_s$	0.130	0.1352
	Web	12	$(45/90/0/ 45)_s$	0.060	0.0624
	Flange	5	(45/90/ 45)	0.025	0.0260
2	Skin	48	$(45/0/ 45/90)_{4s}$	0.240	0.2496
	Cap	52	$(45/0_4/90/0_3/ 45/0)_{2s}$	0.260	0.2704
	Web	24	$(45/90/0/ 45)_{2s}$	0.120	0.1248
	Flange	10	$(45/90/ 45)_2$	0.050	0.0520

3.4 Specimens in Test Plan

The key tests aimed at the evaluation of the *D SIGHT* technology were conducted on built-up hat stiffened panels 30x36 inch (762x914 mm) manufactured in two configurations (12 and 48 ply thick skins). These specimens were built using either a first generation graphite/epoxy (AS4/3501-6) or a graphite/bismaleimide (IM7/5250-4).

A total of four stiffened panels were tested. Two each of the AS4/3501-6 material, one being of the 12 ply lay-up (No. 856) and the other of the 48 ply lay-up (No. 867). Similarly two panels constructed with the IM7/5250-4 material were tested, (No. 860, 12 plies and No. 869, 48 plies).

Some simple specimens were also used to develop various methods of delamination damage introduction. This work was required since methods used to simulate delaminations for ultrasonic methods were previously found to be inadequate for *D SIGHT*. Typically Teflon© inserts have been used but result in a surface perturbation on the bagging side of the laminate which is easily located with *D SIGHT* while no indication could be expected to be observed on the tool side of the laminate. Construction of these simple specimens will be described in the section on Delamination Damage Introduction.

The test plans were expanded through the addition of a honey comb sandwich specimen typical

of E-3 radome construction and an F-16 horizontal stabilizer representing an older aluminum honey comb with graphite/epoxy skins type construction (more recent F-16 stabilizers are fabricated using solid type construction). All these specimens are summarized in **Table 6**.

Table 6: Test Matrix

	STIFFENED PANELS							
	PANEL No.	MATERIAL	No. of PLYS	PRE DAMAGE NDI		DAMAGE by DROP TOWER 0.5 in. Dia. Tip	POST DAMAGE NDI	
				C-SCAN	*D SIGHT*		C-SCAN	*D SIGHT*
1	856	AS4-3501/6	12	Y	Y	39 sites. 1,1.5,3,5,7.5 ft-lb	Y	Y
3	858	AS4-3501/6	12	Y	Y			
4	859	AS4-3501/6	12	Y	Y			
5	860	IM7 5250-4	12	Y	Y	44 sites.1.5, 3,5,7.5,10 ft-lb	Y	Y
7	863	IM7 5250-4	12	Y	Y			
8	864	IM7 5250-4	12	Y	Y			
9	867	AS4-3501/6	48	Y	Y	53 sites 5,7.5,10,15,20,30 ft-lb	Y	Y
10	868	AS4-3501/6	48	Y	Y			
11	869	IM7 5250-4	48	Y	Y	34 sites. 7.5,10,15 20 ft-lb	Y	Y
12	870	IM7 5250-4	48	Y	Y			
	VARIOUS CONSTRUCTIONS					DELAMINATION / DISBOND		
2	857	AS4-3501/6	12	Y	Y	28 sites tested	Y	Y
6	862	IM7 5250-4	12	Y	Y	29 sites tested	Y	Y
13	13	AS4-AlHcomb-Al	12	Y	Y	skin/core disbond, 5 sites	Y	Y
14	852	IM6 1806	36	Y	Y	8 sites tested	Y	Y
15	234A	AS4-3501/6	40	Y	Y	19 sites tested	Y	Y
16	234B	AS4-3501/6	40	Y	Y	6 sites tested	Y	Y
	F-16 HORIZONTAL STABILIZER					DAMAGE		
17	F-16 HStab	gr/ep skins	n/a	Y	Y	23 damage sites by various means	Y	(Y)
		Al honeycomb core		also X-ray			(also X-ray)	
18	E-3	gr/ep skins	n/a	Y	N	as-received, core repairs	N	Y
		Al honeycomb core						

3.5 Surface Preparation

3.5.1 Sanding

All of the built-up specimens in this test program were sanded prior to painting. The procedure involved wet sanding with 220 grit, open cloth, abrasive. The sanding was carried out with a compressed-air driven, orbital, hand-held sander. The surface was sanded until a water-break

condition was achieved.

3.5.2 Painting

a) Paint system

A polyurethane finish paint system was applied to the outer surface of the specimens. This was carried out in accordance with Canadian Forces Technical Orders (C-12-010-010/TP-000). The surface was degreased with paint thinners prior to the application of the epoxy primer coat, (MIL-P-23377). The primer coat and first top coat of polyurethane, (D-12-033-001/SF-000), were roughened by hand sanding prior to the next layer being applied.

b) Color scheme

The second or top coat of the paint system was done in a camouflage scheme with two shades of gray. The paint was applied in a diagonal pattern across the specimens. It was expected that this paint scheme (quite typical for military aircraft) could produce a change in reflectivity of the highlighted surface which in turn might confuse the inspector and lead to some delamination false calls.

The radome and F-16 stabilizer were inspected in as-received condition.

3.6 NDI of Specimens Prior to Damage Introduction

Prior to damage introduction the panels were inspected with both ultrasonic C-Scan and *D SIGHT* techniques.

The ultrasonic C-Scan inspections were carried out at IAR using a reflection pulse-echo method by immersing the specimen in a large water tank. In the reflection pulse echo method, a single transducer was used both as a transmitter and receiver. The transducer was scanned over the test specimen and the reflected signal from a plate located behind the specimen was monitored.

The F-16 stabilizer specimen was too large to be immersed in the IAR C-Scan tank. A through-transmission ultrasonic C-Scan inspection was carried out in the squirter facility at the Quality Engineering Test Establishment (QETE) of the Department of National Defence (DND).

Preliminary *D SIGHT* inspections were carried out at IAR using the Experimental DAIS-250C equipment. Subsequent to this, C-Scan inspection specimens (with the exception of the F-16 stabilizer) were shipped to Diffracto Ltd. for inspection using a simulated DAIS-500 setup. This setup was established based on prior experience using the Experimental DAIS-500 and preliminary studies at Diffracto using simple specimens with delaminations and impacts provided by IAR. In later stages of the project the Prototype DAIS-500 was used for *D SIGHT* inspections.

Most of the *D SIGHT* inspections were carried out using Electron™ highlighter (some of the early work under this project was carried out using the Snoflake™ highlighter which was abandoned due to environmental and safety concerns).

3.7 Delamination and Disbond Damage

3.7.1 Delamination and Disbond Damage Introduction Techniques

The introduction of delamination and disbond damage in both stiffened and honeycomb core composite structures required the development of new techniques. A number of small specimens were fabricated for this purpose.

A composite panel was constructed to investigate a method of forcing delaminations to occur and grow as a result of the panel design. Panel No. 840 was manufactured of AS4/3501-6 material with a 24 ply lay-up modified mid span by terminating four ply groups (3, 4, 4, and 3 plies) symmetric about the mid-plane, at 0.25 inch (6.35 mm) intervals. The panel was designed such that, when axially loaded in tension, a delamination would initiate in the ply drop off area because of the asymmetric load path. The specimens did not perform as intended and construction and testing was halted in favor of methods described below.

The delamination damage and disbonds were introduced by first machining away material from the rear surface of the specimen at the selected site and to a predetermined depth. Typically the machined holes were of ½ inch (12.7mm) diameter. A small instrumented load frame was constructed in which the specimen could be supported while a solid metal probe was pushed against the bottom of the machined hole. The metal probe was fitted into a load cell and the load cell was attached to a mechanical jack. The load cell was calibrated for its maximum capacity of 2000 pounds (8896.4 N). The jack could be positioned within the device to orient it with machined sites which were located across the width of the specimen. The jack was operated manually. The output of the load cell was amplified and displayed on a digital volt meter.

A similar technique was used to create disbonds in a specimen. This type of specimen was constructed of solid skins bonded to two opposite sides of an aluminum honeycomb core (sandwich construction). An access hole was machined through one skin of the specimen to allow for a solid metal probe to be inserted into one of the comb cells. The disbond was created between the intact skin and the core material at the adhesive layer. The panel could be loaded in the load frame in a similar manner as the solid laminate specimens.

The load frame can accommodate specimens up to 38 inches (965 mm) in width. The unsupported area could be adjusted by installing plates with various size holes. The holes in the plates were centered on the damage site and were used to control the maximum damage size.

Edge delamination damage was accomplished by manually driving a metal wedge into the laminate at selected locations around the perimeter at selected ply interfaces.

Four specimens were involved in the development of these damage introduction techniques. From these specimens it was concluded that:

- The removal of material from the rear surface was a suitable method to gain access for the installation of damage at a selected location through the thickness of a solid laminate.
- Repeatable damage could be generated through the use of the load frame and a controlled

loading technique.

- The forced wedge technique could be used to install edge delamination damage at selected locations through the thickness of a solid laminate.
- By drilling through the aluminum skin and loading the specimen with a probe the size of one cell, disbonds could be simulated between the aluminum skin and the honeycomb core.
- Delaminations at a free edge could be created effectively with the load frame and probe.
- Delaminations of a similar area could be created with the load frame and probe.
- The ultrasonic C-Scan inspection could detect all of the damage.

A full description of these initial experiments is described in the references in [3].

3.7.2 Delamination Damage Sites

Damage introduction to simulate delaminations and disbonds were carried out on two stiffened panels, 857 and 862. Forty-four damage sites were machined into each specimen. Not all of the sites were used to create delaminations or disbonds.

Three damage situation types were identified and are shown in **Figure 1**. Damage situation type 2 is reserved for impact damage sites that will be defined later.

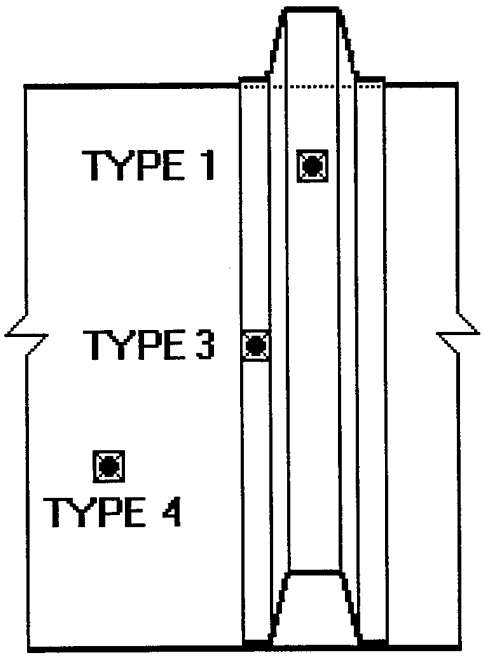

Figure 1: Locations of Damage Situation Types

a) Type 1 sites were centered laterally on the stiffener and a hole was machined through the stiffener base to permit the stiffener to be separated from the skin at both web flanges.

b) Type 3 sites were centered on one flange and material was removed to the bond line between the flange and the rear surface of the skin. Loading at this location would simulate the disbonding of only one flange.

c) Type 4 sites were centered laterally between stiffeners and nominally 75% of the thickness of the material was removed. This site received damage to simulate a delamination within the skin.

Additionally, some edge delamination sites were created by forced wedge at the corners and simulations of flange disbonds were also created at the ends of the stiffeners.

Introduction of delaminations and disbonds into stiffened panels required the machining operations shown in **Figure 2**. These operations were followed by damage introduction procedures described earlier.

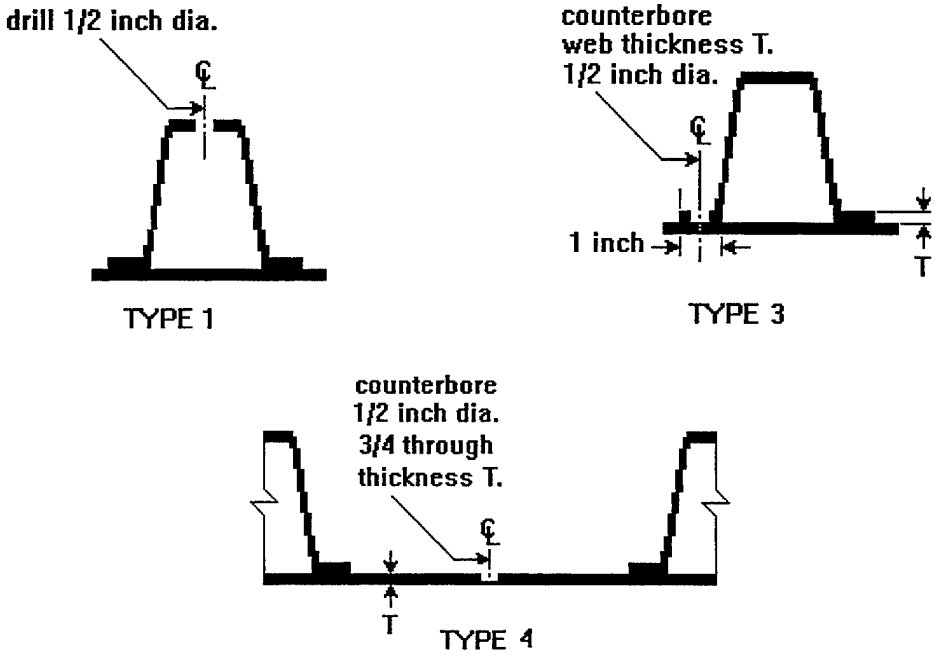

Figure 2: Machining Operations Required for Damage Introduction

3.7.3 Post Damage Summary of Panel No.857

A map of damage sites is shown in **Figure 3**. Site 13 was first damaged in the load frame (situation type 1). Later, both flanges were damaged by forcing a wedge from the free edge until the flange delamination joined with the Site 13 damage (13A). Site 14 was treated similarly. The C-scan results in **Figure 4** show the resulting damage for Site 14A but there is no indication for Site 13A.

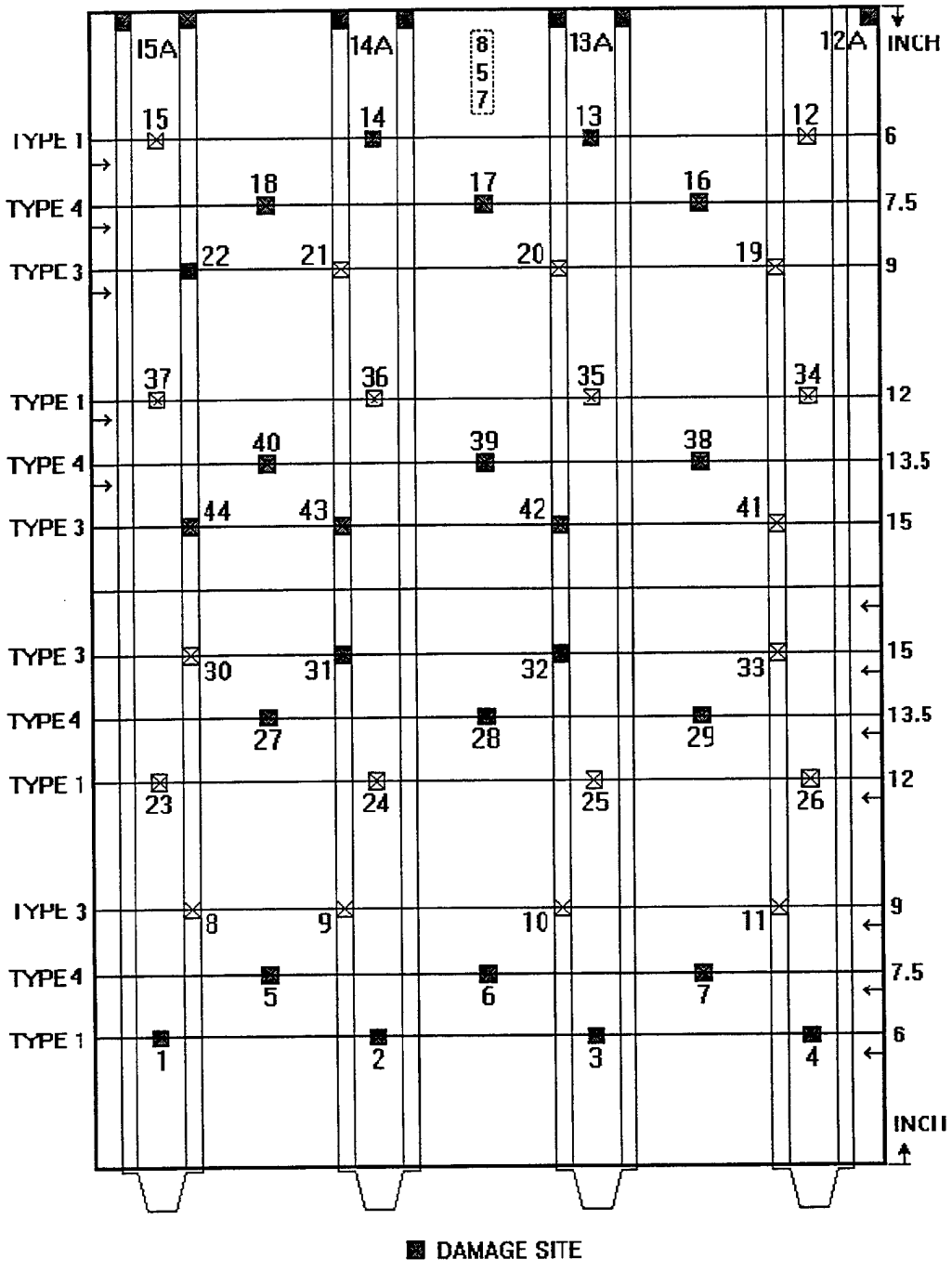

Figure 3: Delamination and Disbond Damage Site Map, Panel No. 857

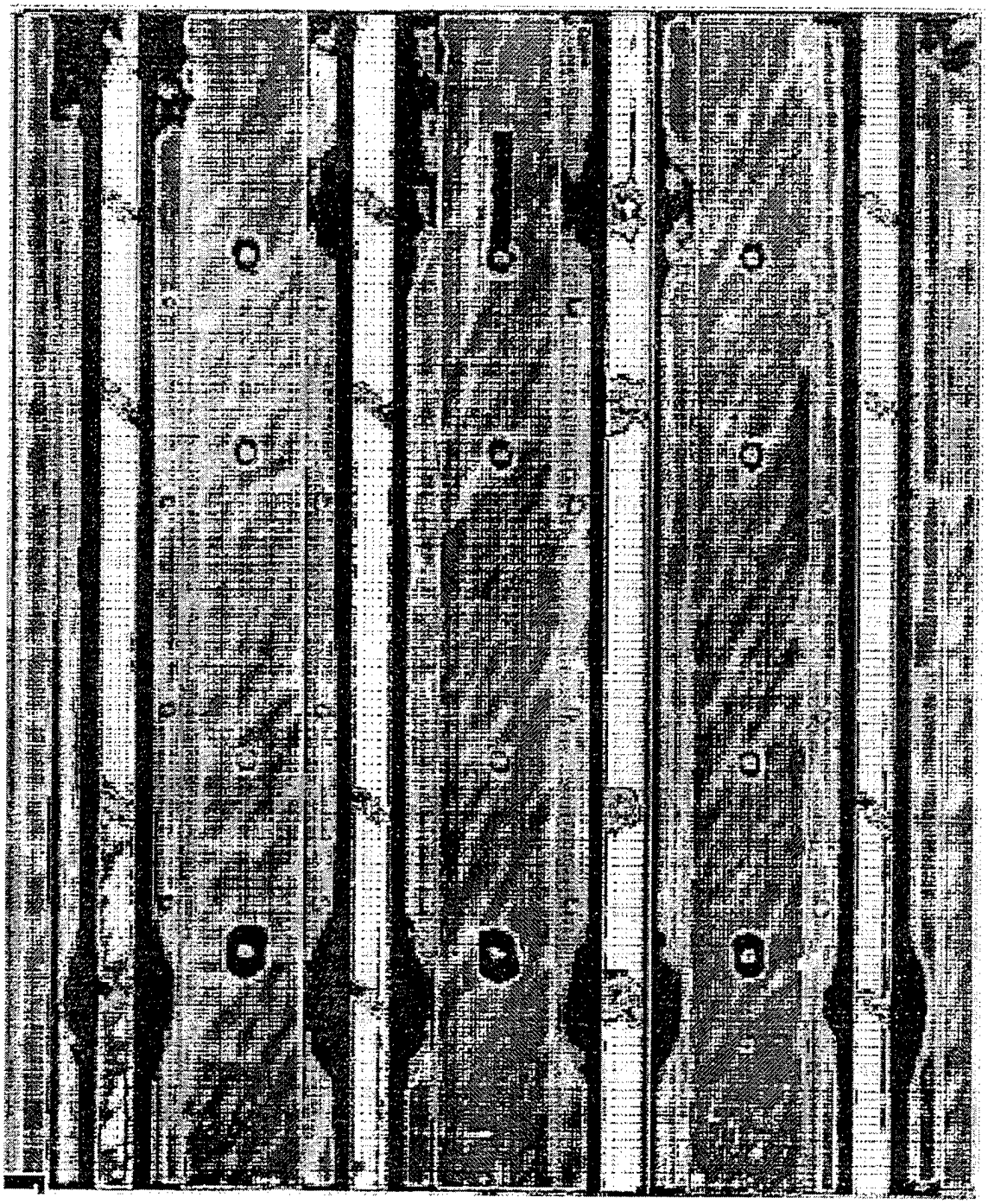

Figure 4: Postdamage C-Scan, Panel No. 857

The *D SIGHT* results in **Table 7** were obtained from the visual analysis of prototype DAIS-500 images using the Analyze Module in the DAIS software. **Figure 5**, **Figure 6**, and **Figure 7** are sample *D SIGHT* images of panel 857.

The panel skin thickness is less over the stiffener than in the bay between stiffeners. This difference can be attributed to the manufacturing process; however, the skin lay-up is 12 plies through out. Type 3 sites had nominally 0.020 inch (0.5 mm) of material removed from the original 0.090 inch (2.3 mm) flange thickness to install the damage close to the level of the bay skin thickness 0.065 inch (1.7 mm).

No Type 1 damage was detected with *D SIGHT*. Type 3 was detected in five out of six sites; however, *D SIGHT* signatures were weak. In both these damage types, the delaminations or disbonds were between the skin and flange. These are both individually balanced lay-ups; therefore, little or no residual curing stress was released in the disbond/delamination process.

In the case of Type 4 sites delaminations were within the skins and closer to the inspected skin surface. All of these defects produced strong *D SIGHT* signatures in spite of the relatively small delamination size. All delaminations were detected (12 out of 12) in spite of the fact that these damage types were, on average, smallest of the three damage situation types. Weak *D SIGHT* signatures were detected at site 12A (corner delamination) and at site 15A (flange disbond).

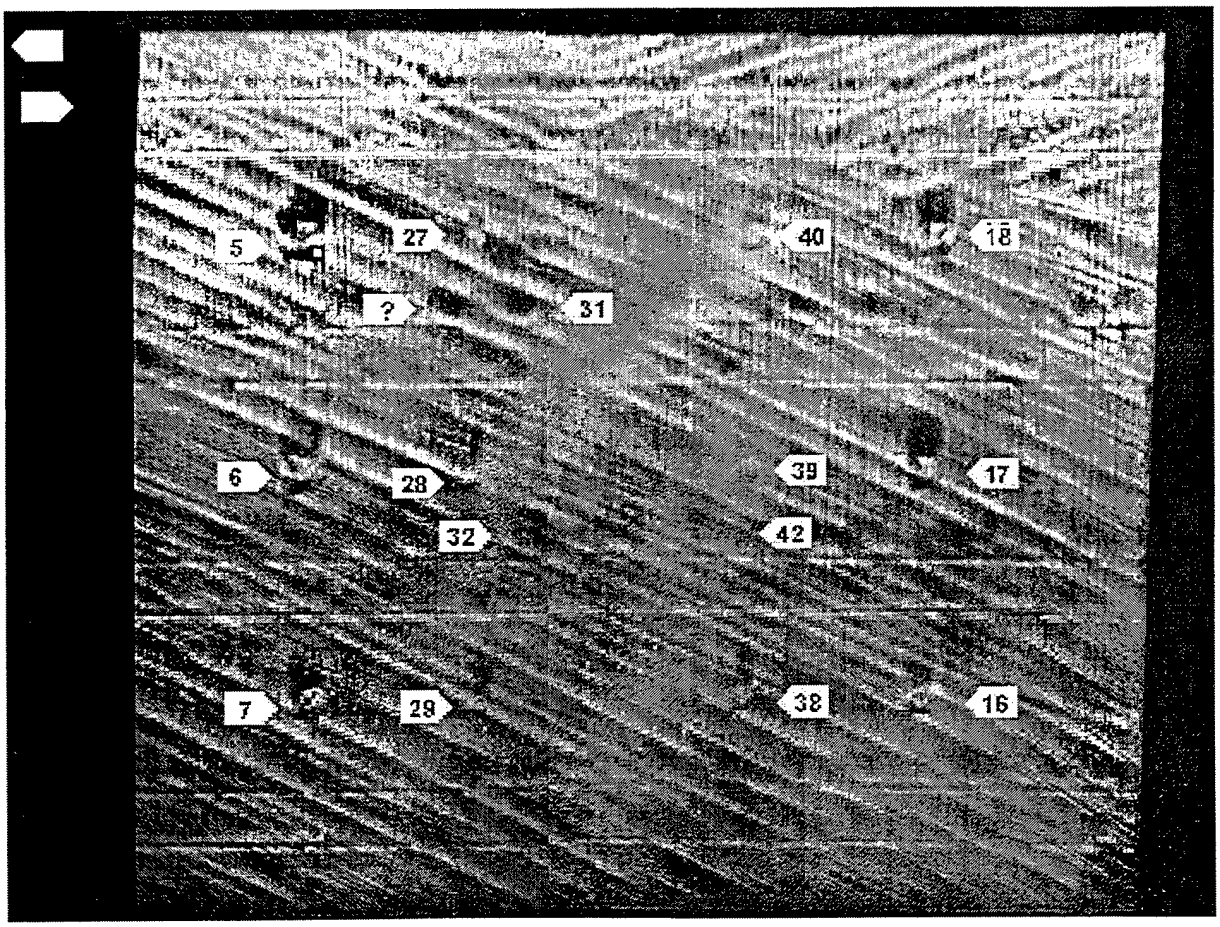

Figure 5: Mosaic of Perspectively Corrected *D SIGHT* Images of Panel No. 857 Using a Simulated DAIS-500 Setup. Numbers Indicate Damage Site Locations as Shown in **Figure 3**. The "?" Indicates a False Signature that was not Found Later Using the Actual DAIS-500 Sensor.

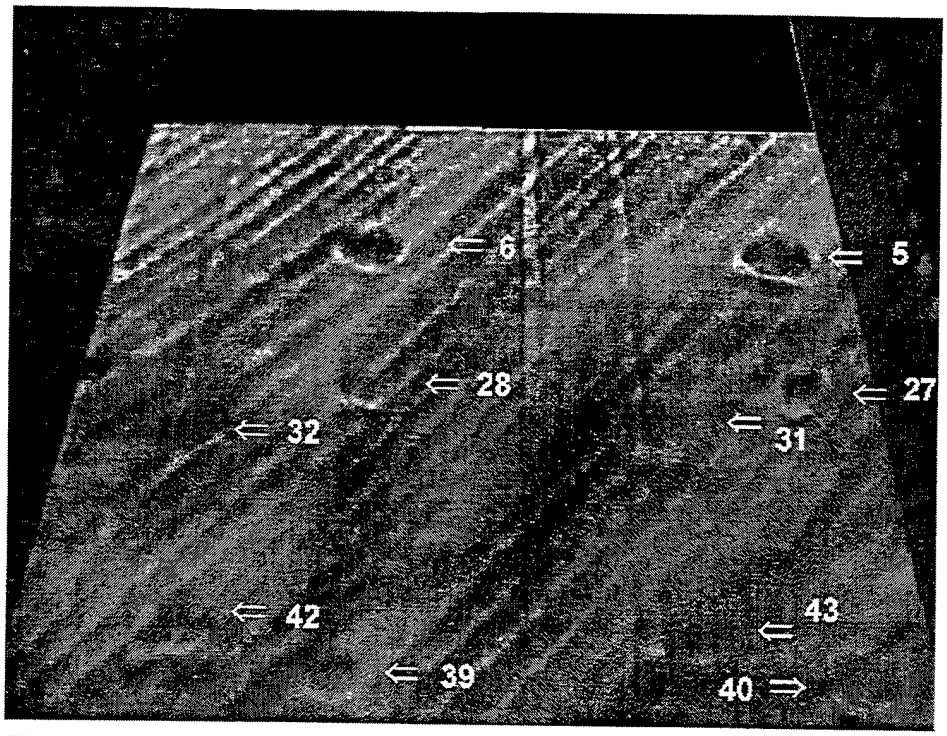

Figure 6: DAIS-500 Image of Panel No. 857 Showing Delamination and Disbond Damage for Numbered Site Locations in **Figure 3**.

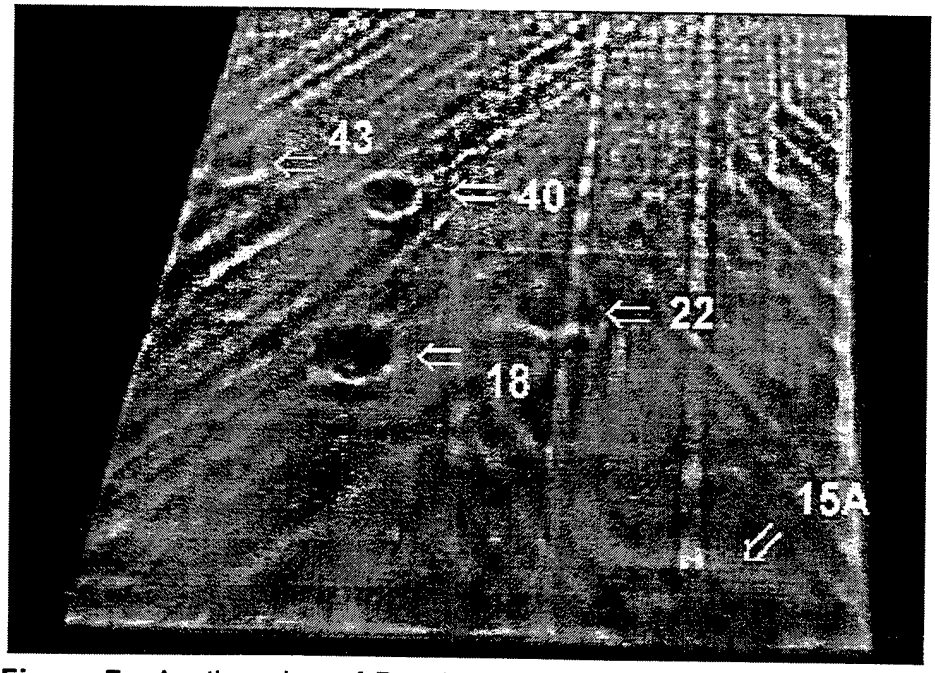

Figure 7: Another view of Panel No. 857 Showing Delamination and Disbond Damage for Numbered Site Locations in **Figure 3**.

Table 7: Test Matrix and Inspection Results, Panel No. 857

DAMAGE INTRODUCTION Panel No. 857							DAMAGE ASSESSMENT		
SITE	TYPE	RESTRAINT AREA (inch)	Maximum Deflection (inch)	Maximum LOAD (lbs.)	Skin Thickness (inch)	Counter-bore (inch)	C SCAN (Y/N)	Damage L xW (inch)	DAIS 500 (Y/N)
1	1	none	0.1	520	0.05		Y	3.57x5.26	N
2	1	none	0.12	720	0.05		Y	4.14x5.28	N
3	1	none	0.12	500	0.05		Y	3.91x4.22	N
4	1	none	0.1	500	0.05		Y	3.11x4.48	N
13	1	none	0.13	600	0.05		N	4.18	N
14	1	none	0.13	500	0.05		Y	4.14x4.33	N
22	3	1.75 dia.	0.06	460	0.091	0.019	Y	1.18	Y
31	3	1.75 dia.	0.05	520	0.091	0.019	Y	1.78	Y
32	3	1.75 dia.	0.1	560	0.090	0.019	Y	3.49	Y
42	3	1.75 dia.	0.1	640	0.090	0.015	Y	2.62	Y
43	3	1.75 dia.	0.06	500	0.091	0.016	Y	2.09	Y
44	3	1.75 dia.	0.07	660	0.091	0.016	Y	2.2	N
5	4	3 dia.	0.13	460	0.065	0.044	Y	1.63	Y
6	4	3 dia.	0.15	460	0.065	0.045	Y	1.48	Y
7	4	3 dia.	0.13	400	0.065	0.043	Y	1.18	Y
27	4	3 dia.	0.1	260	0.065	0.042	Y	0.76	Y
28	4	3 dia.	0.12	240	0.065	0.045	Y	0.8	Y
29	4	3 dia.	0.1	220	0.065	0.043	Y	0.87	Y
16	4	none	0.15	360	0.065	0.045	Y	0.99	Y
17	4	none	0.15	420	0.065	0.045	Y	1.14	Y
18	4	none	0.15	360	0.065	0.045	Y	1.25	Y
38	4	1.75 dia.	0.07	260	0.065	0.045	Y	0.83	Y
39	4	1.75 dia.	0.06	280	0.065	0.042	Y	0.95	Y
40	4	1.75 dia.	0.07	220	0.065	0.044	Y	0.99	Y
12A	(a)	none	n/a	n/a	0.065		Y	1.94x2.13	Y
13A	(b)	none	n/a	n/a	0.065		Y	4.18x7.9	N
14A	(b)	none	n/a	n/a	0.065		Y	4..12x7.83	N
15A	(b)	none	n/a	n/a	0.065		Y	4.12x3.72	Y

(a) edge delamination by forced wedge insertion

(b) flange disbond by forced wedge insertion

3.7.4 Post Damage Summary of Panel No. 862

A map of the damage sites for panel 862 is shown in **Figure 8**. The results of the C-scan and *D SIGHT* inspections for this panel are summarized in **Table 8**.

Panel 857 (AS4/3501-6) and panel 862 (IM7/5250-4) were of identical construction. Comparisons of **Table 7** and **Table 8** show no differences in the ability of *D SIGHT* or C-scan to detect disbond or delamination damage in these panels. Essentially, simulated disbonds (damage situation sites 1 and 3) could either not be detected or produced weak *D SIGHT* signatures. On the other hand, delaminations (damage situation type 4) produced easily located *D SIGHT* signatures.

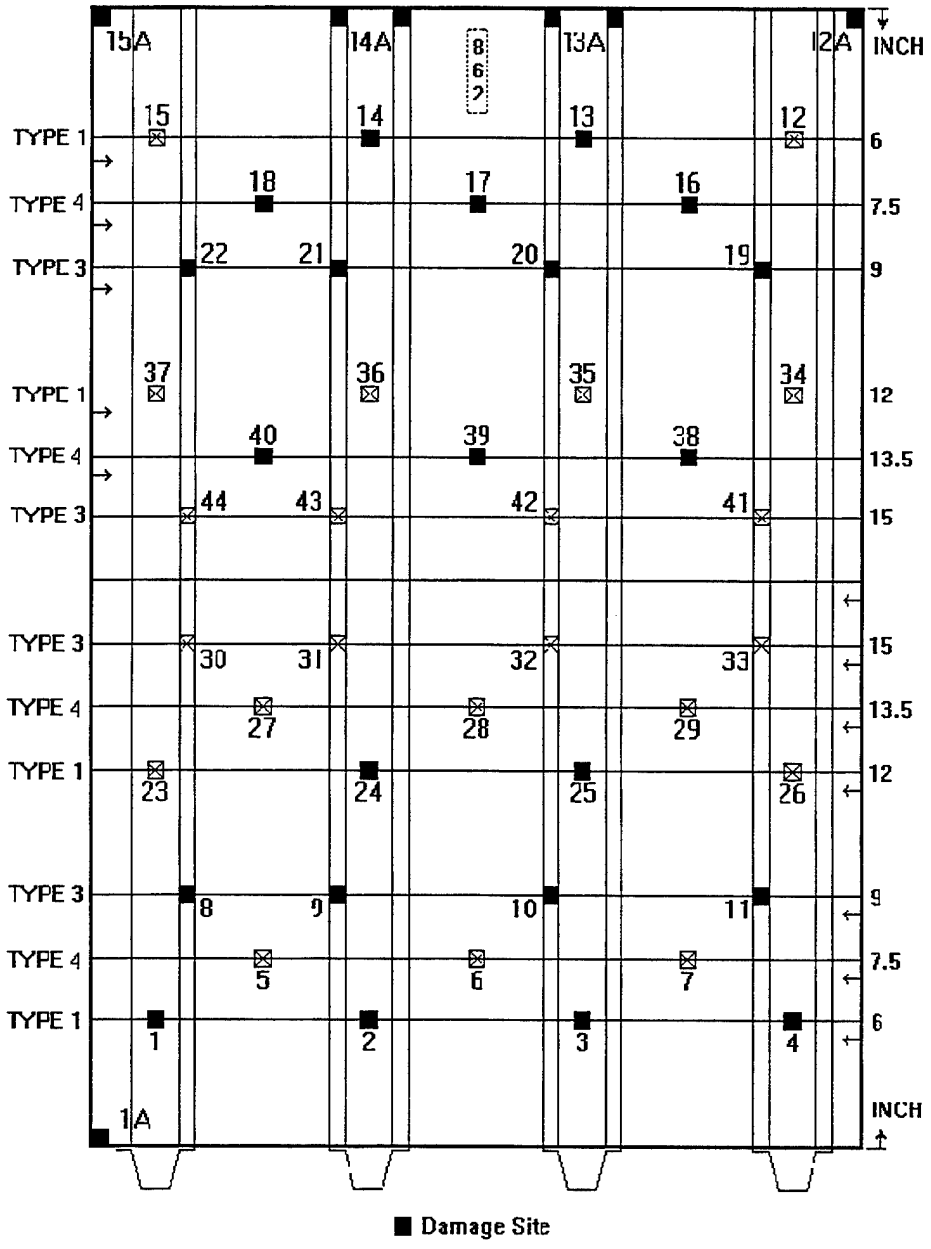

Figure 8: Delamination and Disbond Damage Site Map, Panel No. 862

Table 8: Test Matrix and Inspection Results, Panel No. 862

DAMAGE INTRODUCTION: PANEL No.862							DAMAGE ASSESSMENT		
SITE	TYPE	RESTRAINT AREA (inch)	Maximum Deflection (inch)	Maximum Load (lbs.)	Skin Thickness (inch)	Counter-bore (inch)	C SCAN Detect (Y/N)	Damage L x W (inch)	DAIS 500 (Y/N)
1	1	none	0.12	620	0.06		Y	3.76x3.23	N
2	1	4 x 4.5	0.1	640	0.06		Y	4.79x3.65	N
3	1	4 x 4.5	0.1	600	0.062		Y	3.53x3.34	N
4	1	4 x 4.5	0.06	500	0.062		Y	3.23x3.08	N
13	1	none	0.1	800	0.061			0.93x3.53	N
14	1	none	0.11	700	0.062		N	4.56x3.38	N
24	1	none	0.1	560	0.06		Y	3.8x4.03	N
25	1	none	0.15	880	0.062		Y	4.22x4.03	N
8	3	3 dia.	0.1	560	0.087	0.011	Y	2.81x0.49	N
9	3	3 dia.	0.08	580	0.086	0.011	Y	2.85x1.44	N
10	3	3 dia.	0.08	680	0.089	0.011	Y	2.58x>1	N
11	3	3 dia.	0.08	800	0.086	0.011	Y	2.96x1.52	Y
19	3	1.75 dia.	0.3	840	0.087	0.014	N		N
20	3	1.75 dia.	0.3	800	0.090	0.011	N		N
21	3	1.75 dia.	0.3	800	0.089	0.008	Y	1.94x	N
22	3	1.75 dia.	0.3	660	0.092	0.011	Y	1.78x	N
5	4	Not tested	n/a	n/a	0.062	0.042	Y	0.61	Y
6	4	Not tested	n/a	n/a	0.064	0.042	Y	0.68	Y
7	4	Not tested	n/a	n/a	0.061	0.041	Y	0.61	Y
16	4	3 dia.	0.11	520	0.062	0.041	Y	1.78x1.37	Y
17	4	3 dia.	0.12	560	0.058	0.041	Y	1.86x1.4	Y
18	4	3 dia.	0.15	560	0.064	0.039	Y	1.82x1.21	Y
27	4	Not tested	n/a	n/a	0.062	0.040	Y	0.61	Y
28	4	Not tested	n/a	n/a	0.064	0.040	Y	0.61	Y
29	4	Not tested	n/a	n/a	0.061	0.041	Y	0.64	Y
38	4	3 dia.	0.09	360	0.062	0.041	Y	1.1	Y
39	4	3 dia.	0.11	420	0.058	0.040	Y	1.25	Y
40	4	3 dia.	0.105	300	0.064	0.040	Y	0.99	Y
1A	(a)	none	n/a	n/a	0.062		Y	1.06x2.85	Y
12A	(a)	none	n/a	n/a	0.06		Y	1.21x2.88	Y
13A	(b)	none	n/a	n/a	0.061		Y	7.6x4.22	Y
14A	(b)	none	n/a	n/a	0.062		N	???	N
15A	(a)	none	n/a	n/a	0.065		Y	1.02x0.99	Y

(1) effect of rear surface material removal

(a) edge delamination by forced wedge insertion

(b) flange disbond by forced wedge insertion

3.8 Impact Damage

3.8.1 Equipment and Damage Types

The instrumented drop-weight impact test facility was used to introduce impact damage. The system installed at IAR is a Dynatup Model 8200 drop-weight impact system (drop tower) with GRC 730-I data acquisition and analysis instrumentation manufactured by General Research Corporation. The drop tower was modified by increasing the size of the base plate and raising it off the floor to accommodate the positioning of the test specimens. The specimens were fixed in their test position by wedges between the base plate and the specimen. This configuration also allowed for the positioning of the drop tower directly on very large specimens. A selection of indentor tip shapes is available. In this project both 0.5 and 1.0 inch (12.7 and 25.4 mm) diameter spherical tips were used.

Most of the tests involved IAR-built stiffened panels described earlier. Four damage situation sites were selected for impact damage introduction as shown in **Figure 9**. The situation types described below are identical to those used in the delamination and debonding study with the addition of damage situation type 2.

- Type 1 situation sites were centered on the skin over the stiffener.
- Type 2 situation sites were centered on a web section of the stiffener.
- Type 3 situation sites were centered over the flange of the stiffener web. Impacts at Type 3 situation sites were intended to produce disbond damage between the flange and the skin.
- Type 4 situation sites were centered on the skin between stiffeners.

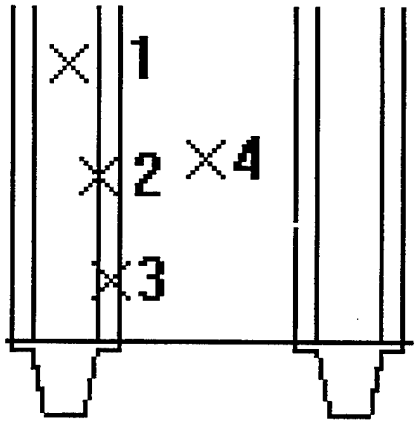

Figure 9: Impact Damage Situation Types

The test sites were located so that the damage from one site would not extend into another. The sites were planned with the aid of a diagram for each specimen and the locations were marked temporarily on the surface for alignment. A typical damage site map is shown in **Figure 10**.

STIFFENED PANEL DAMAGE and LOCATION

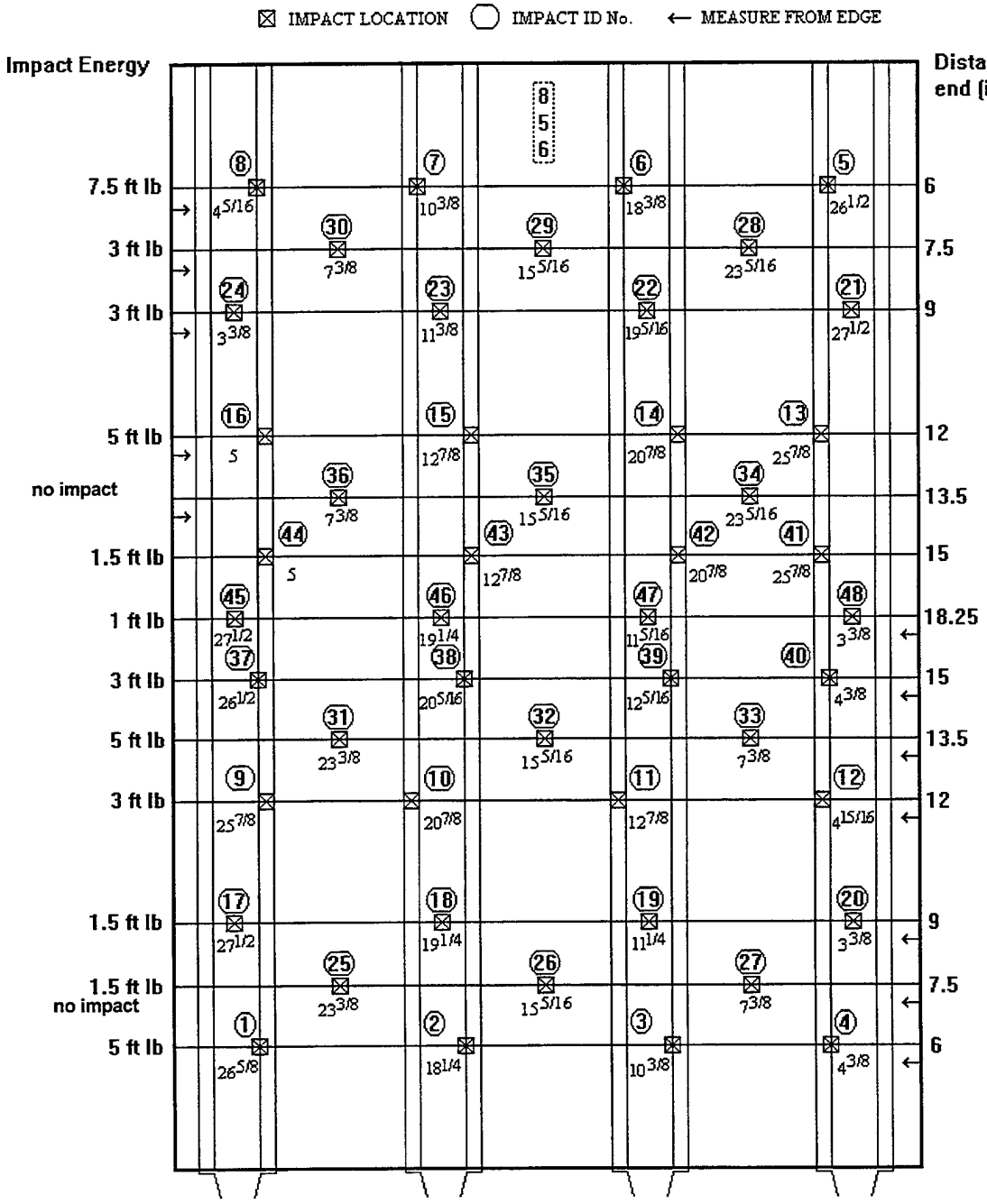

Figure 10: Typical Impact Damage Site Map, Panel 856

3.8.2 Summary and Analysis of Impact Damage

Four stiffened panels were used in the assessment of DAIS-500 impact damage detection capability: panels 856 and 860 were of thin 12 ply construction while the panels 867 and 869 were 48 ply thick. Panels 856 and 867 are made of AS4/3501-6 while panels 860 and 869 are made of IM7/5250-4.

Each panel was subjected to impact damage according to a damage site plan (see **Figure 10** for the plan for panel 856). Subsequent to impact damage panels were inspected with the DAIS-500 and C-scan. A typical DAIS-500 image with impact damage indications is shown in **Figure 11**.

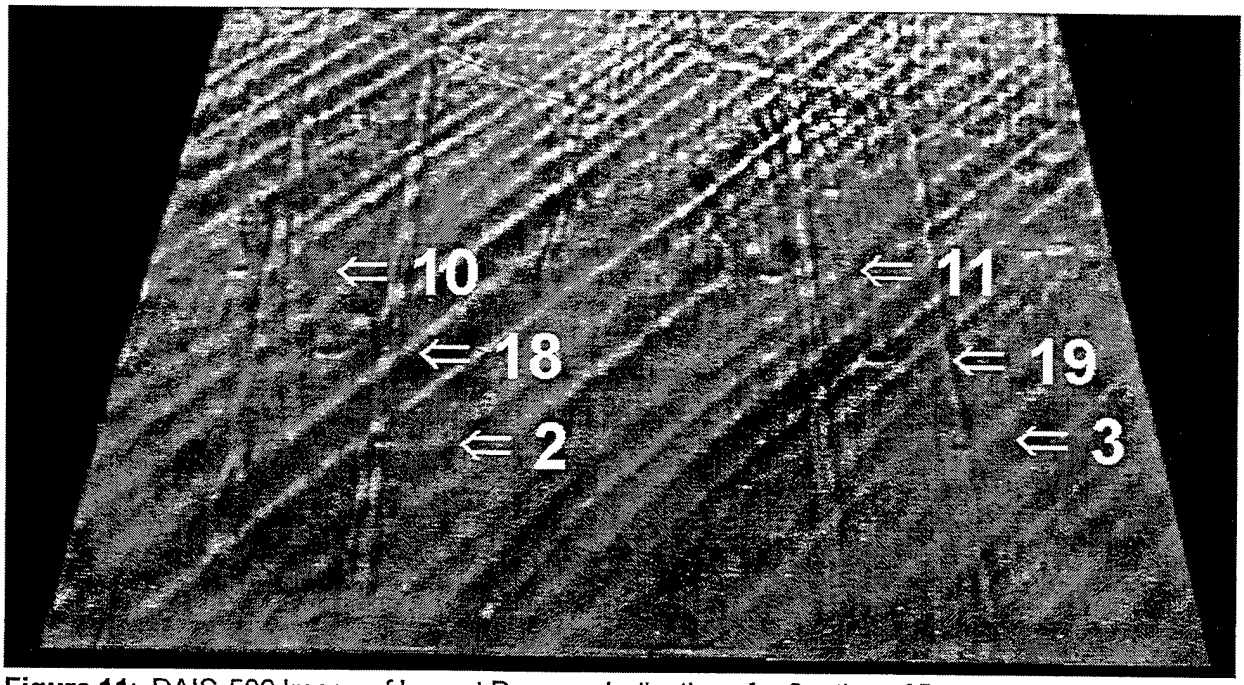

Figure 11: DAIS-500 Image of Impact Damage Indications for Section of Panel 856. The numbers correspond to the damage sites in **Figure 10**.

Table 9 is typical of tables prepared for these panels. It combines the information on impact location, energy, indent depth, largest dimension of damage as measured in a C-scan and an indication on *D SIGHT* inspection result (detected or not using DAIS). Complete data can be found in [3]. Over 178 individual impact events were generated. The results from all panels are summerized in **Table 10** and **Figure 12**.

Table 9: Test Matrix and Inspection Results, Panel 856. [D=detected, N=not detected]

Impact		Impact Energy		Load (lb.)	Indent Depth (in.)	Paint	C-Scan	*D SIGHT*
Site No.	Situation Type	Plan (ft lb)	Test (ft lb)			light (lt) dark (dk)	(inch) D/N	DAIS-500 D/N
45	1	1	1.01	310	0.001	dk	0.49	D
46	1	1	1.04	327	0.001	dk	0.49	D
47	1	1	1.03	350	0.001	dk	0.44	D
48	1	1	1.04	347	0.001	lt	0.59	D
17	1	1.5	1.69	419	0.002	dk	0.64	D
18	1	1.5	1.68	437	0.002	dk	0.64	D
19	1	1.5	1.65	424	0.002	lt	0.59	D
20	1	1.5	1.67	411	0.002	lt	0.54	N
21	1	3	3.17	439	0.015	dk	0.49/1.9	D
22	1	3	3.17	468	0.007	dk	0.49/1.8	D
23	1	3	3.17	437	0.012	dk	0.73/2.0	D
24	1	3	3.14	424	0.012	lt	1.0/2.0	D
37	2	3	2.97	766		dk	N	N
38	2	3	2.98	1597.92		dk	N	N
39	2	3	3.01	1233.6		dk	N	N
40	2	3	2.99	848		lt	N	N
1	2	5	5.13	1060	0.002	dk	N	D
2	2	5	5.1	1534	0.001	dk	N	D
3	2	5	5.13	1555	0.001	lt	N	D
4	2	5	5.1	650	0.001	lt	N	N
5	2	7.5	7.56	1869	0.006	dk	0.44	D
6	2	7.5	7.56	1548	0.005	dk	0.39	D
7	2	7.5	7.59	1663	0.004	lt	0.34	D
8	2	7.5	7.53	1256	0.003	lt	0.78	D
41	3	1.5	1.56	327		dk	N	N
42	3	1.5	1.55	488	0.001	dk	0.93	D
43	3	1.5	1.56	398	0.001	dk	0.83	D
44	3	1.5	1.56	319		dk	N	N
9	3	3	3.22	423	0.001	dk	0.73	D
10	3	3	3.19	545	0.002	dk	1.37	D
11	3	3	3.2	487	0.001	dk	1.13	D
12	3	3	3.2	449	0.001	lt	1.32	D
13	3	5	5.21	489	0.001	dk	0.98	D
14	3	5	5.21	689	0.004	dk	1.17	D
15	3	5	5.26	697	0.005	dk	1.57	D
16	3	5	5.24	463	0.001	lt	0.88	D
25	4	1.5	1.59	235		dk	N	N
26	4	1.5						
27	4	1.5						
28	4	3				dk	N	N
29	4	3				dk	N	N
30	4	3				lt	N	N
31	4	5	4.93	131	0.007	dk	2.0	D
32	4	5	4.99	121	0.007	dk	2.5	D
33	4	5	4.96	118	0.005	lt	2.0	D
34-36	4							

Table 10: Number of impact events per site type and number of sites detected using various NDI methods

Panel	Site Type	Total Impacts	Total C-Scan	Total dent	Total damage C-Scan+dent +DAIS 500	**DAIS-500 detected**	DAIS-500 Confirmed by C-Scan	DAIS-500 Confirmed by Dent	DAIS-500 Not detected by C-scan	C-Scan Not detected by *D SIGHT*	C-S or DAIS not detected by dent
856	1	12	12	12	12	**11**	11	11	0	1	0
856	2	12	4	8	8	**8**	4	8	4	0	0
856	3	12	10	10	10	**10**	10	10	0	0	0
856	4	7	3	3	3	**3**	3	3	0	0	0
860	1	12	12	12	12	**12**	12	12	0	0	0
860	2	12	3	8	10	**10**	3	8	7	0	2
860	3	12	9	8	10	**8**	8	8	0	1	1
860	4	9	3	3	3	**3**	3	3	0	0	0
867	1	13	9	9	9	**9**	9	9	0	0	0
867	2	16	0	8	10	**4**	0	2	4	0	0
867	3	15	10	10	10	**7**	7	7	0	3	0
867	4	9	6	5	6	**5**	5	5	0	1	0
869	1	12	10	10	10	**10**	10	10	0	0	0
869	2	8	8	8	8	**2**	2	2	0	6	0
869	3	8	8	7	8	**5**	5	5	0	3	1
869	4	9	6	7	7	**4**	4	4	0	2	1
	Total	**178**	**113**	**128**	**136**	**111**	**96**	**107**	**15**	**17**	**5**

DAIS-500 inspection produced 4 false calls.

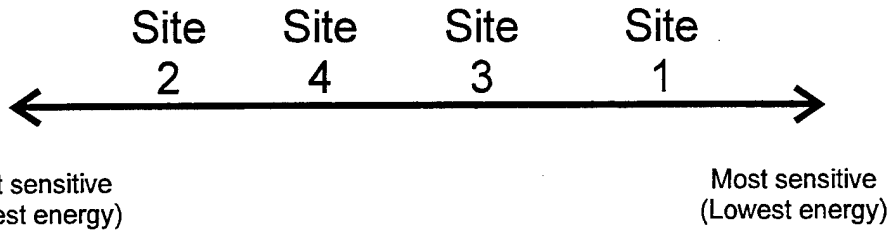

Figure 12: Site type sensitivity to impact damage as measured by impact energy required to generate *D SIGHT* detectable damage

Based on data on inspection results for each panel the largest impact energy required to produce *D SIGHT* detectable damage was at situation type 2 (over the web of the stiffener - **Figure 9**). C-Scan indications for this situation type were also small and generally *D SIGHT* indications were observed before C-Scan damage was reported. Situation type 1 (at the center of the stiffener - **Figure 9**) required the least energy to produce detectable damage. Situation type 4 (mid-bay between stiffeners - **Figure 9**) required less energy than situation type 2 but more than situation type 3 (over the stiffener flange). This "impact energy vs. situation scale" was the same for both panel materials and while the energy required for thicker panels was obviously larger, the scale was the same (**Figure 12**). Since the highest reductions in panel compressive strength were observed for panels impacted at mid-bay, the fact that at these situations smaller dents could be expected should be considered in future studies of stiffened panels [5].

Table 10 summarizes some of the data presented for each panel individually. When conducting the analysis it should be kept in mind that the impact energies used in the stiffened panel tests were intentionally small. The aim was to generate damage which would allow an evaluation of the DAIS-500's threshold of detection capability. Thus out of 178 impacts only 136 have produced detectable damage (either through C-Scan (113 calls), dent (128 calls) or DAIS-500 (111 calls)). The DAIS-500 inspection took place several months after the impact events and dent measurements took place. Because of this time lag and the dent relaxation effects (see section 3.8.3), there are 21 (out of 128) sites where dents were not detected with DAIS-500, but were observed just after impact. It should be noted that some dents were extremely small and could be located only with DAIS.

Impact indentation produces a very distinct *D SIGHT* signature which is rather easily distinguished from *D SIGHT* signals originating from other surface perturbations (compare Fig.11 and Fig 6). This observation is supported by the fact that only 4 false calls (out of 115) were produced during stiffened panel DAIS-500 inspections (a false call rate of 3.5%). In some of the more significant impacts, apart from the dent *D SIGHT* signature, the delamination signature could also be observed. This further facilitates impact damage identification.

In **Table 10** it can be seen that in panels 856, 860 and 867 situation 2 impacts resulted in 15 impacts detectable with DAIS-500 but not identified as damaged on C-Scans. This is partly related to the rigid support provided in this situation by the web of the stiffener and the difficulty of performing C-Scan inspections in this area. When situation 2 is excluded from consideration, then the remaining 82 DAIS-500 calls were all confirmed by C-Scan.

At lower impact energies, such as 10 to 15 ft-lb or 13.6 to 20.4 J, impact dents in IM7/5250-4 panels are about 30% smaller while C-Scan damage size is comparable. At higher energies over 50 ft-lb or 68 J, the dent depths in IM7/5250-4 are less than 50% of the dent depths in AS4/3501-6 panels of the same thickness and construction.

Current certification requirements for composites are driven by impact visibility or barely visible impact damage which is measured by impact dent depth. Thus for certification purposes, IM7/5250-4 structures have to be subjected to much higher impact energies resulting in higher damage levels than AS4/3501-6 structures. A 0.014 in (0.36 mm) deep dent required 30 ft-lb (41 J) impact in AS4/3501-6 versus 50 ft-lb (68 J) in IM7/5250-4. It is postulated that the application of DAIS with its better than visual inspection sensitivity could lead to certification for composites based on impact cumulative probability of occurrence. This would lead to structures being subjected to the same impact energy levels independent of the material from which they were fabricated. The ultimate benefit of this approach is increased design strain levels and lighter structures.

The largest C-Scan observed damage without *D SIGHT* indications in 12 ply panels was 0.8 inch (20 mm) diameter (situation 3). In the 48 ply panels this damage was 0.96 in. (24 mm). The indent depths could not be measured reliably using a dial gauge for some *D SIGHT* detected impact sites (below 0.001 inch or 0.025 mm). The barely visible threshold (1 to 2.5 mm deep dent) required currently for certification purposes can only be reached through much higher energy impacts (over 50 ft-lb or 68 J for the 48 ply skins) severely degrading structure strength. Based on an in-service survey reported in [6], the cumulative probability of occurrence of a 60 J impact is less than 0.01. From this it also follows that current structures, while providing the ability to sustain rather severe impact damage, are often heavier than they would need to be in an operational scenario if *D SIGHT* inspections were available and performed regularly. A trade-off study may establish the cost and operational benefits of operating lighter aircraft structure requiring DAIS deployment with possibly more frequent minor repairs against those of operating heavier, less efficient structures. Such a study would be of immediate use in light of the weight problems of some widely publicized programs such as the V-22.

A study to assess the possibility that two adjacent impact events, both below the BVID threshold, may reduce the strength of a composite primary structure to below the required residual strength (limit load) would be beneficial. No such studies were published in the open literature.

The threshold of *D SIGHT* detection might be affected by general surface conditions (i.e. noise level). The surfaces of the stiffened panels were not perfectly smooth. In actual aircraft structures both smoother and coarser surfaces can be found. No effect of the camouflage paint scheme texture or color was observed on impact damage detectability in this study.

3.8.3 Impact Indent Relaxation

Several impacts were performed on stiffened panels with the aim of monitoring indent depth evolution with time. Because most impacts in the panels were performed at very low energy levels aimed at establishing the threshold of detection for DAIS 500 these often have resulted in indent depths at the limit of practical depth measurement with a dial gauge. Other methods of measurement (i.e. Shadow Moiré) were deemed too cumbersome for use on a large number of indents. Thus, in the relaxation study somewhat larger impact energies were selected. This was also done in order to demonstrate that the relaxation occurs in the generally accepted BVID (Barely Visible Impact Damage) zone of indent depths (0.05 to 0.1 inch - 1.2 to 2.5 mm).

Impacts were limited to site types 1 and 4. The tests results are presented in **Table 11**. Indent reductions of over 30% of the original depth were measured. This is similar to the reductions reported by the authors earlier using simple coupon specimens. However, in this study, only the factor of time is included. Larger reductions could be expected if the panels were exposed to cyclic loading, temperature and humidity.

The data in **Table 11** show that impacts which initially are above BVID can relax below that level. Since most aircraft structures in service today have been certified without taking account of this phenomenon, it is possible that critical damage may remain undetected for an extensive period of time seriously degrading residual strength in certain number of these structures.

The magnitude of the observed reductions indicates that indent relaxation must be accounted for in damage tolerance tests of composite structures.

The larger impact energies used in this part of the project provided further evidence that IM7/5250-4 requires higher impact energies to create indents with a depth equal to those observed in AS4/3501-6 panels.

Table 11: Impact Indent Depth Reduction Measurements

Test No.	Site Type	Load (ft-lb)	Damage C-Scan (inch)	Indent Depth (inch)						% Change	Note
				1	2	3	4	5	6		
856-49	1	4.86	0.84	0.053	0.053	0.053		0.045	0.04	25	BTP
856-52	1	5.16	0.91		0.075	0.075		0.058	0.059	21	BTP
856-31	4	4.93	2	0.01	0.009	0.009	0.008	0.007	0.006	40	
856-32	4	4.99	2.2		0.019	0.018	0.018	0.017	0.014	26	
856-33	4	4.96	1.9			0.012	0.008	0.008	0.008	33	
856-34	4	7.71	0.77x5.0			0.081		0.07	0.07	14	BTP
860-49	1	4.49		0.019	0.018	0.018	0.018	0.014	0.014	26	
860-50	1	5.17			0.034	0.032	0.032	0.029	0.028	18	
860-51	1	5.09				0.009	0.009	0.009	0.009	0	
860-52	1	5.06					0.03	0.023	0.022	27	
860-54	4	7.71	0.70	0.005				0.003	0.003	40	
869-41	1	20.06	2.6x1.5	0.011				0.01	0.01	9	
869-42	1	25.4	2.9x1.5	0.014				0.011	0.011	21	
869-45	1	45.54	3.9x1.5	0.021				0.019	0.013	38	BTP
869-46	1	56.72	3.9x1.5	0.043				0.039	0.034	21	BTP
869-43	4	30.08	1.9	0.01				0.006	0.006	40	
869-44	4	51.05	3.3x4.4	0.014				0.013	0.013	7	BTP
869-47	4	60.73	4.6x5.1	0.015				0.015	0.015	0	
867-57	1	20.4	2.4x1.5	0.014				0.01	0.009	36	
867-58	1	25.26	3x1.5	0.02				0.016	0.013	35	
867-60	1	45.52	3x1.5	0.104				0.102	0.086	17	BTP
867-35	4	30.38	3	0.015				0.012	0.01	33	
867-37	4	50.93	2.7	0.062				0.062	0.058	6	BTP

Columns 1 to 4 are measurements taken immediately after each (successive) impact
Column 5 -12 hours after impact
Column 6 - 24 hours after 5
C-Scan damage - diameter or rectangular dimensions shown
BTP - broken top plies

3.9 Radome

In the early stage of the project, a field trip to Tinker AFB had involved the Experimental DAIS 500 inspection of the surface of the E-3 AWACS rotodome outer surface. Later a flat specimen was provided by Boeing to IAR. The specimen was 14.5 in wide, 47 in long and 2 in thick, (368 x 1195 x 49 mm). The specimen was of a sandwich construction, honeycomb core with composite skins. The outside surface skin had a rubber coating. This specimen had received nine repairs ranging from 0.5 to 1.25 inches in diameter, (12.7 to 31.75 mm). Only two of the repairs were through the thickness and in both these instances the dimpled rubber outer covering was not replaced. Unspecified damage was introduced into the specimen at WL prior to shipment of the specimen for *D SIGHT* inspection. No additional damage was introduced intentionally at IAR. The specimen was inspected with both C-Scan and *D SIGHT*.

The ultrasonic C-Scan of this specimen could not detect the repaired areas or any other damage. This was apparently because of highly attenuating nature of the rubber coating. The black, pebbled, rubber outer surface had proved difficult to highlight with a liquid on the rotodome. *D SIGHT* images were taken of the specimen using a laboratory setup with both a "point" and "broad" or extended light source. A broad source is more diffuse and decreases the sensitivity to high frequency noise and fine features. The point light source was set up at a shallower angle.

The repairs on the panel can be seen in ambient light, because of differences in color. The "point" source *D SIGHT* setup was very sensitive to the skin waviness but only one site was marked as a possible defect indication. The broad light source setup seemed to be able to pick-up the same indication site plus two other sites. All suspect sites are marked in the *D SIGHT* images shown in **Figure 13** and **Figure 14**.

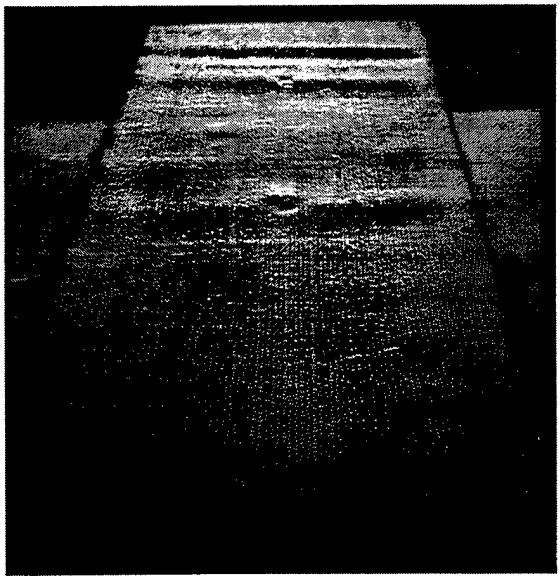

Figure 13: Radome under point source lighting with suspected indications marked by an arrow

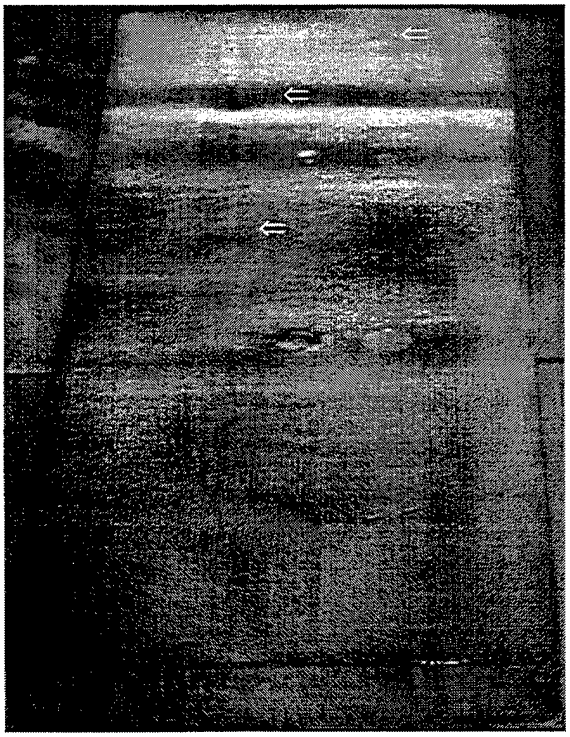

Figure 14: Radome under broad source lighting with suspected indications marked by an arrow

Although the inner surface of the rotodome may not be inspected under in-service conditions, the inner surface of the specimen was imaged in the laboratory. In addition to the repair sites, possible impact damage sites were detected.

D SIGHT inspections of the two sides of the radome specimen revealed that some perturbations on the specimen surface were not detected with the "point" light source setup. Results of *D SIGHT* inspections should be compared with known defect sites by the personnel who performed the damage introduction work.

3.10 F-16 Horizontal Stabilizer

3.10.1 Predamage Inspection and Damage Introduction

A complete horizontal stabilizer from a USAF F-16 aircraft was provided to IAR. No information was available on the composite skin material lay-up or variations in construction throughout the specimen; however, it was evident that it represented an older type honeycomb core with graphite/epoxy skin construction. The specimen had been repaired in a number of locations on the lower surface. The decision was made to perform NDI tests in an attempt to document any existing damage and to develop NDI procedures which would be used after damage was introduced at IAR. The C-scan revealed variations in skin thickness, repairs and some areas of lower transmissivity. No areas showing skin to core disbonding were evident (see **Figure 15**).

Each damage site was documented, just prior to damage introduction, with the experimental DAIS 250C. This helped to further document some repairs in the lower surface. The upper surface was found free of significant damage. In some areas (i.e. around the pivot) the surface was found to be unusually rough making damage detection difficult.

A radiographic inspection was carried out prior to damage introduction at QETE/DND. The damage site map, **Figure 16**, shows how the upper surface was divided into 16 zones. These zones represent the coverage and identification of the X-ray exposures, (nominally 12 x 17 inches (30.5 x 43.2 cm)). X-rays did not indicate any damage other than the areas of repair identified through the C-Scan and *D SIGHT* inspections.

Five types of damage were selected for introduction into the specimen upper surface. The drop tower impact test facility was used to introduce impact damage at 13 locations with energies ranging from 3.82 to 32.04 ft-lb, (5.18 to 43.44 Joules). Impact No. 1 was conducted with a 0.5 inch (12.7 mm) diameter indentor. This impact, at 5.47 ft-lb (7.32 Joules), resulted in a near penetration of the skin. All subsequent impacts were carried out with a 1 inch (25.4 mm) diameter spherical tip indentor. The remaining damage events were uninstrumented and carried out manually.

At three sites an access hole was drilled through the lower surface skin. A metal probe was inserted into one cell of the honeycomb core and the upper skin was disbonded from the core by forcing the specimen down onto the stationary probe. The DAIS 250C inspection head was located over the site to monitor the damage growth.

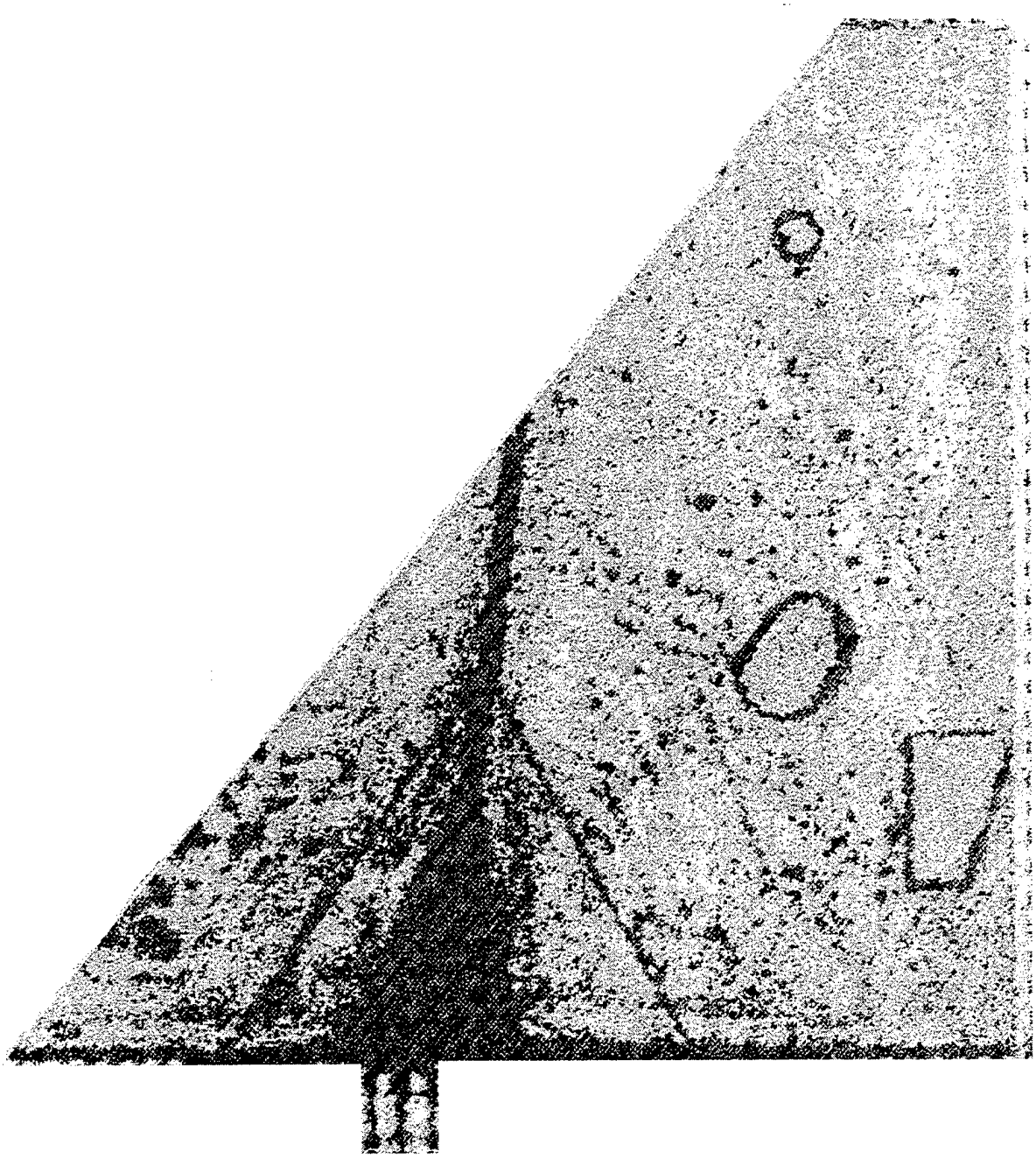

Figure 15: C-scan of F-16 Horizontal Stabilizer as Received

Hammer drop tests were carried out at two sites. This was a simulation of a tool-drop event. A standard ball-peen hammer, (2.5 lb/1.12 kg) was dropped from a height of three feet (0.3 m) onto the upper surface.

To simulate foreign object damage (FOD) at an oblique angle the ball-peen hammer was used to strike the upper surface. Four tests were carried out. A mylar sheet was placed over the upper surface to prevent the hammer from marking the paint.

At the leading edge there is a metal edge protector. The leading edge was struck with the hammer and the area was inspected for damage on both the upper and lower surfaces.

Seven location types were selected for damage introduction. The sites were selected to take advantage of the variation in core thickness, internal structure and repaired areas (see **Table 12**)

Table 12: Description of F-16 Site Type Locations

Type	Description
1	Leading and trailing edges
2a	Repaired, thin section, core and lower skin replaced
2b	Repaired, thick section, core and lower skin replaced
3	Thick section, composite skin/al honeycomb core, original condition
4	Central joint, composite skin/al honeycomb splice
5	Pivot root, composite skin over solid metal
6	Thin section, composite skin/al honeycomb core, original condition

Damage was introduced at 23 sites on the upper surface of the specimen. The damage sites are identified by making use of the X-ray zone numbers (1 to 16) in **Figure 16**.

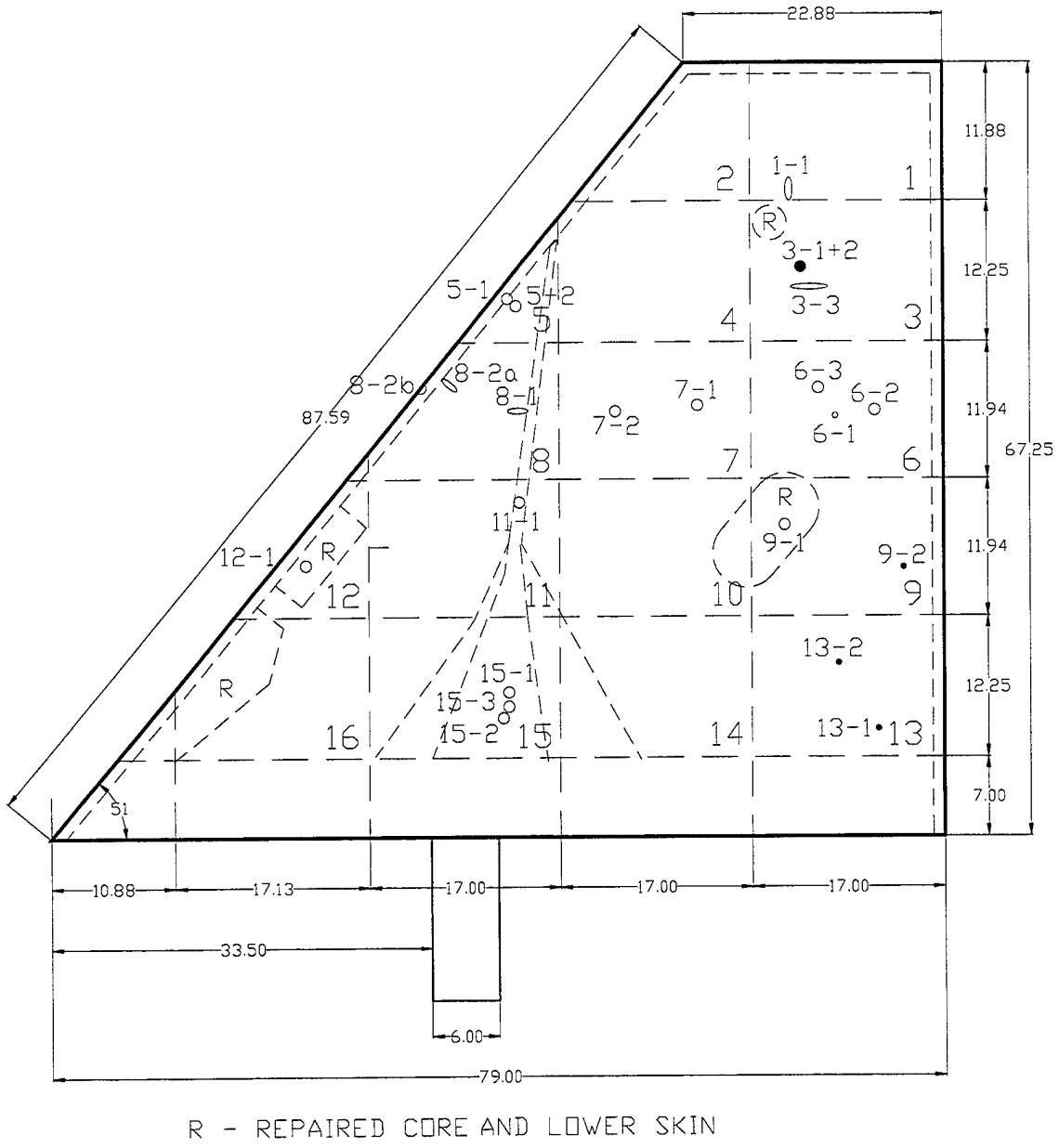

Figure 16: F-16 Damage Site Map and X-ray Inspection Zones

3.10.2 Postdamage Assessment

A posttest C-scan inspection was carried out in the same manner as the pretest inspection. The resolution of the inspection was not suitable to discriminate the damage caused by any of the tests (see **Figure 17**). A more detailed inspection using portable C-Scan equipment in pulse-echo mode did not provide definitive results as the technique could not discriminate damage from the variations in adhesive layer thickness between the thin composite skin and aluminum honeycomb core.

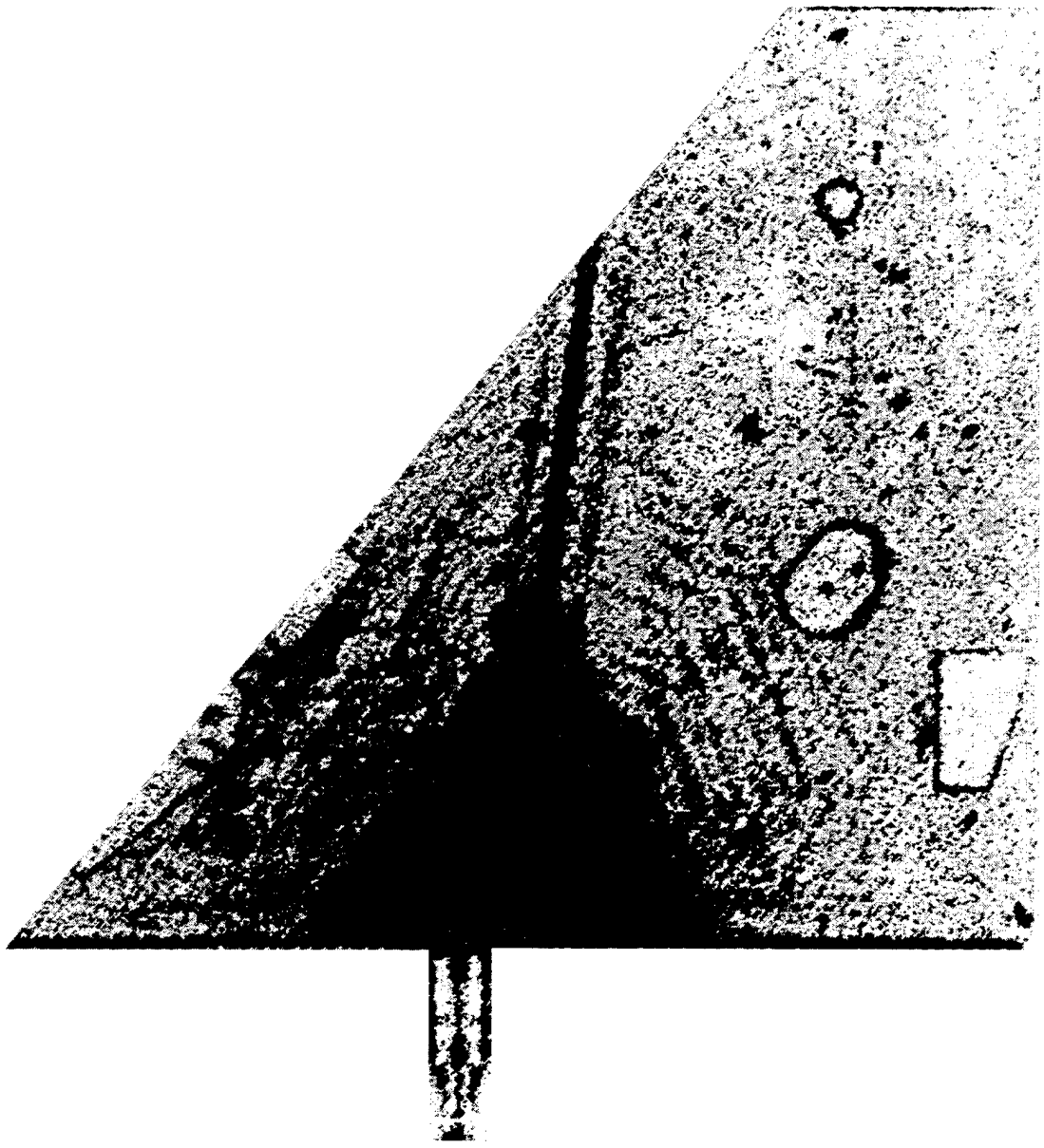

Figure 17: C-Scan of the F-16 Stabilizer after Damage Introduction

A radiographic inspection was carried out after all of the tests were complete. The posttest radiographs were identified in the same manner as the pretest exposures. The results are summarized in **Table 13**.

All of the damage sites were inspected with the DAIS 250C immediately after damage introduction. The stabilizer was inspected with DAIS 500 prototype once the system became available. The DAIS 500 images were analyzed by an inspector without prior knowledge of implanted damage type and location. The results are summarized in **Table 13**.

3.10.3 Discussion of Results

The X-ray images taken prior to testing were used to define repaired areas and changes in construction within the specimen. They were also used to plan the damage introduction sites. The X-ray images from prior to and after damage introduction tests were directly comparable. The X-ray film visual inspection results are contained in **Table 13**. Test 1 used a 0.5 inch (12.7 mm) spherical tip on the drop tower and resulted in a near penetration of the composite skin yet no evidence of damage to the core appears in the X-ray. Test 5, carried out with an inch (25.4 mm) diameter tip does show slight evidence of crushed honeycomb core. The three skin disbond tests, (14, 15 and 16), each showed damage to the core material. The leading edge impact in Test 23 resulted in only a subtle marking on the metal insert and no apparent damage to the core material.

The squirter system ultrasonic C-Scan inspections covered the entire specimen. The predamage C-scan and X-ray information was used to revise the C-Scan settings to improve damage resolution. Thus the predamage and postdamage inspection images were considerably different. In spite of this the C-Scans of the full stabilizer could not provide suitable resolution or comparative details to allow the determination of changes as a result of the damage introduction tests. Subsequently portable ultrasonic C-Scan system was used, at various damage sites, but without success. It is expected that further attempts could have produced more positive C-Scan results; however, as with the stiffened panels, the aim was to generate data on the threshold of detection for *D SIGHT* and not to improve C-Scan inspection procedures.

DAIS 500 inspection produced more calls than installed damage sites. These can not be regarded as false calls as X-ray and C-Scan procedures were not capable of detecting most of the introduced damage. It should be noted; however, that all confirmed damage sites (X-ray post-damage inspection) were identified with DAIS 500. As well all DAIS 250C isolated damage locations (using DAIS 250C smaller field of view) were also found by the inspector using DAIS 500 prototype.

Table 13: Test Matrix and Inspection Results of Damage

DROP TOWER IMPACT DAMAGE

TEST No.	IMPACT ZONE	ZONE TYPE	DROP TOWER		*D SIGHT* IMAGE	DAMAGE DETECTION			
			TIP DIA. (in)	FORCE (ft-lb)		DAIS 250C (D/T/N)	DAIS 500 (D/T/N)	X-ray (D/Dc/N)	C-SCAN (D/N)
1	6	6	0.5	5.47	6-1	D	D	N	N
2	7	3	1	5.36	7-1	D	D	N	N
3	15	5	1	5	15-1	N	N	N	N
4	11	4	1	10	11-1	D	D	N	N
5	6	6	1	5.25	6-2	D	D	Dc	N
6	6	3	1	3.8	6-3	D	D	N	N
7	9	2b	1	3.84	9-1	D	D	N	N
8	7	3	1	3.82	7-2	D	D	N	N
9	5	1	1	4.51	5-1	N	N	N	N
10	5	1	1	3.78	5-2	D	D	N	N
11	12	2a	1	3.91	12-1	D	D	N	N
12	15	5	1	15.82	15-2	T	N	N	N
13	15	5	1	32.04	15-3	T	N	N	N

OTHER DAMAGE

TEST No.	IMPACT ZONE	ZONE TYPE	DAMAGE TYPE	*D SIGHT* IMAGE	DAMAGE DETECTION			
					DAIS 250C (D/T/N)	DAIS 500 (D/T/N)	X-ray (D/Dc/N)	C-SCAN (D/N)
14	13	6	skin/cell disbond	13-1	D	D	D	N
15	13	6	skin/cell disbond	13-2	D	D	D	N
16	9	6	skin/cell disbond	9-2	T	N	D	N
17	3	6	hammer drop	3-1	D	D	N	N
18	3	6	hammer drop	3-2	D	D	N	N
19	1	6	FOD	1-1	D	D	N	N
20	3	6	FOD	3-3	D	D	N	N
21	8	3	FOD	8-1	D	D	N	N
22	8	1	FOD	8-2a	D	D	N	N
23	8	1	leading edge	8-2b	D	D	Dc	N

D - Detected

N - Not detected

Dc - Detected by comparison of before and after X-rays

FOD - Foreign Object Damage

3.11 Conclusions

3.11.1 Delaminations and Disbonds

A new method of controlled delamination and disbond introduction in composites was developed.

DAIS 500 was shown to be capable of detecting delaminations and disbonds in locations where residual stress released when the damage was created have been significant enough to produce surface perturbations. Applicability of DAIS for these types of damage NDI will depend on particular structure and knowledge of what constitutes significant damage.

Image enhancement and analysis methods should be considered for *D SIGHT* delamination detection.

3.11.2 Impact Damage

DAIS 500 ability to detect impact damage at very low impact energy levels is comparable to ultrasonic C-Scan (113 vs. 111 calls).

In F-16 horizontal stabilizer DAIS 500 detected 20 out of 23 damage sites. Very low level of damage introduced at IAR in order to test DAIS 500 threshold of detection capability proved in most cases too low for X-ray (5 out of 23) and ultrasound techniques used (none detected).

Very low false call rate in impact damage detection was observed with DAIS 500 (3.5%).

Extent of impact damage (C-Scan signature and indentation) in stiffened panels depended largely on the location of impact vs. stiffener position.

Significant differences were observed in the response to impact between the AS4/3501-6 and IM7/5250-4. The same energy impact produced indents 30% to 50% less deep in IM7/5250-4 panels. In order to generate indent of the same depth in both systems nearly 70% higher energy was required in IM7/5250-4.

Incorporation of DAIS systems into composite aircraft structures NDI could open a new approach to certification based on cumulative probability of impact occurrence rather than on BVID requirement. Significant structural weight savings should be possible.

3.11.3 Impact Dent Relaxation

Impacts which initially are above BVID limit can relax below that level. Since most aircraft structures in service today have been certified without taking account of this phenomenon, it is possible that critical damage may remain undetected for extensive period of time seriously degrading residual strength of these structures.

The magnitude of observed reductions (over 30%) indicates that indent relaxation must be accounted for in damage tolerance tests of composite structures.

4 HIGHLIGHTER SELECTION

4.1 Introduction

The process of inspecting a surface with *D SIGHT* relies on two reflections of light off the surface. The specular component of these reflections must be high or else the diffuse scatter component prevents the formation of the primary signature on the retroreflector with sufficient clarity to *D SIGHT* properly. When the surface is not naturally reflective, it can be made artificially reflective by applying a thin liquid coating called a highlighter that decreases the diffuse scatter and increases the specular reflection. Surfaces with high reflectivity are usually called "glossy." The type of liquid used and its properties along with the condition of the surface determines the extent to which the surface reflectivity can be improved from its natural state.

Besides the reflectivity issue, the properties of the highlighter also impact other important issues such as the health and safety of personnel and the environment, physical effects on paint and materials, removal and disposal, and ease of application. All these factors must be considered before selecting a highlighter for a specific inspection application.

Military aircraft with composite skins are generally painted with a dull matte finish. Even when stripped of paint, composites are not sufficiently reflective enough to be inspected without highlighting. For this reason it will be necessary to find a suitable highlighter that not only works well in improving reflectivity but is also safe and user friendly.

4.2 Highlighters

4.2.1 Desirable Properties

The following list of properties are considered desirable for a highlighter and form a set of criteria to evaluate various highlighters.

1. applies easily and wets surface well without running while cutting through grime and dirt on the surface

2. settles to an even film in less than 10 seconds regardless of the skill level of the operator or the method of application

3. maintains film thickness (low evaporation rate) for a 30-minute period

4. gives all surfaces the reflectivity of mirrored glass

5. does not damage underlying paint and materials

6. washes off readily with water or leaves no residue

7. nonflammable and nontoxic with no appreciable odor

8. environmentally friendly for storage and disposal

9. low cost per application.

No single highlighter to date has been found that satisfies all these criteria. It will be necessary to determine which of these criteria are the most important in the military environment.

4.2.2 Commercial Types

Several commercial highlighters are available along with a number of commercial solvents and penetrating oils that behave like highlighters. In general, a highlighter has two competing components: a thin liquid that settles quickly and a thicker liquid that slows evaporation. Highlighters are typically liquid and remain wet during use. Glossy paint or highlighters that dry can also serve the same purpose provided their removal is easy or not important. RD-100 is a black commercial highlighter that works well for human visual inspection after it dries, but does not work well with *D SIGHT* since its sheen is too dull. It can be removed with hot water provided it does not set for an extended period of time.

Table 14 lists some known highlighting fluids and their constituent components. It has been learned that Exxsol-D-120, a sample of which was originally received from an automotive manufacturer in Europe, is not available in the United States. Despite the potential problem of availability, it will be included in the analysis.

Table 14: Commercial Highlighters

Trade Name	Components
Kroil	light penetrating oil
Progal	alcohol based degreaser
Chemlite 215	solvent highlighter
Snoflake	kerosene based highlighter
P-3 Hilite SG	glycol based highlighter
Electron	dielectric solvent
Exxsol D 120	aroma free test fuel (gasoline)

It is difficult to predict which highlighter will be effective from its physical properties on a given surface. The physics and chemical behavior of the highlighters on specific surfaces must be tried experimentally. For example, **Table 15** lists some of the important physical parameters that should be useful to evaluate the highlighter but these parameters do little to help find an acceptable highlighter.

Table 15: Physical Highlighter Properties

Highlighter	Viscosity (cps)	Surface Tension (dynes/cm)	Density (gm/cm^3)	Refractive Index
Kroil	3.6	27.3	0.860	1.468
Progal	1.1	22.2	0.750	1.417
Chemlite 215	6.3	27.6	0.820	1.455
Snoflake	1.6	25.4	0.802	1.447
P-3 Hilite SG	9.6	28.3	1.005	1.395
Electron	1.0	25.0	0.782	Unknown
Exxsol D 120	4.5	Unknown	0.820	1.450

4.3 Highlight Quality

Most of the highlighters listed above have been used in automotive applications on sheet metal and plastic skin panels. Snoflake and Chemlite 215 have also been used on military and commercial aircraft. Only Electron and Exxsol-D-120 have not been tested or used extensively as highlighters.

Judging the quality and acceptability of highlighters is difficult due to the many requirements they must satisfy. From an imaging point of view, the criteria most important relate to reflectivity and evaporation rate. Both of these interact and define a period of time that is optimal for imaging purposes. It has been found that a standard gloss meter is unacceptable to measure the reflectivity of a wet surface. As a result, Diffracto has been evaluating highlighters with a measure of reflectivity called DORRI, (Distinctness-of-RetroReflected-Image). This measure is similar to the Distinctness-of-Image (DOI) measure except that it makes use of a retroreflector. Since *D SIGHT* uses a retroreflector in the standard optical arrangement, the measurement of reflectivity incorporating a retroreflector is not only appropriate but will respond to the same surface characteristics as *D SIGHT*.

The DORRI number is a measure of light dispersion caused by the underlying surface roughness even through a transparent liquid film in a specified window of interest. A mirror finish will have a DORRI number of 100. It is known that light returning from a retroreflector to the source disperses slightly about one degree. A profile of this light distribution back at the light source has a characteristic bell-shaped intensity profile and a fixed transition slope (ie. slope at maximum rate of change of intensity). When the light reflects off a surface with increasing levels of surface roughness, the intensity profile broadens considerably reducing the transition slope because the surface roughness has increased the diffuse scatter. By comparing the transition slope of a given surface to a mirror surface, the level of diffuse scatter can be measured. The ratio of the transition slope for a surface and a calibrated transition slope of a mirror defines the DORRI number. To determine the transition slope, two images are acquired, one with the light source slightly further away from the lens than the other. The intensities at these two locations are normalized with respect to light power to form a contrast slope. It is these contrast slopes that are actually used to form the DORRI number. Diffracto's TPS (Test Plaque Station) is equipped with this

measurement ability and has been used in the tests reported here.

The performance of a highlighter can be measured with DORRI in two ways: a high DORRI number close to 100 indicates that the highlighter is creating surface reflectivity close to that of a mirror and by monitoring the DORRI number continuously over time from the moment of application, the settling time, steady-state time and evaporation rate can be determined. The effects of wiping and direction of wiping can also be evaluated.

The effectiveness of four highlighters were evaluated ranging in viscosity from 1 to 9.6. These included Snoflake, Chemlite 215, P3 Hilite, and Electron. Each highlighter was applied by hand wiping onto a sheet metal sample which was then placed in the TPS-2 for DORRI evaluation. The sensitivity to settling and reflectivity is greatest when the wiping direction is perpendicular to the optical axis of the camera. Four or more separate trials were performed for each highlighter to eliminate variations in application. **Figure 18** shows the DORRI number plotted against time. All four highlighters show lower reflectivity during the first minute after application but settle out and remain constant for at least five minutes. The steady-state level, however, differs. After 3 minutes the average steady-state DORRI reading is as follows:

Snoflake 97.0
Electron 88.1
Chemlite 215 . . . . . 87.3
P3 Hilite 71.5

These steady-state DORRI numbers are subtle indicators of highlight quality in the worst case application. Low DORRI numbers indicates that streaks may persist for a long time without settling completely. In a vertical (parallel to optical axis) wiping direction, the steady-state levels are all high and closer to each other across highlighters partly due to the fact that streaks generate micro valleys that maintain reflectivity toward the retroreflector. Snoflake shows the highest reflectivity and the least variation even when wiped across the FOV. Chemlite 215 shows the greatest variation from trial to trial. Except for P3 Hilite, which tends to be too viscous, the other three highlighters all have good reflectivity properties. Choosing between them should be based more on other factors than their ability to improve surface reflectivity.

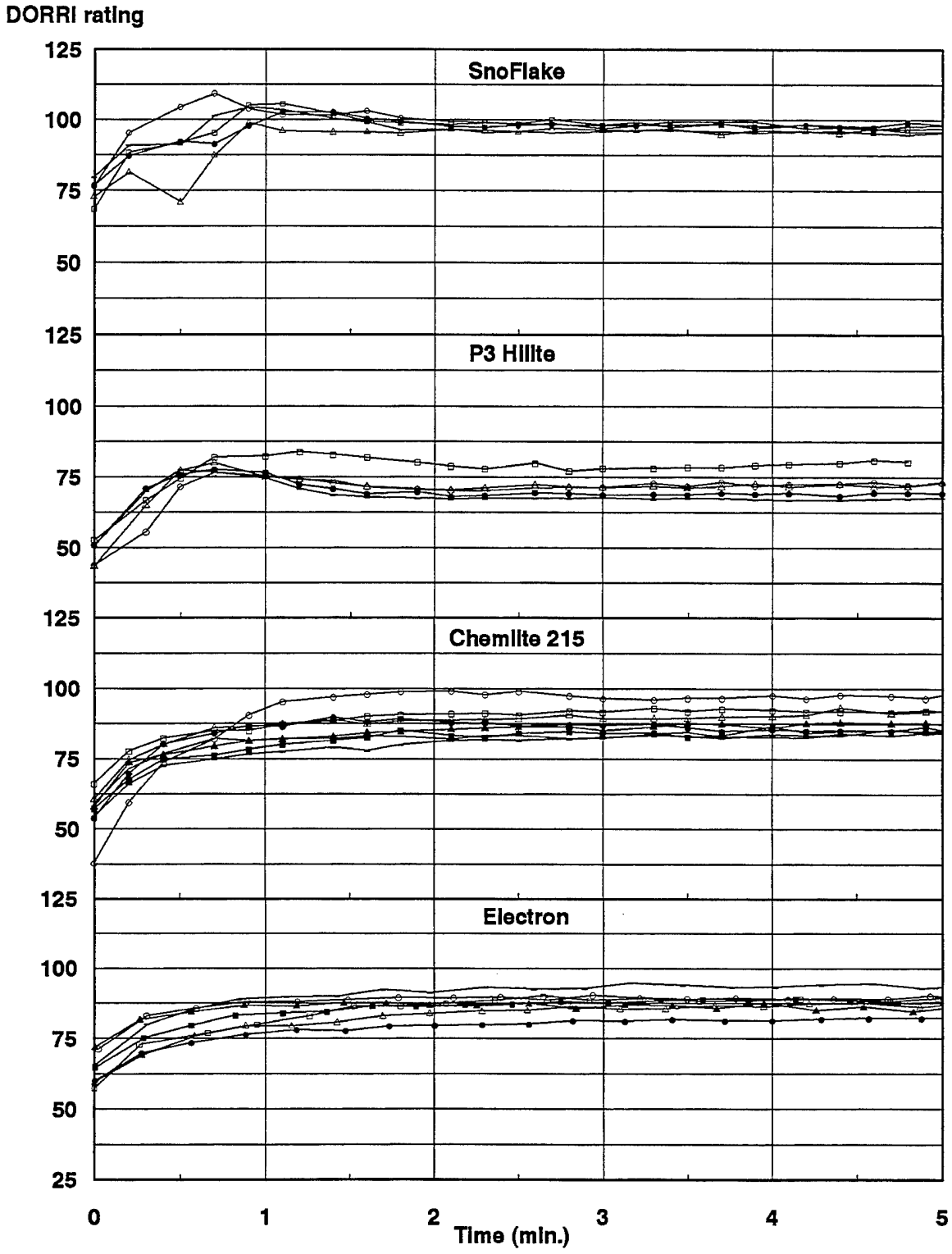

Figure 18: DORRI Reflectivity vs. Time for Different Highlighters

Table 16 summarizes known pros and cons with each highlighter and rates the highlighters from experience in lab and field use.

Table 16: Rating of Highlighters

Highlighter	Pros	Cons	Rating
Electron	- settles quickly - cuts through grime - minimal odor - environmentally safe - leaves no residue - non-reactive - non-toxic	- evaporates in 10 minutes - flash point: 147° F. - more than 5 times cost of Snoflake	1
Snoflake	- settles quickly - evaporates slowly - cuts through grime	- flash point: 146° F. - strong kerosene odor - leaves oil residue	2
Chemlite 215	- settles quickly - evaporates slowly - water soluble - no strong odor - flash point: > 200° F.	- does not cut through grime - too viscous - leaves sticky residue	3
Exxsol D 120	- no strong odor - flash point: 239° F.	- evaporates slowly - residue dries on surface	4
Kroil	- settles quickly - similar to Snoflake	- health and safety hazard - evaporates slowly - leaves oily residue - objectionable odor	5
Progal	- settles very quickly - leaves no residue	- evaporates too quickly - combustion hazard	6
P-3 Hilite SG	- no strong odour	- too viscous	7

4.4 Application Methods

There are several methods that can be used to apply highlighters (see **Table 17**). The physical properties of the highlighter can influence the choice, however, there can be other problems associated with the application method. These methods and their pros and cons are summarized in the following table.

Table 17: Highlighter Application Methods

Method	Pros	Cons
Spraying	- quick application	- high equipment cost - atomizes into fine mist - tendency to run - does not clean surface - tendency to create orange peel finish
Rolling	- non-directional finish - easy to apply	- does not clean surface - difficult to remove excess - leaves dirt and contaminates in place
Wiping	- cleans surface during wiping - possible to control fluid thickness - easy to control application area	- leaves directional streaks - difficult to find wiper material

Spraying highlighter is generally not recommended because it has a tendency to contaminate the air with a fine mist that could be explosive and a health hazard. Rolling is a good highlighting method except for the initial application. One of its major drawbacks is that it leaves dirt on the surface that shows up as noise in the image. Hand wiping with a cloth is acceptable for small areas but with large aircraft surfaces wiping with a sponge on the end of a pole is a good compromise. Wiping the surface helps to prime the surface and clean it of dirt and grime. The biggest drawback of wiping is the directional streaks that may be created depending on the wiper, technique, direction of application and highlighter properties. Streaks on military aircraft are generally not an issue due to the high initial roughness of these surfaces.

4.5 Recommendations

Although Electron has been rated first, this rating is based on its potential from lab experience rather than on extensive field experience. Its primary advantages over Snoflake relate to health and safety and the absence of a residue on the surface. Electron is also approved by USAF as a Class 2 Solvent Remover satisfying MIL-I-5135D and MIL-I-25135E specifications.

Snoflake is an excellent highlighter but is often criticized for its strong kerosene smell which is similar to JP4 jet fuel. Approval of Snoflake for use in military hangars as an NDI fluid may be extremely difficult and some air force bases have already prevented its use during demonstrations. Chemlite 215 is a good highlighter but requires that the surface be clean. The residue can be washed off with water whereas Snoflake residue must be removed with a solvent. Based on the available evidence, Electron is recommended as the highlighter of choice since it leaves no residue, is environmentally safe, cuts through grime, is nonreactive with other materials, and produces an acceptable surface reflectivity.

Because of these desirable properties, Electron should be actively used in lab and field trials to gain additional experience with its application, highlight quality for *D SIGHT*, evaporation rate, cutting ability, and operator acceptability on actual aircraft surfaces. Except for its low flash point, Electron has many of the desirable highlight properties outlined earlier in this report.

5 HARDWARE DEVELOPMENT

5.1 Sensor Optimization

The process of optimizing *D SIGHT* optical parameters involves several factors including external considerations such as weight, size, and ease of use. In this case, optimization means finding a set of parameters such as camera distance, angle, light source position and type, and retroreflector position so that the *D SIGHT* signatures of delaminations and impact have maximum visibility (i.e., sensitivity) and contrast in the image. Of particular importance to this process is the availability of impacted and delaminated samples, a physical characterization of the defective areas in terms of severity and physical indication, the types of structures and physical constraints on the inspection process, an understanding of the *D SIGHT* process and its configuration to enhance the physical indications, and the constraints on the geometry of the sensor.

To determine how well a given set of parameters performs in maximizing visibility and contrast, a set of experiments were undertaken to compare the original DAIS-500 sensor with other optical configurations. The test configurations were established from the perceived deficiencies in the DAIS-500 sensor and the knowledge of how to improve signature contrast from the understanding of the *D SIGHT* process. After the selection of an optimal configuration, a new sensor was built and tested on the impacted and delaminated samples.

5.1.1 DAIS-500 Deficiencies

The originally developed DAIS-500 sensor has already been used extensively to inspect aircraft at military hangars and outdoors on tarmacs both for inspection of impact damage as well as corrosion on lap joints. From this experience, two types of deficiencies have been observed: lack of physical ruggedness of the sensor and low contrast signatures when inspecting for delaminations or disbonds.

The ruggedness issue will be addressed during the discussion of the new sensor design. The lack of contrast issue is one reason for the need to modify the basic DAIS-500 configuration and is believed to be a result of a grazing angle that is too large for the type of physical indication created by delamination indications. Disbonds and delaminations tend to have lower spatial frequency content compared to impact damage sites so it will be necessary to improve the sensitivity to these spatial frequencies while preserving the signature response to impact damage. The DAIS-500 field of view is determined by the 32 degree grazing angle of the camera resulting in a disparity between the grazing angles at the front and back of the field of view that causes a sensitivity change. Lowering this grazing angle will improve the sensitivity change from front to back but may increase the disparity in the spatial resolution at these two extreme points. The DAIS-500 was also found to be sensitive to surface noise. A broader light source has the effect of reducing this noise but must not be broadened to the point where the signatures from impact damage are reduced significantly.

To address some of these problems, a set of optical arrangements will be configured to determine how to decrease the sensitivity change across the field of view but improve the sensitivity of the

sensor to lower spatial frequencies of delamination indications while preserving the response to impact damage sites.

5.1.2 Optimization Criteria

The goal of the optimization process for delaminations and impact damage is to change the optical parameters of the DAIS-500 sensor so that the following criteria are satisfied:

- maintain approximately the same field of view as the DAIS-500 (3.125 sq ft)
- preserve signature contrast for impact damage indications
- change the shape of the field of view from a trapezoid to a rectangular footprint for ease of placement
- decrease sensitivity disparity for a given indication along the field of view (i.e., top to bottom in image)
- increase signature contrast for low spatial frequency delamination indications
- reduce the amount of high frequency surface noise appearing in the DAIS-500 image from composite fiber/pattern read-through.

5.1.3 Design of Experiments

To address the problems of the DAIS-500 for the detection of both delamination and impact damage indications, the following parameters were changed and the resulting images evaluated:

- the base grazing angle of the camera to the surface was lowered from 32 degrees to 27 and 22.5 degrees. The sensitivity of *D SIGHT* to lower spatial frequencies increases with a decreased grazing angle of the camera. Also, the sensitivity disparity decreases due to the smaller change in solid angle from the camera to the two extreme points of the field of view.
- the distance of the retroreflector to the surface was increased from 18 inches to 22 and 30 inches. Again, as the retroreflector distance to the surface is increased, *D SIGHT* becomes more sensitive to lower spatial frequencies on the surface.
- the light source with a 1.4 inch reflector was changed to a 2 inch reflector to broaden the light source and reduce the amount of high frequency noise appearing in the image.
- a new camera was obtained with a ½ inch format and 2 stops better sensitivity to obtain greater depth of field as well as weight reduction.

5.1.4 Optimization Sample Set

The optimization of *D SIGHT* for delaminations relies heavily on acquiring a suitable and representative sample of defective specimens that can be used to fine tune the optical parameters. At present, only delaminations created in a laboratory environment are available. Specimens from actual aircraft have not been found.

Table 18 gives a list of the specimens received to date for optimization and their known delamination condition. Included in the table is the approximate size of the specimen, its surface condition and number of defects. Impact damage specimens from the DND impact detection contract will be used to verify that their signatures are not degraded by any proposed changes.

Figure 19 shows the narrow composite specimens along with peak profile heights and widths of edge delaminations that were found from physical profiling. **Figure 20** shows similar data on the central delaminations of the three composite sheets. It should be noted that specimen 234A, which was artificially delaminated in 9 locations, did not produce any measurable physical indications in the middle top two locations and very little on the bottom right. A CMM profile of each column, from top to bottom, is given in **Figure 21**.

Table 18: Sample Parts for Optimization

Part ID	Dimension (inches)	Surface Condition	Delamination
848-1	2 x 11.5	no paint	edge (4700 lb)
848-2	2 x 11.5	no paint	edge (4800 lb)
848-4	1.5 x 11.5	no paint	edge (3700 lb)
484-6	1.5 x 11.5	no paint	edge (3750 lb)
S1	2 x 11.5	no paint	edge (knife)
S2	2 x 11.5	no paint	edge (knife)
sheet	20.5 x 23.5	no paint	6 - various sizes
honeycomb	15.5 x 23	no paint	3 - various sizes
234A	15 x 17	no paint	9 - various sizes

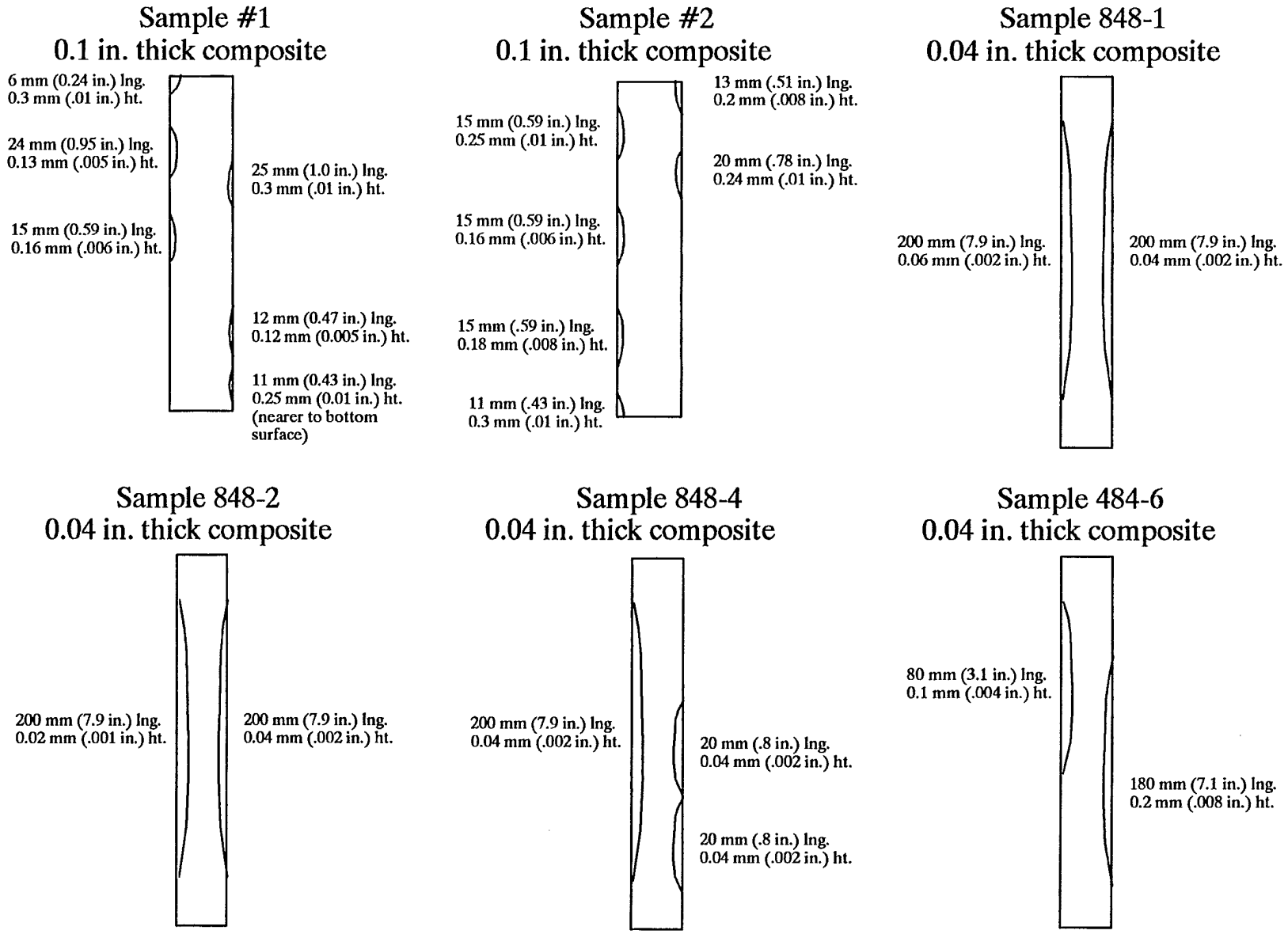

Figure 19: Dimensions of Edge Delaminations

Honeycomb Sample

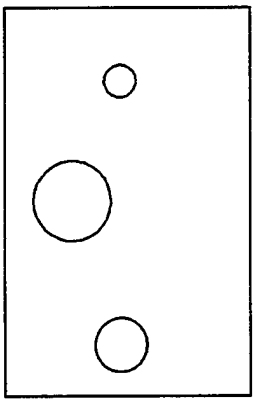

52 mm (2 in.) diam.
0.13 mm (.005 in.) ht.

116 mm (4.6 in.) diam.
1.24 mm (.05 in.) ht.

82 mm (3.2 in.) diam.
0.25 mm (.01 in.) ht.

Single Sheet Composite Sample

36 mm (1.44 in.) diam.
0.13 mm (.005 in.) ht.

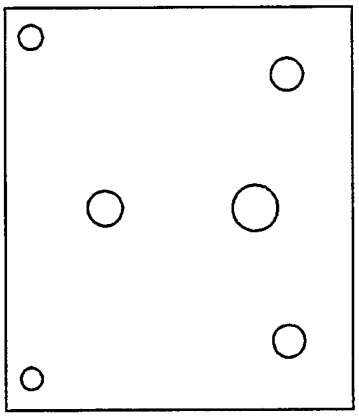

51 mm (2.02 in.) diam.
0.17 mm (.007 in.) ht.

50 mm (1.97 in.) diam.
0.15 mm (.006 in.) ht.

69 mm (2.71 in.) diam.
0.30 mm (.012 in.) ht.

32 mm (1.25 in.) diam.
0.07 mm (.003 in.) ht.

51 mm (1.99 in.) diam.
0.13 mm (.005 in.) ht.

Composite Sample 234A

31 mm (1.22 in.) diam.
0.04 mm (.002 in.) ht.

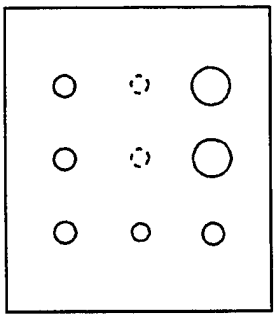

69 mm (2.71 in.) diam.
0.21 mm (.008 in.) ht.

32 mm (1.26 in.) diam.
0.05 mm (.002 in.) ht.

70 mm (2.76 in.) diam.
0.14 mm (.006 in.) ht.

29 mm (1.14 in.) diam.
0.04 mm (.002 in.) ht.

31 mm (1.22 in.) diam.
0.01 mm (.0004 in.) ht.

24 mm (0.95 in.) diam.
0.02 mm (.001 in.) ht.

Figure 20: Dimensions of Artificial Delaminations on Three Composite Sheets

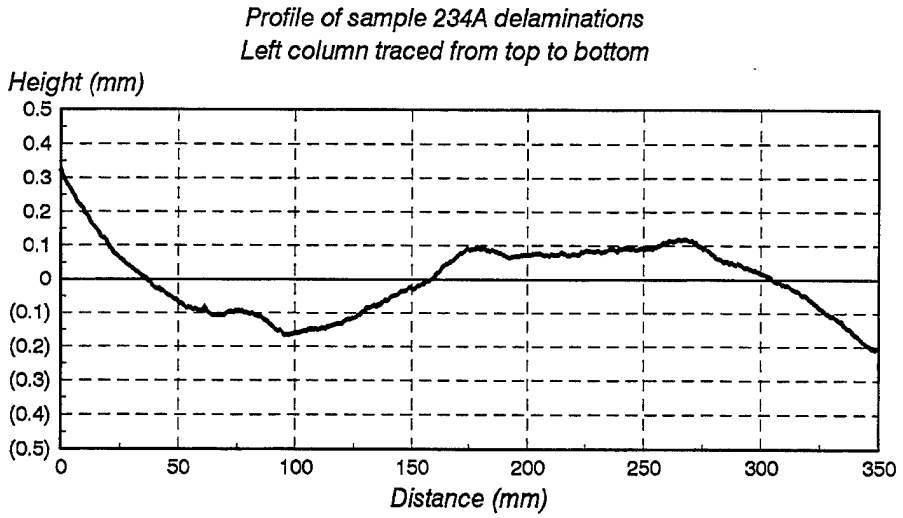

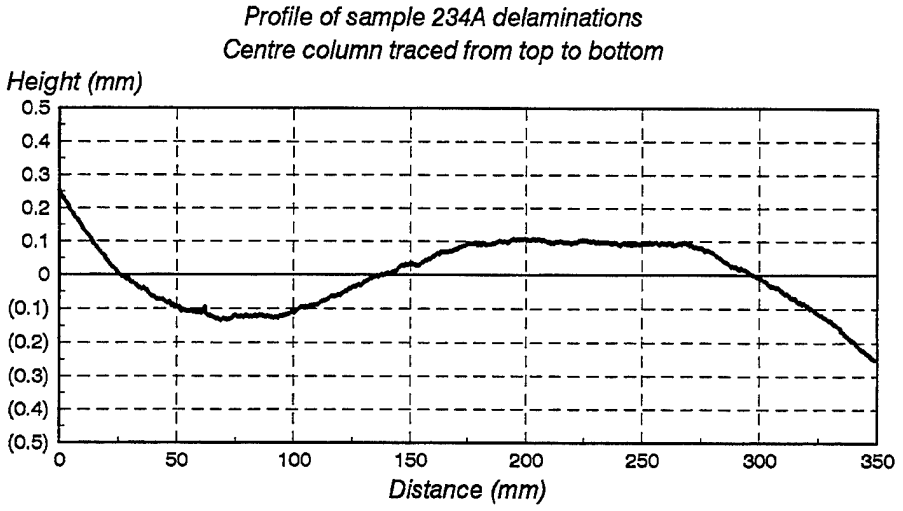

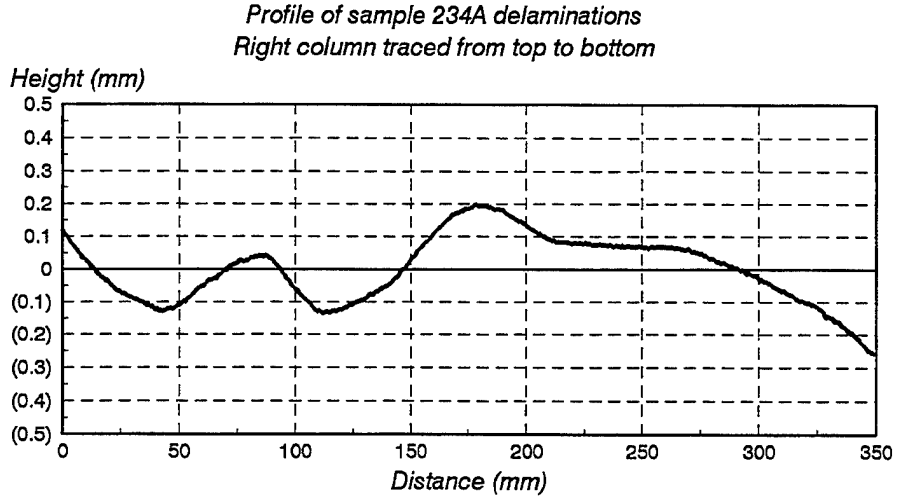

Figure 21: CMM profiles of specimen 234A

5.1.5 Experimental Results

The effect of the parameter changes proposed above can be subdivided into the effects on image signatures from impact damage and delamination indications, and the effects on the package dimensions and the optical path folding possibilities. Both these effects are important. It will be necessary to find a compromise that satisfies the criteria as much as possible yet result in a package that is not too large or too complicated to construct.

Figure 22 shows a *D SIGHT* image from a DAIS-500 of a collection of specimens with both impact damage and delaminations. By using a broader light source, the high frequency noise on the composite surfaces is attenuated as shown in **Figure 23**. The signatures of the delaminations are improved with a broader light source and a lower base grazing angle of the camera at 22.5 degrees, shown in **Figure 24**. Unfortunately, the resulting package with this optical configuration is over 1 foot longer than the DAIS-500. To reduce this package size, a wider angle lens was used and part of the field of view was masked off leaving approximately 3 sq ft. **Figure 25** shows the resulting image. This configuration, although better for packaging, suffers from a loss of magnification and spatial resolution. As a compromise, the grazing angle was increased to 27 degrees at 52 inches and the retroreflector was brought closer to the surface at a distance of 22 inches. **Figure 26** shows the resulting image and indicates that there is sufficient sensitivity to both impact damage and delaminations. Although this configuration results in a package that is slightly longer than the DAIS-500, it has a rectangular footprint, good sensitivity to both impact damage and delaminations, and reduced image noise.

Figure 27 and **Figure 28** show the carbon fiber sheet imaged using this configuration, while **Figure 29** shows the resulting image on a honeycomb panel. The same panel is shown in **Figure 30** along with a simulated delamination indication formed on sheet metal having a nominal diameter of one inch and a height of 0.001 inch. **Figure 31** shows the six edge delamination specimens using this same optical configuration. Some of these edge delaminations do not image well, partly due to their small size, and partly due to the location and orientation of the indication with respect to the view point of the sensor. There is not enough surface to image these edge delaminations from a direction perpendicular to the edge delaminations. To date, this configuration is favored as an alternative for the DAIS-500.

The new camera was used in **Figure 31** to inspect the nine artificially created delaminations on specimen, 234A. The upper two middle delaminations are not visible as would be predicted by the profile traces which showed no height indications at these locations and the bottom right delamination signature is almost not visible in the image (i.e., height = 0.0004 in).

Because the array format of the new camera is smaller than the original camera, the closest lens available to be equivalent to the 25 mm lens used with the original camera is a 20 mm lens (i.e., should be 18.75 mm). To maintain the same FOV as with the original camera, the distance of the new camera must be 1.43 m (56.25 in) for a rectangular footprint of the same area.

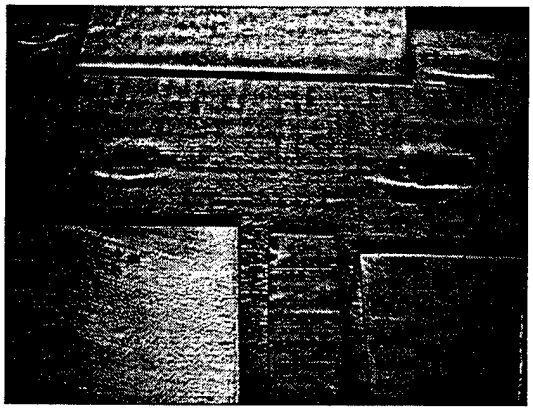

Figure 22: Original DAIS-500 configuration

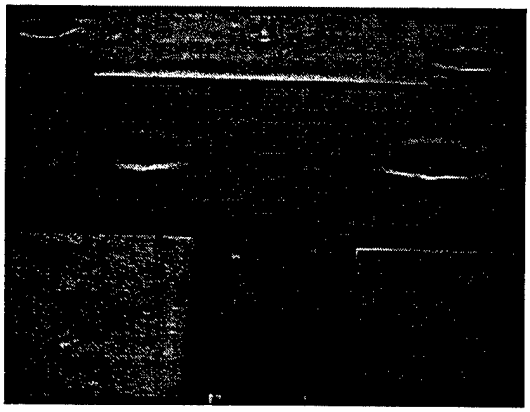

Figure 23: DAIS-500 with broad light source

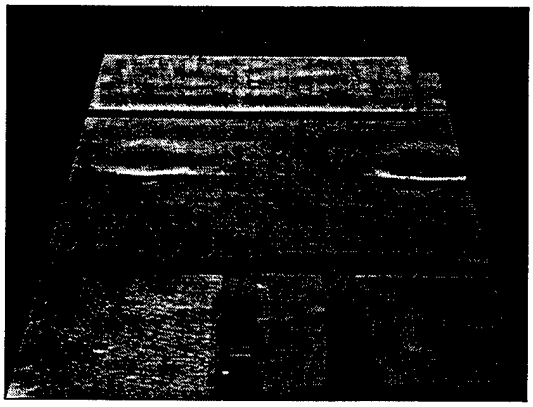

Figure 24: 35 mm lens, camera at 22.5 deg., camera to surface = 68 in., retro to surface = 30 in.

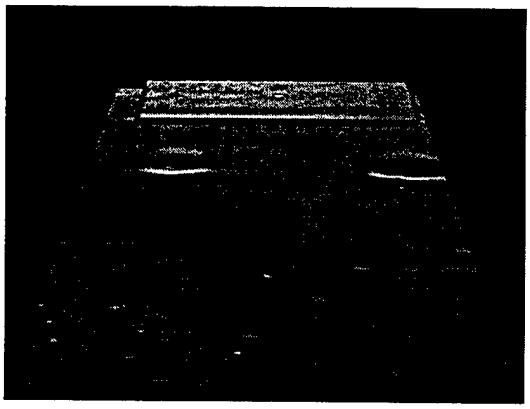

Figure 25: 25 mm lens at 22.5 deg., camera to surface = 58 in., retro to surface = 22 in.

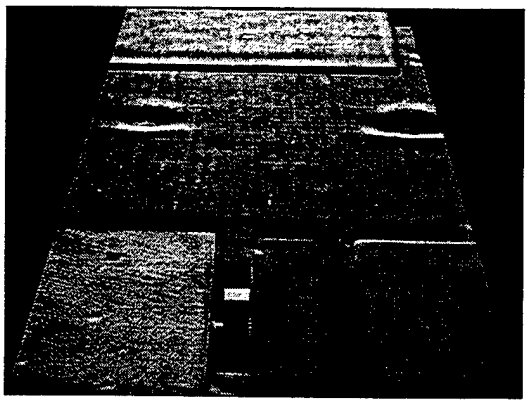

Figure 26: 25 mm lens at 27 deg., camera to surface = 52 in., retro to surface = 22 in.

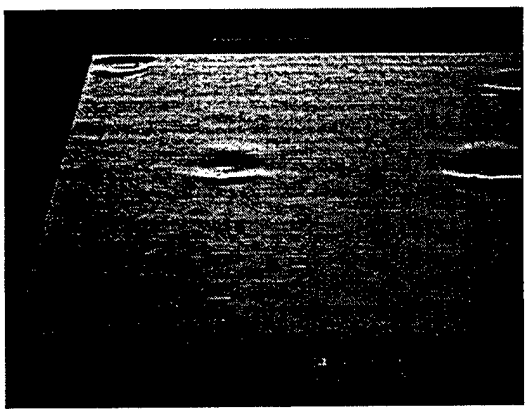

Figure 27: Left side, carbon fiber sheet, same setup as **Figure 26**

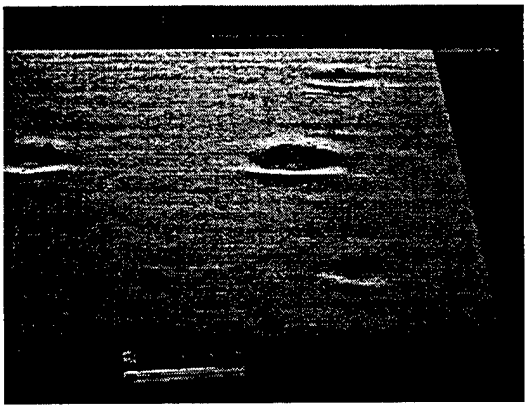

Figure 28: Right side, carbon fiber sheet, same setup as **Figure 26**

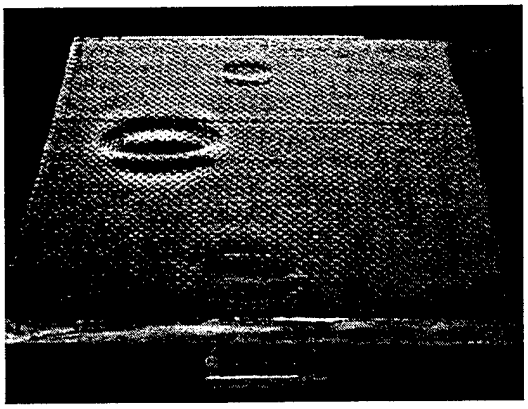

Figure 29: Honeycomb delamination, same setup as **Figure 26**

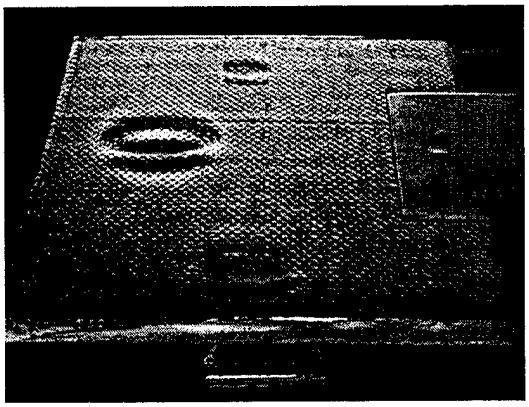

Figure 30: Honeycomb delamination with simulated sheet metal delamination on right side, 1" diameter, 1 mil high

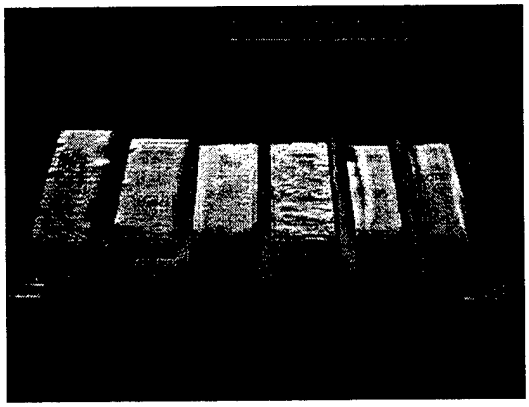

Figure 31: All edge delamination samples. Left to right, sample 1, sample 2, 848-1, 848-2, 848-4, and 484-6

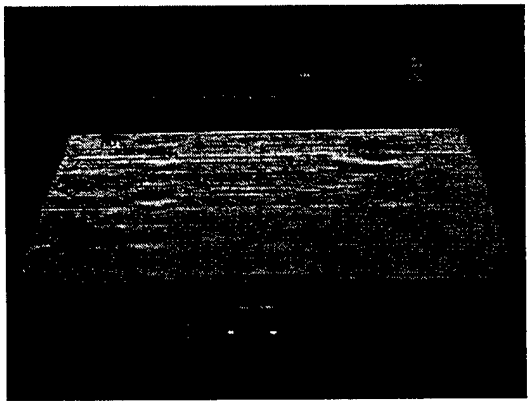

Figure 32: Specimen 234A using new camera

5.2 Hardware Description

Based on the sensor optimization and new improved host hardware, the new DAIS system consists of the following components with the sensor power supply being integrated with the host:

- *D SIGHT* image acquisition sensor
- host controller
- pendant controller
- printer

These components are depicted in **Figure 33** in the typical configuration. The purpose of the system is to acquire *D SIGHT* image data from aircraft surfaces for visual interpretation by an inspector. The system also provides the ability to display and print the image data for interpretation, store and retrieve the image data for record keeping, record analysis results and repair areas and permit user input of identifying information.

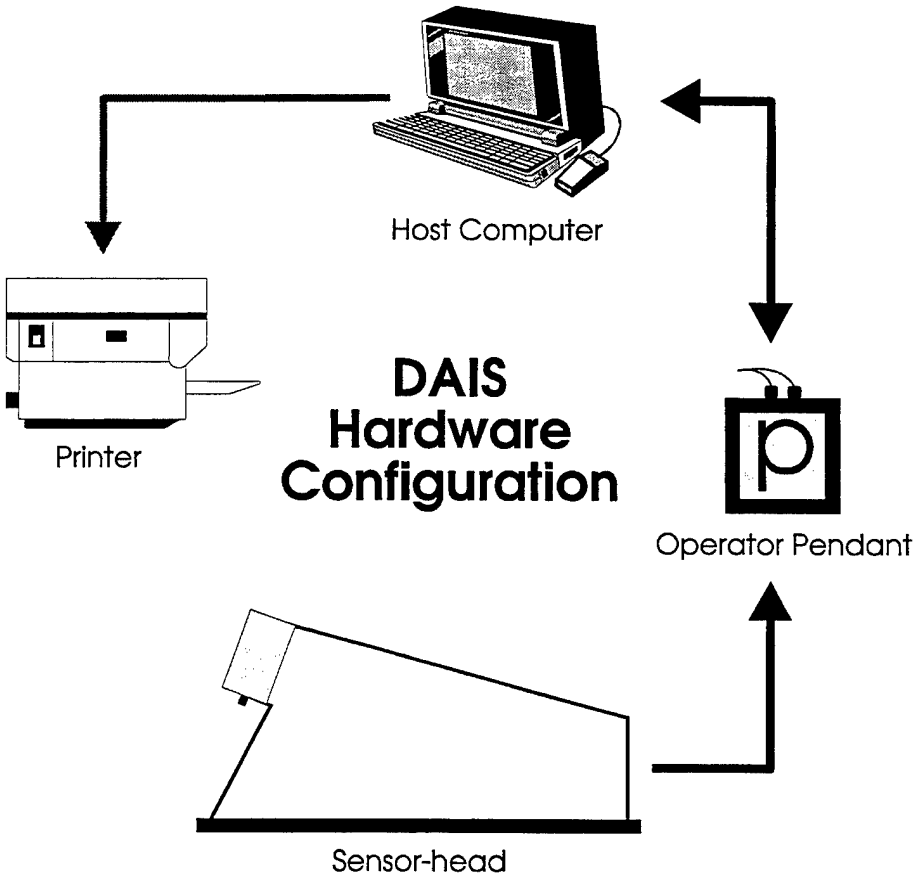

Figure 33: DAIS Hardware Configuration and Connections

5.2.1 Host Controller

The host controller consists of an industrial PC/AT computer with an LCD VGA display monitor, keyboard, and disk drives as well as hardware necessary for image capture, communication with the pendant and sensor and printing functions. Image video display capability is provided at the host on the 10 inch VGA display. User input is made through keyboard entry and a built-in mouse.

The power and control modules for the remote pendant and sensor reside in the host controller enclosure in an extended chassis. A custom cable connect panel is supplied to interface to the special boards and power modules. The system can be powered with switchable 120/240 VAC.

The minimum computer specifications are as follows:

- 486-66Mz processor
- 16 MB RAM
- 1.44 MB, 3.5" disk drive
- 540 MB hard drive
- parallel port
- TFT LCD 10' VGA monitor (256 simultaneous colors)
- 101-key keyboard
- built-in mouse

Additional hardware included:

- 8 bit, 640x480 image capture board
- D/A I/O board for light control
- power supplies for pendant and sensor

5.2.2 Pendant Controller

A portable pendant device is an integral part of the system to provide control of the sensor functions at a remote location from the host. The pendant is connected to the host by a cable approximately 30.5 m (100 ft) to minimize the movement of the host controller during inspection tasks. A cable, about 4.5 m (15 ft) in length is provided to connect the remote pendant to the sensor. Each cable is equipped with industrial connectors and mating connectors are provided on the sensor, pendant, and host controller. An industrial custom cable is provided for RS-170, VGA signals, RS-232 signals, power, and sense lines.

The pendant consists of a TFT LCD 10 inch VGA video display monitor with an integral touch screen for user input of control commands. The monitor and cable connectors are packaged in an industrial enclosure with convenient handles. The pendant will provide full control of image acquisition and the ability to display video and system menu items. The new pendant and host computer are shown in **Figure 34**.

5.2.3 DAIS-500 Sensor

The DAIS-500 sensor consists of an enclosure with integral handles, a CCD camera and lens, a white light source, a retroreflective screen, and glass mirrors to reduce package size. The optical components for the sensor have been optimized to maximize detection sensitivity for impact damage, delaminations, and disbonds. The camera, lens, light source, and electronics are enclosed in a self-contained module equipped with a filtered fan system in order to protect the components from dust and contamination. A thermal switch is included to protect the components from excessive heat in case of component failure or blocked air circulation.

Each sensor is equipped with an identification (ID) number chip to identify it uniquely to the DAIS system. In addition, a solid-state CCD camera is provided with a industrial camera lens. A low power white light source is provided with a bulb life exceeding 2000 hours. For ease of cleaning,

a commercial retroreflector is used with a protective coating.

The sensor enclosure for the DAIS-500 sensor is a hybrid design having both rigid end caps to protect critical components and a central cloth/frame section to reduce weight. The enclosure serves two purposes: to support the internal optical components and geometry and to block ambient light that would reduce image contrast and sensitivity from entering the inspection area. Manipulation of the sensor into any orientation is made possible by rigid handles at approriate locations. The enclosure footprint and field of view are rectangular in shape and the inspection area has a 2 to 1 aspect ratio. No-mar feet and a light blocking rubber skirt are provided at the base of the sensor to reduce possible damage to the aircraft surface and to prevent ambient light from entering the sensor. The completed sensor is shown in **Figure 35** and a drawing showing internal structure is shown in **Figure 36**.

The sensor specifications are given below:

• camera type	CCD, ½" format, 768x494 pixels
• camera orientation	normal view
• camera to surface distance	1.43 m (56.25 in.)
• surface to retroreflector	559 mm (22 in.) (nominal)
• camera grazing angle	27 degrees
• camera lens	20 mm @ f11, fixed focus
• lamp reflector diameter	halogen with integral 50 mm (2 in.) stipple reflector
• effective lamp location	38 mm (1.5 in.), off-axis, below lens
• retroreflector	3M, Scotchlite 3290, coated
• field of view	355 mm x 762 mm (14" x 30")
• weight	8.2 kg. (18 lbs)

5.2.4 Printer

The system printer is a commercial monochrome laser printer with 600 DPI or better (color printers are available as an option). The printer is equipped with a standard letter paper tray. Connection of the printer to the host controller is provided with standard printer and power cables.

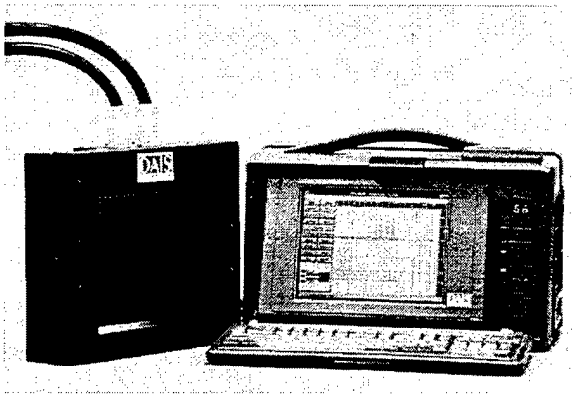

Figure 34: Pendant and Computer Host

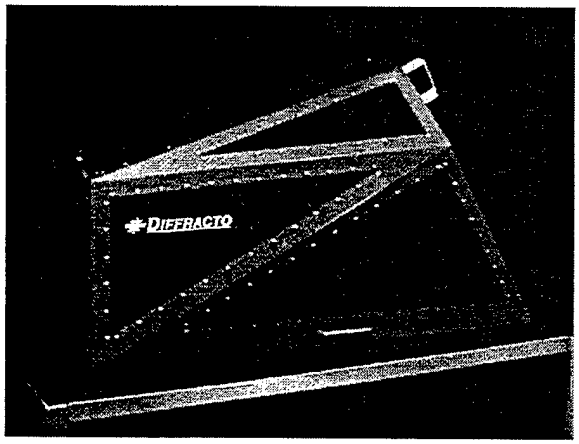

Figure 35: DAIS-500 Prototype Sensor

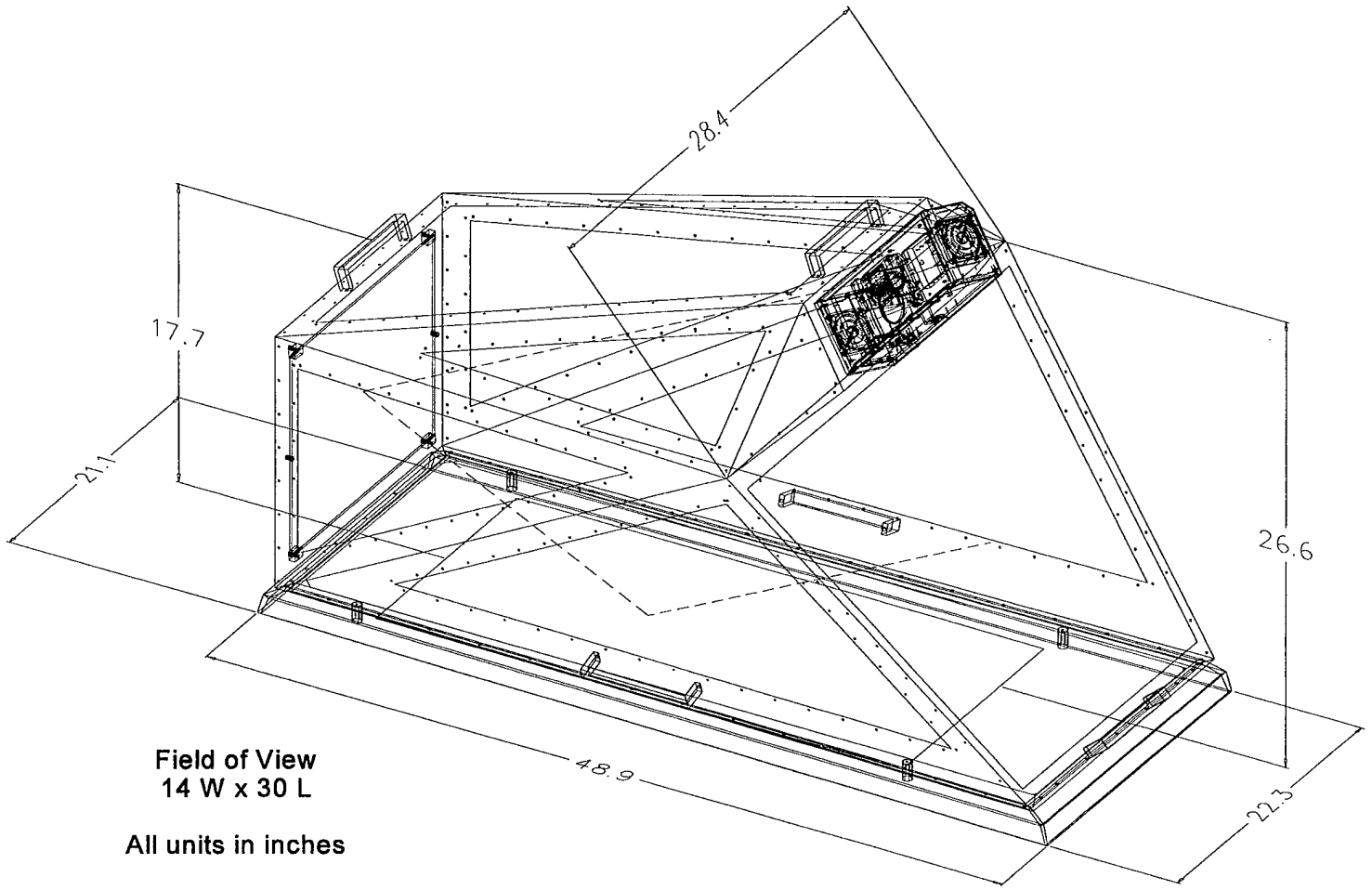

Figure 36: DAIS-500 Sensor Drawing

6 SOFTWARE DEVELOPMENT

6.1 General

The problem of coordinating and finding inspection data from specific locations on the aircraft has led to the development of a graphical user interface for the collection, retrieval and analysis of image data based on the concept of a turtle diagram. A turtle diagram is an unfolded planar diagram of the aircraft surface. **Figure 36** shows a turtle diagram with the basic characteristics required: reference labels having meaning to the aircraft and NDI technician and critical placement positions for the inspection along lap splices representing areas requiring inspection. Reference to the image data can be made by selecting the box associated with the position on the aircraft drawing.

DAIS software uses this Windows graphical user interface during the inspection process both at the host and pendant. In addition, a modular structure is used to simplify and isolate major functions that need not require all system hardware. The Windows software environment is ideal for this modularity and has the added capability of simultaneously displaying live video in a window and graphics on a VGA monitor.

The software structure for DAIS is based on five broad operational requirements that have been identified for the inspection system: inspection plan creation, sensor installation and calibration, image acquisition, image analysis and reporting, and repair planning. Only the sensor install/calibrate module and the image acquisition module require connection of the entire system

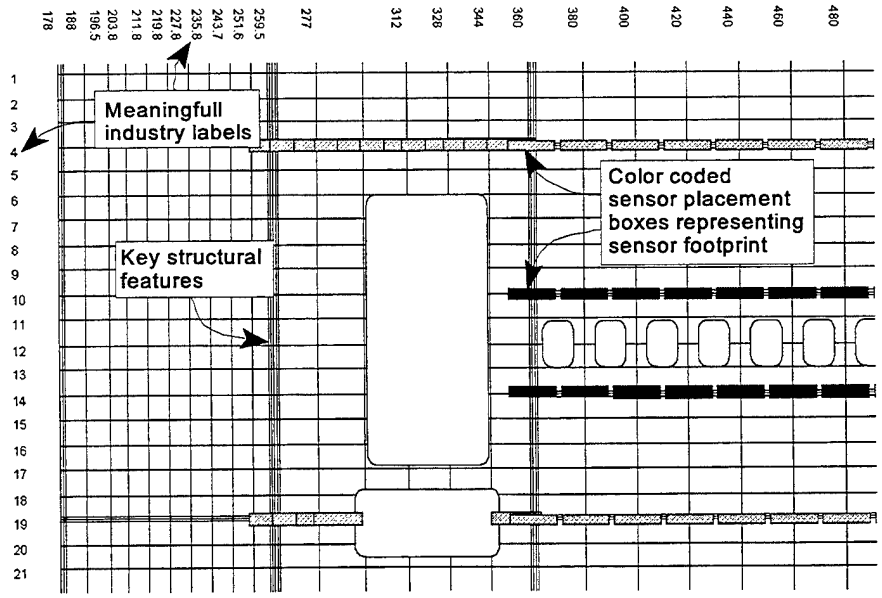

Figure 37: Example Turtle Diagram with Sensor Placements

hardware; otherwise, the remaining modules could be used at the host in the NDI shop.

6.2 DAIS File Structure

Three main types of files in the DAIS system will record the inspection activities. The inspection plan files (.PLN) are designed once for a specific aircraft type and can be reused or modified depending on maintenance requirements and schedules. The aircraft work files (.AIR) embody a particular inspection plan file (i.e. contain the plan within it) along with the inspection status, analysis results, repair results and image filenames for a particular aircraft tail number. The aircraft work file will incorporate information from the acquisition module, the image analysis module and the repair module as it is updated. All image data will be stored in individual files in either Bit Mapped image file format (.BMP) or in Tagged Image File Format (.TIF) depending on the user's preference. The names of the image files will be created automatically from information related to the position of the placement in the plan, the sequential group number, and the sequential number of the placement within the group. Users will interface to these image files graphically through the turtle diagram. The aircraft work file could be archived for comparison with future inspections even if all the images associated with it have been deleted, since it records the defects found and any repair actions on the turtle diagram and not the images themselves. **Figure 38** shows the five modules schematically and the corresponding input and output files.

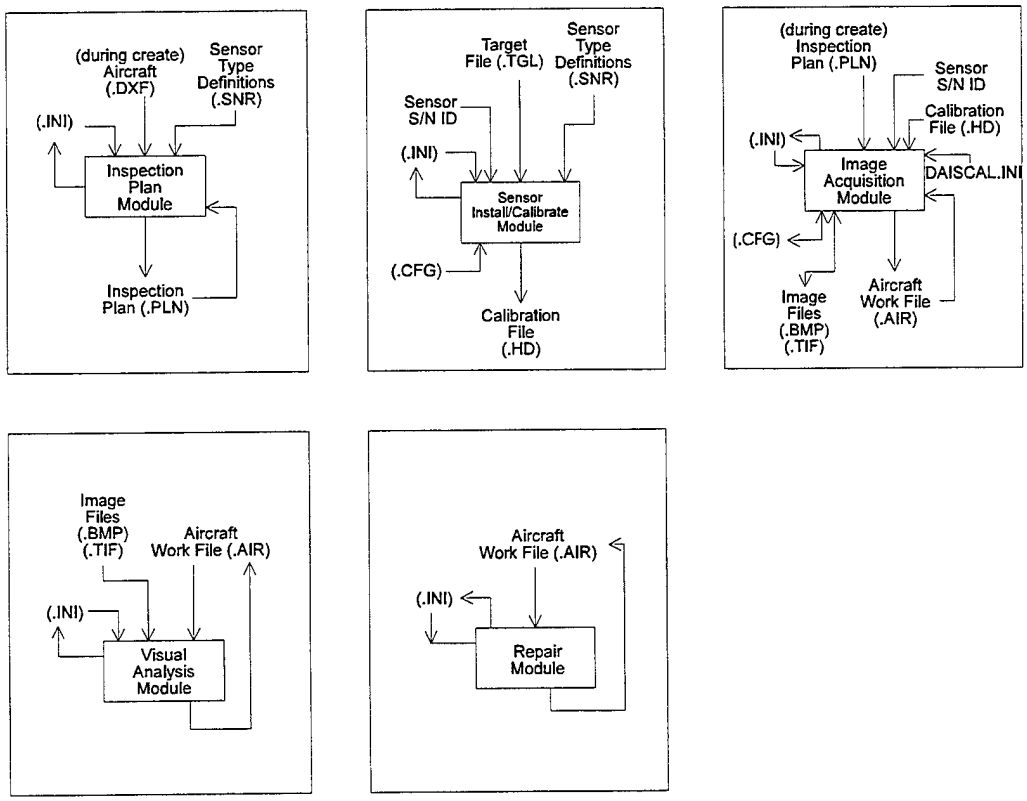

Figure 38: Relationship of DAIS Modules and System Files

6.3 Description of Program Modules

6.3.1 Inspection Plan Module

The inspection plan module is basically a graphical editor that creates an inspection plan from an existing planar drawing of the aircraft (turtle diagram) and the footprint of sensors needed to accomplish the desired inspection. The goal of this module is to allow an experienced inspector to design a plan of inspections for a set of DAIS sensors from the inspection requirements of a regular maintenance schedule or service bulletin. The inspection plan can then be executed by NDI technicians who will be guided by the plan each time the inspection is needed. This will result in a consistent set of inspections that can be compared over time. The aircraft drawing is presumed to already exist and must satisfy a limited set of constraints during its creation. Once an inspection plan is created it can be used over and over again. More than one inspection plan may be created due to different inspection schedules or needs.

Table 19 summarizes the functions and the menu system for inspection planning.

Table 19: Inspection Plan Menu Items

Menu Item	Submenu Item	Button	Function
File	Create...		Loads aircraft drawing file(s) and user information for a specific aircraft given by its tail number, etc. to create an inspection plan file (.PLN)
	Open...	File	Opens an existing plan file
	Modify...		Modifies the list of drawing DXF files and the user header information
	Save	Save	Saves the changes to the opened plan file
	Save As...		Saves the changes to the inspection plan in a new file
	Close		Closes the opened plan file without leaving the program
	Print Turtle Diagram...		Prints the turtle diagram to the system printer specified
	Printer Setup...		Allows configuration of printer settings
	Exit	Exit	Exits the program to Windows

Table 19 (cont'd)

Menu Item	Submenu Item	Button	Function
Page	Select Page...	Page	Displays a list of available plan pages for selection
	Previous Page		Loads previous page in plan file from the current page
	Next Page		Loads next page in plan file from the current page
Zoom	Zoom Full		Sets turtle diagram size to include the entire diagram in the display window
	Zoom In	Zoom +	Enlarges the size of the turtle diagram by the selected zoom increment and centers it about the position of the cursor
	Zoom Out	Zoom -	Reduces the size of the turtle diagram by the selected zoom increment and centers it about the position of the cursor
	Zoom Increment...		Sets the zoom increment as a percent of full scale to 1,5,10 or 25%
Group	New...	New	Starts a new group definition
	Rename...	Rename	Renames the selected placement group
	Merge...	Merge	Merges the two selected groups using the name of the first
	Delete	Delete	Deletes the selected placement group
	Edit Group	Edit Group	Selects placement group for editing of placements
Placement	Settings...	Settings	Sets sensor model, orientation, overlap, and surface radii parameters for subsequent placement operations
	Change...	Change	Allows setting changes to an individual placement
	Single	Single	Creates a single placement on the turtle diagram with a mouse click
	Line	Line	Creates a line of sensor placements on the turtle diagram based on two point specification
	Array	Array	Creates an array of sensor placements on the turtle diagram based on three point specification

Table 19 (cont'd)

Menu Item	Submenu Item	Button	Function
	Delete	Delete	Deletes a single placement
	Close Group	Close Group	Terminates editing of placements in current group
Options	Units...		Selects English (in) or Metric (mm) units
Help	Contents...		Displays contents of help document
	Using Help...		Explains how to use help
	About...		Displays release version of program

6.3.2 Install/Calibrate Module

The install/calibrate module is intended to be used infrequently; it is required whenever a new sensor is purchased or when a spatial recalibration is warranted due to sensor repair, sensor damage, or hardware component drift. Each sensor is equipped with an ID number chip that will allow its identification to the system in terms of sensor type, model number and its unique spatial calibration to a known spatial calibration target. The spatial calibration is needed to allow the removal of the "keystone" or perspective effect found in all *D SIGHT* images as well as aircraft surface curvature by making the image appear as a flat, top-view image. The calibration results in a set of parameters for a spatial camera model and does not relate to defects or defect calibration whatsoever. **Table 20** summarizes the functions and menu items for installing and calibrating.

Table 20: Install/Calibrate Menu Items

Menu Item	Submenu Item	Button	Function
Install...		Install	Reads ID number from sensor and user selects DAIS model number
Calibrate...		Calibrate	Provides parametric spatial calibration of camera for removal of perspective distortion in saved images
List...		List	Generates printable list of installed sensors along with calibration status
De-install...		De-install	Allows user to remove sensor from active list of available sensors
Help...	Contents...		Displays contents of help document
	Using Help...		Explains how to use help
	About...		Displays release version of program
Exit			Exits program to Windows

6.3.3 Acquisition Module

The image acquisition module is a key module that uses an existing inspection plan, designed for a specific aircraft type and maintenance schedule, and applies it to a particular aircraft tail number. The goal of this module is to remove the burden of where to inspect and what has been inspected already by providing a graphical color display of the inspection areas that have or have not been inspected, and the remaining inspection areas. In addition, the module will automatically prompt the technician to position a specific sensor in preplanned areas that cover a logical section (i.e., top of wing) of the aircraft. Each logical section or group created by the inspection planner, however, can be selected arbitrarily by the technician depending on the availability of that area for inspection. The module also removes the burden of managing images and filenames by allowing the position of the inspection area on the turtle diagram to define an internal filename that can be accessed graphically rather than by a filename. An aircraft work file will keep track of the inspections already completed and any outstanding inspections. This file may be opened and closed as many times as needed over the course of the inspection process until all the inspections are finished. The file is also available for image analysis of already completed inspections or repair planning before the remaining inspections are finished.

The primary video window displaying the *D SIGHT* image is shown in **Figure 39**. The light is automatically adjusted to a preset target level and the image will remain live for a preset time.

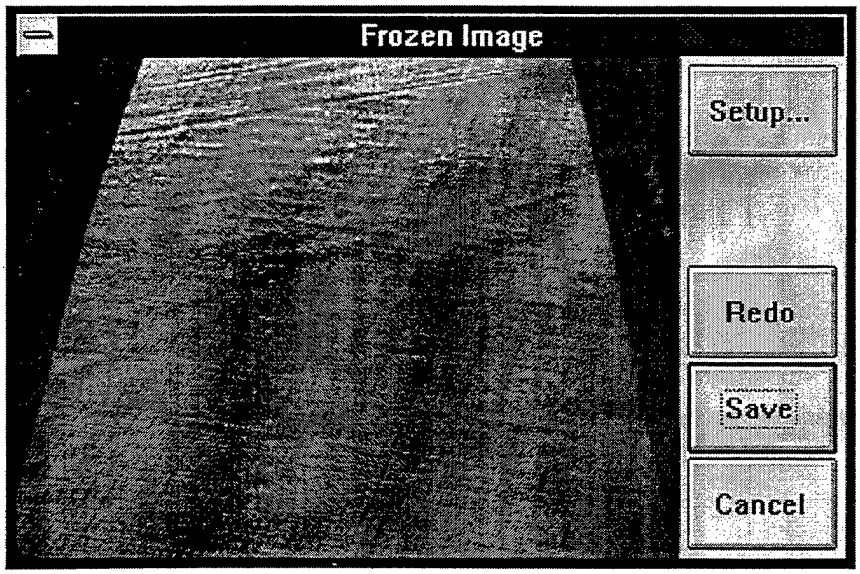

Figure 39: Image Acquisition Display Window

Table 21 summarizes the functions and menu for the acquisition program.

Table 21: Acquisition Menu Items

Menu Item	Submenu Item	Button	Function
File	Create...		Loads inspection plan file (.PLN) and user information for a specific aircraft given by its tail number, etc. to create an aircraft work file (.AIR)
	Open...	File	Opens an existing aircraft work file
	Modify Header...		Modifies the user header information
	Save	Save	Saves the changes to the opened aircraft work file
	Close		Closes the opened aircraft work file without leaving the program
	Exit	Exit	Exits the program to Windows
Page	Select Page...	Page	Displays a list of available plan pages for selection
	Previous Page		Loads previous page in inspection plan from the current page
	Next Page		Loads next page in inspection plan from the current page
Zoom	Zoom Full		Sets turtle diagram size to include the entire diagram in the display window
	Zoom In	Zoom +	Enlarges the size of the turtle diagram by the selected zoom increment and centers it about the position of the cursor
	Zoom Out	Zoom -	Reduces the size of the turtle diagram by the selected zoom increment and centers it about the position of the cursor
	Zoom Increment...		Sets the zoom increment as a percent of full scale to 1,5,10 or 25%
Group	Open	Open	Opens an existing placement group
	Close	Close	Closes the opened placement group
Image	Acquire...	Acquire	Displays live image capable of being saved for the particular placement box highlighted
	Recall...	Recall	Displays a stored image file for the particular placement box highlighted

Table 21 (cont'd)

Menu Item	Submenu Item	Button	Function
	Redo...	Redo	Allows a saved image to be overwritten with a new image for the specified placement box
	Skip	Skip	Allows the current placement box to be by-passed during acquisition
Options	Transform Images		Recalled images are perspectively corrected if checked
	Enhance Contrast		Sets image contrast parameter
	Enhance Sharpness		Sets image sharpness parameter
	Units...		Selects English (in) or Metric (mm) units
	Image Format...		Select Windows Bitmap format (.BMP) or Tagged Image File Format (.TIF)
Help	Contents...		Displays contents of help document
	Using Help...		Explains how to use help
	About...		Displays release version of program

6.3.4 Analysis Module

The image analysis module is also a key module that allows the inspector to visually analyze each *D SIGHT* image associated with every sensor placement for defects in normal or perspectively corrected form. The turtle diagram interface makes this process easy by showing which areas have been inspected and analyzed, where the defects are located and their severity. The turtle diagram allows the inspector to systematically analyze the entire set of images without the burden of filenames and the need to keep track of which areas are complete. The inspector will have the ability to mark defect type and severity for an inspection footprint from a list of types and severities. The inspector will also have the ability to mark an inspection area for reacquisition, if the image quality or sensor position is incorrect, or to include a note/comment. The analysis module will permit partial analysis of the already completed inspections to keep the inspection process as flexible as possible.

Table 22 summarizes the available functions for the analysis module:

Table 22: Analysis Menu Items

Menu Item	Submenu Item	Button	Function
File	Open...	File	Opens an existing aircraft work file (.AIR)
	Modify Header...		Modifies the user header information
	Save	Save	Saves the changes to the opened aircraft work file
	Close		Closes the opened aircraft work file without leaving the program
	Print Images...		Prints the images from the specified group or page
	Print Turtle Diagram...		Prints the turtle diagram to the system printer specified
	Printer Setup...		Allows configuration of printer settings
	Exit	Exit	Exits the program to Windows
Page	Select Page...	Page	Displays a list of available plan pages for selection
	Previous Page		Loads previous page in inspection plan from the current page
	Next Page		Loads next page in inspection plan from the current page
Zoom	Zoom Full		Sets turtle diagram size to include the entire diagram in the display window
	Zoom In	Zoom +	Enlarges the size of the turtle diagram by the selected zoom increment and centers it about the position of the cursor
	Zoom Out	Zoom -	Reduces the size of the turtle diagram by the selected zoom increment and centers it about the position of the cursor
	Zoom Increment...		Sets the zoom increment as a percent of full scale to 1,5,10 or 25%
Group	Open	Open	Opens an existing placement group
	Close	Close	Closes the opened placement group
Image	Analyze...	Analyze	Displays stored image for the particular placement box highlighted for visual interpretation and recording of results on turtle diagram
	Recall...	Recall	Displays a stored image file for the particular placement box highlighted

Table 22 (cont'd)

Menu Item	Submenu Item	Button	Function
	Redo...	Redo	Allows an analyzed image for the highlighted inspection box to be re-evaluated
	Skip	Skip	Allows the current placement box to be by-passed during visual interpretation and analysis
Options	Transform Images		Recalled images are perspectively corrected if checked
	Enhance Contrast		Sets image contrast parameter
	Enhance Sharpness		Sets image sharpness parameter
	Units...		Selects English (in) or Metric (mm) units
Help	Contents...		Displays contents of help document
	Using Help...		Explains how to use help
	About...		Displays release version of program

The critical display of the image is provided in a dialog box shown in 73. If the image in the placement box indicates corrosion and is marked accordingly, the placement box is marked in red on the turtle diagram on exit with an OK. The aircraft work file is then updated with the defect type and severity. If no corrosion is found, the placement box is marked with green on exit with an OK.

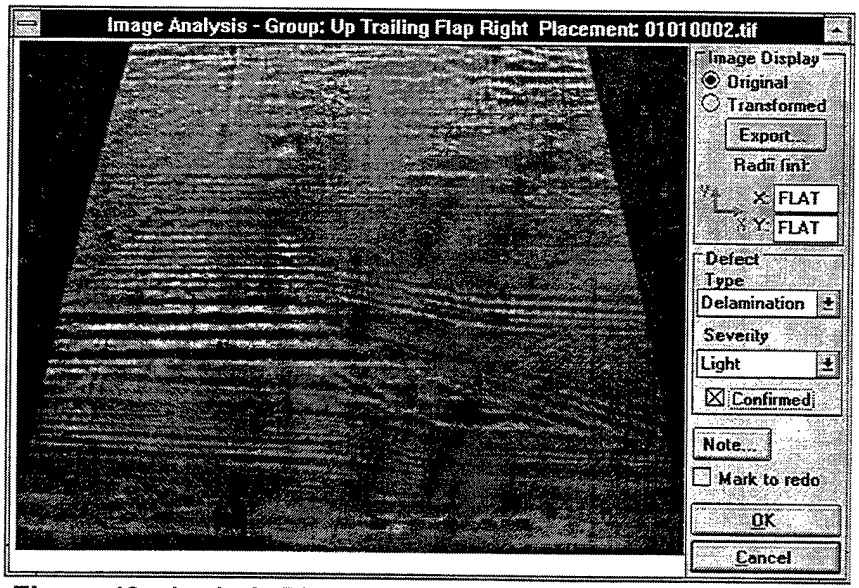

Figure 40: Analysis Dialog Box for Viewing and Marking Defects

When images need to be printed, a new menu is presented that includes several criteria for selecting the images that are desired. Menu functions are listed in **Table 23**.

Table 23: Image Print Menu Items

Menu Item	Submenu Item	Button	Function
Page	Select Page...	Page	Displays a list of available plan pages for selection
	Previous Page		Loads previous page in inspection plan from the current page
	Next Page		Loads next page in inspection plan from the current page
Zoom	Zoom Full		Sets turtle diagram size to include the entire diagram in the display window
	Zoom In	Zoom +	Enlarges the size of the turtle diagram by the selected zoom increment and centers it about the position of the cursor
	Zoom Out	Zoom -	Reduces the size of the turtle diagram by the selected zoom increment and centers it about the position of the cursor
	Zoom Increment...		Sets the zoom increment as a percent of full scale to 1,5,10 or 25%
Selection	All on Page	All	Selects or Deselects images from all placement boxes on the current page
	All with Color	Color	Selects or Deselects images from all placement boxes with the selected color
	All with Severity	Severity	Selects or Deselects images from all placement boxes marked with defects with the selected severity level
	by Group	Group	Selects or Deselects images for a group by clicking on any member of the group
	by Placement	Placement	Selects or Deselects images for individual placements from any group by clicking on the placement box
Options	Transform Image		Sets flag to perspectively correct images (if calibrated) prior to printing or display
	Enhance Contrast		Increases image contrast if set
	Enhance Sharpness		Increases image sharpness if set

Table 23 (cont'd)

Menu Item	Submenu Item	Button	Function
	Units		Selects English (in) or Metric (mm) units
Cancel		Cancel	Cancel image printing and exit print menu
Print...		Print...	Display print dialog box for selection of copies, resolution, and printer setup functions including paper type, orientation, and driver options

6.3.5 Repair Module

The repair module is intended to produce a repair plan that may span several inspection areas or fractions of them. By observing the locations and severity of defects, the engineer can propose a repair strategy for the affected areas from a knowledge of the aircraft, physical constraints, and defect locations. The resulting marks on the turtle diagram should provide a visual repair plan for the affected areas, including any special instructions regarding the repair. The repair plan can also be tagged with completed repairs.

Table 24 summarizes the functions and menu for the repair program:

Table 24: Repair Planning Menu Items

Menu Item	Submenu Item	Button	Function
File	Open...	File	Opens an existing aircraft work file (.AIR)
	Modify Header...		Modifies the user header information
	Save	Save	Saves the changes to the opened aircraft work file
	Close		Closes the opened aircraft work file without leaving the program
	Print Turtle Diagram...		Prints the turtle diagram to the system printer specified
	Printer Setup...		Allows configuration of printer settings
	Exit	Exit	Exits the program to Windows
Page	Select Page...	Page	Displays a list of available plan pages for selection
	Previous Page		Loads previous page in inspection plan from the current page

Table 24 (cont'd)

Menu Item	Submenu Item	Button	Function
	Next Page		Loads next page in inspection plan from the current page
Zoom	Zoom Full		Sets turtle diagram size to include the entire diagram in the display window
	Zoom In	Zoom +	Enlarges the size of the turtle diagram by the selected zoom increment and centers it about the position of the cursor
	Zoom Out	Zoom -	Reduces the size of the turtle diagram by the selected zoom increment and centers it about the position of the cursor
	Zoom Increment...		Sets the zoom increment as a percent of full scale to 1,5,10 or 25%
Repair	Create	Create	Starts the definition of a new repair zone including the ability to draw a rectangular area over the turtle diagram and textual information
	Delete	Delete	Deletes one of the existing repair zones
	Confirm	Confirm	Indicates that the repair is complete by changing the color of the repair zone to green (complete) from red (planned) or vice-versa
	Redo	Redo	Marks individual placement boxes for re-acquisition by changing color to yellow
Options	Units...		Selects English (in) or Metric (mm) units
Help	Contents...		Displays contents of help document
	Using Help...		Explains how to use help
	About...		Displays release version of program

7 FIELD TRIAL SUMMARY

During the course of this program, DAIS-500 prototype equipment (and DAIS-250C equipment designed for corrosion detection under a different program) were tested and demonstrated at six different military locations on a variety of different components and materials typically over a 1-2 day period. A detailed trip report for each of these trips is included in the Appendix. There were two main reasons for conducting these field trials. First, the hangar environment and physical constraints imposed by a variety of aircraft would be fed back to the design of the inspection equipment. Second, the NDI inspectors and other military personnel would be able to critique the equipment for its user friendliness, usefulness, and its sensitivity to a variety of defect types on actual aircraft and component lab specimens.

The field trials were conducted at the following sites:

Northrup-Grumman, Louisiana (2 trips)
Tinker AFB, Oklahoma
Kelly AFB, Texas
Hill AFB, Utah
Whiteman AFB, Missouri
McClellan AFB, California

In addition to these field trials, the DAIS-500 was left at Tinker AFB and McClellan AFB for an extended period of time to allow NDI personnel to evaluate and to obtain experience with the equipment.

The aircraft inspected by the DAIS-250C sensor included the modified B-707 in the JSTARS program while the DAIS-500 sensor was used to inspect components or sections of the following aircraft for impact damage, delaminations, and disbonds: B-52, KC-135, B1-B, E-3, B1, C-5, T-38, F-16, F-18, B-2 and A-10A (corrosion).

Early in the program and field trials, it became apparent that the kerosene-based highlighter, Snoflake, would be unacceptable in military hangars due to its health and safety concerns, as well as the potential to react with components and their adhesives, paint, etc. At Kelly AFB, for example, Snoflake was not permitted to be used on C-5 components. Instead, WD-40 had to be substituted, however, this light oil does not have good highlighter properties. Ultimately, a dielectric solvent called Electron, which is currently an accepted solvent in the military, was suggested by McClellan AFB personnel as a highlighter for *D SIGHT*. This solvent became the highlighter of choice when compared to Snoflake even though optically Snoflake is the better highlighter. Electron was used at all facilities thereafter without any problems or complaints with the exception of Whiteman AFB.

At Whiteman AFB, no liquids were permitted on the non-reflective surfaces of the B2 bomber other than water and alcohol. As a result, the first attempt to use a thin solid film or "dry" highlighter in the field was tried with a breadboard attachment to the DAIS-500. The effort was successful in that it demonstrated the feasibility of using such an attachment in place of a liquid highlighter. Further development is needed to determine how the solid film highligher differs from the liquid in terms of signatures or whether the solid film masks defect indications.

Throughout the field trials, it also became evident that the Window's user interface to the computer and pendant was easily understood by most people with some computer experience. The "turtle

diagram" or planar diagram of the aircraft surface for locating areas to be inspected with sensor placement boxes was easily understood and became a powerful method to find image data quickly for any given area of the aircraft. It captures what is to be inspected, in what location, and whether the image data has been acquired and/or analyzed. Many participants had positive comments about this color-coded graphical method of organizing the inspection and the resulting image data.

Most people at the field trials were surprised by the apparent visual enhancement provided by *D SIGHT* the first time they see it in operation. In these field trials, there were no exceptions. Since most NDI personnel are use to ultrasonic inspection for composites because they "see" deep into the material with sound waves, they are skeptical of a device that only infers what is going on below the surface from surface evidence especially in the case of delaminations and disbonds. In most cases they are unaware that a delamination does in fact produce a subtle indication at the surface and because *D SIGHT* is so sensitivity to small perturbations on the surface, it can detect the presence of the delamination by its effect on the surface geometry. There were many situations were *D SIGHT* showed indications of a delamination but coin tapping could not confirm its presence. Although this type of false-call is undesirable, the goal of this program was to develop a sensor that could find candidate areas quickly over large surface areas for further evaluation by more precise instruments. In this regard, the DAIS-500 performed this function well from all indications during the field trials. The detection of impact damage is easier for people to accept but again, the extent of subsurface damage may not be easily determined without further evaluation.

Throughout the field trials, the greatest concern to the contract participants was whether the size of the DAIS-500 was too large for ease of use during regular inspections. There were several times when the size of the sensor seemed to be too large for certain inspections especially when the sensor had to be held with extended arms or for an extended period of time. One of the difficulties was the inability to see around the sensor to position it properly on the surface. A second was the weight of 18 lbs (8.2 kg). With two people holding the sensor, the task became much easier. Unfortunately, this would require two technicians on the sensor and one at the control pendant. It will have to be determined if the use of so many technicians is justified in relationship to the area inspected and speed of inspection. In many cases the sensor was being used for demonstration on small lab specimens rather than its intended use on large aircraft surfaces. In this context, the large sensor size and footprint is not unreasonable.

The field trials were an important part of the development process. Much was learned and the exposure gained from the field trials is beneficial for possible introduction of the system to the NDI community in the ALC's.

8 CONCLUSIONS

A new method of controlled delamination and disbond introduction in composites was developed early in this program. In-service experience with DAIS should result in the creation of a data base of natural delamination and disbond surface perturbations which are needed to provide ultimate validation of this method. The DAIS-500 was shown to be capable of detecting delaminations and disbonds in locations where residual stress, released when the damage was created, have been significant enough to produce surface perturbations. Applicability of DAIS for these types of damage NDI will depend on particular structures and a knowledge of what constitutes significant damage.

The ability of the DAIS-500 to detect impact damage at very low impact energy levels was found to be comparable to ultrasonic C-Scan (113 vs. 111 calls). In the case of the F-16 horizontal stabilizer, the DAIS-500 detected 20 out of 23 damage sites. Very low levels of damage, introduced at IAR in order to test the DAIS-500 threshold of detection capability, proved in most cases too low for X-ray (5 out of 23) and ultrasound techniques (none detected). A very low false call rate for impact damage detection was observed with the DAIS-500 (3.5%). The extent of impact damage (C-Scan signature and indentation) in stiffened panels depended largely on the location of impact vs. stiffener position. In addition, significant differences were observed in the response to impact between the AS4/3501-6 and IM7/5250-4 composite materials. The same energy impact produced indents 30% to 50% less deep in IM7/5250-4 panels. In order to generate an indent of the same depth in both systems nearly 70% higher energy was required for IM7/5250-4.

Impacts which were initially above the BVID limit were found to relax below that level. Since most aircraft structures in service today have been certified without taking account of this phenomenon it is possible that critical damage may remain undetected for an extended period of time seriously degrading the residual strength of these structures.

At the start of the program, an excellent but unacceptable kerosene-based highlighter was being used during inspections. Tests with Electron, both in the lab and on-aircraft, indicate that this environmentally friendly dielectric solvent will satisfy both the optical requirements of *D SIGHT* and the health and safety concerns of the inspectors.

The optical geometry of the DAIS-500 sensor was designed based on the visibility of signatures from both small impact damage indications, delaminations and disbonds. The sensor has been found to be very sensitive, however, its size and weight is open to criticism and may be excessive for ease of inspection. At 18 lbs (8.2 kg) the sensor is awkward to operate by a single inspector although it does inspect about 3 ft^2 (0.27 m^2) per sensor placement.

The introduction of the "turtle diagram" or planar, unfolded diagram of the aircraft surface has been received well by the inspectors in the field trials. The diagram is color coded and provides a quick and easy way to determine the status of the inspection as well as the inspection requirements. Image data management is enhanced significantly with the Windows-based software during inspection and during subsequent visual analysis.

9 RECOMMENDATIONS

Based on the work during this program, the following recommendations are proposed:

- Image enhancement and analysis methods in software should be considered for *D SIGHT* impact damage and delamination detection.

- The software should be modified to allow components to be tracked rather than aircraft since many components such as flaps end up on several aircraft over their life time.

- The software should be modified to allow inspection data from multiple sensors inspecting the same aircraft to be merged into one overall summary turtle diagram rather then as separate diagrams.

- The magnitude of impact dent relaxation (over 30%) indicates that indent relaxation should be accounted for in damage tolerance tests of composite structures in future studies.

- Incorporation of DAIS systems into composite aircraft structures NDI could open a new approach to certification based on cumulative probability of impact occurrence rather than on the current BVID requirement due to its sensitivity. Significant structural weight savings should be possible. Feasibility and trade-off studies should be undertaken.

- Efforts to reduce the size of the DAIS-500 should be initiated to make the system more user friendly and easier for inspectors to manipulate the sensor on-aircraft.

- The development of a solid film highlighter should be pursued to avoid the use of a consumable liquid which is not permitted on some aircraft surfaces like the B-2.

10 REFERENCES

[1] J.W. Lincoln, "Certification of Composites for Aircraft," Proceedings of the USAF ASIP Conference, Dec. 1986.

[2] F. Schur, "Inspection of Carbonfiber Repairs," Air Transport Association Nondestructive Testing Forum, Long Beach, CA, 1991.

[3] R.W. Gould, J.P. Komorowski, "Detection of Impact Damage and Delaminations with Large Area Composite Inspection System - DAIS-500," National Research Council Canada, Institute of Aerospace Research, Ottawa, ON, LTR-ST-2031, Oct. 1995.

[4] S. Lee, W. Ubbink, P. Brisebois and N. Dery, "Design and Manufacture of Hat-Stiffened Composite Panels," National Research Council Canada, Institute of Aerospace Research, Ottawa, ON, LTR-ST-1996, February 1995.

[5] R.S. Whitehead, "Certification of Primary Composite Aircraft Structures," Proceedings of the 14th Symposium ICAF, pp. 587-617, 1987.

[6] H.P. Kan, R.S. Whitehead, E. Kautz, "Damage Tolerance Certification Methodology for Composite Structures," NASA CP3087, pp. 479-498.

11 PUBLICATIONS

The following is a list of other publications that were generated and presented at various conferences during the course of this project.

[1] J.P. Komorowski, R.W. Gould, F. Karpala, O.L. Hageniers, "Inspection of Composite Aircraft Structures Using *D SIGHT,*" Proceedings 39th International SAMPE Symposium, Anaheim, CA, April 11-14, 1994.

[2] O.L. Hageniers and F. Karpala, "Composite NDE - A Rapid Scan Technology," ASNT Proceedings, Spring Conference 1995, Las Vegas, NV, March 20-24, 1995.

12 APPENDIX: TRIP REPORTS

12.1 Northrup-Grumman/JSTARS

12.1.1 Original Trip

Although not a primary task of the contract, a field trip was organized to perform corrosion inspection involving a USAF purchased 707 aircraft being converted from the commercial transport role under the Joint Surveillance Target and Attack Radar System (JSTARS) program. The conversion is being carried out at the Northrop Grumman Corp. JSTARS facility in Lake Charles, Louisiana. The *D SIGHT* inspection involved Jerzy P. Komorowski, Ronald W.Gould from IAR/NRC and Dr. Frank Karpala, from Diffracto Ltd. and took place on June 14, 1994. The Northrop representative and escort was Mr. George Hilton.

All airframes were Boeing 707-300/400 aircraft previously flown by commercial operators. Aircraft P5 (tail number N 861BX) was chosen because it had only a light level of conversion maintenance activity and because the belly skins were planned to be removed within 6 months allowing for a correlation study with the *D SIGHT* findings. The aircraft was stripped of all paint.

Unpacking and setting up of the DAIS equipment took less than 20 minutes. Mr. Gould and Dr. Karpala formed the DAIS inspection team. The inspection was focused on the aircraft belly as these panels are all supposed to be replaced allowing for future correlation with the DAIS findings. Unaided visual inspection of lap areas did not reveal any significant evidence of corrosion, however several repair patches were found including a large section of skin which had been replaced from BS360 to BS480 - S25R to S27R (S27R is a new lap splice). The upper row of rivets in S25R were replaced by drilling out the countersink and the installation of larger button head rivets.

The original DOS based system software and breadboard hardware were used for this field trip. Approximately 400 feet of lap and butt splice lengths were covered during the 6:44 hr inspection. The inspections were interrupted occasionally so that the acquired *D SIGHT* images could be printed. This considerably slowed the inspection and is generally not necessary. However, for this inspection the printed images were made available for immediate interpretation by the participants. Also it should be mentioned that the DAIS operators were working in an extremely hot and humid environment and the printing offered needed rest. Some time was also taken to move the stands which were needed above Stringer 19. Thus, given the conditions in the Northrop hangars 2 days would have been required to complete the inspection of all fuselage lap splices.

Initial inspection of the *D SIGHT* images revealed a slight shift of focus towards the far end of the field of view. This could not be easily adjusted on site. The next DAIS head currently under construction should address this deficiency by offering a longer field of view which will therefore be simpler to adjust and focus will be easier to maintain. Other DAIS modifications were also discussed with Dr. Karpala.

Several Northrop engineers and managers came to briefly observe the DAIS inspection and discuss the system operation. One suggested that a scroll print of the lap splice might be useful.

An interest in the inspection of the wing leading edge-to-spar joint was expressed. Unfortunately the limited time did not allow for this inspection to be carried out. This application will be given consideration in the future.

The *D SIGHT* images were interpreted by Mr. Komorowski. In addition to corrosion, some areas showed evidence of abrasive grinding (i.e. S25R 600F to G - top row of rivets). Since this process is not easy to control, usually excessive amounts of material are removed which makes eddy current or ultrasonic verification of corrosion thinning difficult. The original B-707 lap splice construction does not involve bonding or sealant but it is not known if any sealant was introduced during aircraft maintenance. If such records exist they should be corroborated with the *D SIGHT* findings as excessive use of sealant may produce *D SIGHT* images similar to corrosion pillowing.

All *D SIGHT* images and some of the photographs of the inspected aircraft were organized using desk top publishing software. Each image location was verified using the photographs provided by Mr. Buynak. The images were analyzed on a computer monitor and corrosion indications were marked on a "turtle" diagram. Generally the inspection revealed that a rather large proportion of the aircraft seems to be affected by corrosion which was not evident in an unaided visual inspection. It should be cautioned that previous maintenance and heavy use of sealant may be partly responsible for this result. On the other hand, the findings are consistent with the age of the airframe and typical corrosion locations (heavier corrosion was found in the lower joints).

12.1.2 Follow-up Trip

A one day follow-up visit was made on April 8, 1995 to the Lake Charles, LA. facilities of the Northrop Grumman Corporation. The visit was to carry out a close visual inspection for corrosion of lap and circumferential splice joints on a B-707 airframe being converted to JSTARS configuration. The visit was made by Mr. R. Gould and hosted by Mr. G. Hilton.

On the day of the visit, skin panels 48L and 48R, were temporarily back in position on the airframe. A box of scrapped parts was located near the airframe. With the help of Mr. Hilton some 13 skin panels were salvaged from the box. During the day skin panel 48L was taken off the airframe and also inspected. The lap and circumferential joints of those skin panels adjacent to panel 48L were also inspected on the airframe.

All of the available skin panels were visually inspected on both the outer and inner surface of each joint. The results of these inspections were recorded manually. A Polaroid instant still camera was used to document one area of one panel. The photographic results were judged to be unsuitable and no additional images were taken.

The airframe was originally constructed without the use of an adhesive in the construction of the lap or circumferential splices. The presence and location of faying surface sealant, as detected during the inspections, has been included in the reports of the condition of the skin panels. The presence of this sealant should be considered as an indication of repairs having been carried out at these locations. The faying surface sealant was not removed for the inspection but spot checks of the condition of the underlying skin material were made.

The close visual inspection determined the extent of surface affected by corrosion but not the level

of corrosion related to thickness loss. At one location on skin panel No. 19L the corrosion was completely through the skin thickness (0.075 in). In three instances, sections of joint had been abraded to remove corrosion product. The extent of this activity has been recorded but no assessment of the level of corrosion, (remaining thickness) was made. However, based on visual assessment of corrosion product accumulation an approximate corrosion level rating was used by the inspector and recorded.

The position of the corrosion that was detected has been reported on a turtle map for each skin panel. The report for each skin panel also includes the DAIS 250C corrosion inspection results. In some cases the level of corrosion has been included in the notes attached to the maps. It should be noted that the *D SIGHT* inspection turtle maps were prepared to indicate only areas of relatively continuous or discontinuous corrosion whereas the close visual inspection results are more detailed. The *D SIGHT* inspection results should be reviewed and replotted in equivalent detail to the visual inspection reports.

The following is a list of the skin panels inspected:

Forward belly, left-hand side	-	7L, 11L, 12L, 18L, 19L.
Forward belly, right-hand side	-	11R, 18R, 19R, 24R.
Aft belly, left-hand side	-	40L, 41L, 48L.
Aft belly, right-hand side	-	41R, 45R.

The skin panels have now been stored separately at Northrop Grumman Corp. Based on the results from both types of inspections, sections from these skin panels could be removed and retained for further analysis.

12.2 Tinker AFB (OC-ALC)

A visit was arranged for Jan. 19-20, 1994 to introduce the DAIS system to the ALC personnel (mainly NDI) at Tinker Air Force Base and to gather information on the most common NDI tasks and structures that are typically inspected. Additionally, feedback from NDI personnel would be used in later stages of the contract. Contract participants were Jerzy Komorowski, Omer Hageniers, and Charlie Buynak.

Although the project was supposed to address large area composite inspection, Diffracto was asked to demonstrate both the corrosion and composite inspection *D SIGHT* sensors (DAIS-250C and DAIS-500 respectively). The air force base is the home of the B-52, B-1, KC-135 and E-3 aircraft. Mr. Karl E. Kraft of OC-ALC/TIESM was hosting the visit. The visit started with a meeting in the conference room. The contract participants were introduced to the ALC personnel in attendance:

Mr. Jackie Frye	OC-ALC/LAPPI
Mr. Kris Garriot	OC-ALC/LAKRA
Mr. Steward Williams	OC-ALC/LTPPBC
Ms. Hoang K. Nguyen	OC-ALC/LAKRA
Mr. Jon Kimmel	OC-ALC/LAKRA

These ALC personnel represent the two sides of NDI efforts at the ALC: research and production. The goals of the project and purpose of the visit were explained and the principles of *D SIGHT* were presented.

Following the meeting the inspection team demonstrated the DAIS equipment at the adjacent composite repair shop and learned about current NDI problems with composites. The next day additional components were inspected in the B1-B overhaul hangar. The following is a list of components inspected during the field trip, typical inspection problems and the most significant in-service damage problems.

1) B-52 radome, glass-fiber/epoxy and paper (nomex) honeycomb sandwich, skin delaminations or disbonds apparently caused by impact (bird strikes), inspection method: coin tapping. The radomes inspected were stripped of paint and required the use of highlighter (Electron was used). The delaminated areas identified were about 25 mm in diameter. The defects were not apparent in the *D SIGHT* images.

2) KC-135 radome, construction similar to 1), radome was painted black and was quite reflective but not very clean, defects and inspection method as in 1). No defects found which would be apparent in *D SIGHT*.

3) B1-B horizontal stabilizer leading edge about 4 m long 0.3 m wide at the root, glass/fiber epoxy and foam core sandwich, numerous small delaminations or disbonds apparently caused by impact damage, inspection method coin tapping. The surfaces were coated with flat gray paint. No significant *D SIGHT* signatures could be distinguished which would correlate with coin tapping findings.

4) A 900 x 80 mm about 40 ply thick laminate graphite/epoxy coupon was shown and under *D SIGHT* seemed to contain traces of stitching. The coupon was apparently typical to B-2 laminate construction. No defects were found and none were known to be present.

5) Permission was obtained to perform an inspection on an E-3 radome. The aircraft was in the hangar for minor repair and was due to fly the same day. The rear part of the fuselage and the radome were surrounded by special purpose scaffolding called a "Texas tower." The tower consists of two symmetric parts (left and right) which are rolled into place on special rails built into the floor in the corner of the hangar. The top floor of the tower offers access to the lower surface of the radome while the top of the radome can be walked on for inspection. The glass/fiber paper (nomex) honeycomb radomes are apparently laid up on male molds. As a result the external surface is quite rough - showing typical honeycomb read-through. The lower surface contained numerous wrinkles (excess resin flow). The composite sections of the rotating radome were painted with shiny black paint which did not require highlighting. The most common defects - disbonds/delaminations are typically found on the leading edge. The source of damage is attributed to bird impact or ground handling. One such damage site was marked with chalk and had a diameter of about 30 mm. Several *D SIGHT* images of the area were recorded; however, the delaminations were not apparent.

6) Sections of two horizontal stabilizers were inspected, removed from aircraft. These were placed top side down on dedicated stands. The leading edge (curved) of one contained similar delaminations as the leading edge inspected on the previous day. Close examination (tapping and a trace on the surface) indicted that at least some of these delaminations had a square or diamond shape - typical of a manufacturing flaw, not of impact damage. The trailing edges of these stabilizers are of sandwich construction (glass fiber/epoxy on aluminum honeycomb core). The skins appear flat. *D SIGHT* inspection revealed several possible impact damage sites. Coin tapping did not indicate any damage.

7) B-1 Weapons bay door. Removed from aircraft, on a stand and in vertical position. The outside skin of these doors is approximately 10 mm thick graphite/epoxy flat. This skin is stabilized with honeycomb. *D SIGHT* inspection revealed one possible impact site: again, coin tapping was not successful in identifying delamination.

8) Upper wing to body fairings, removed from aircraft. Solid graphite/epoxy laminate have complex curvatures. Inspections have not revealed any defects.

All B1-B parts were painted with various shades of gray (camouflage) the transitions from one shade to another were quite distinct in *D SIGHT* images. The new highlighter (Electron) was used for virtually all inspections. However, on the horizontal stabilizer several areas were highlighted with Snoflake. There were no readily apparent differences in the quality of highlighting.

At the conclusion of the meeting a discussion was held among the participants. Buynak suggested that the minimum size of defect the system should be able to locate is 3/4 inch. Several concerns were expressed about this number:

a) The original contract statement of work was aimed at inspection of large area composite primary structure. It was written almost 3 years ago when it seemed that USAF will be dealing with large solid laminate composite structures (B-2, F-22). While the B-2 program has shrunk significantly, there are other solid primary structures which should not be overlooked such as the F-16 horizontal stabilizers. While not very big on their own, because of the large number of aircraft involved all together they represent a very large surface requiring inspection. A visit to an ALC which is tasked with F-16 maintenance should be included in the task.

b) The 3/4 inch limit does not seem to be related to the structural integrity requirement since the components which we inspected are generally not too significant structurally. It is more likely that this represents the typical inspection limit for ultrasonic equipment. *D SIGHT* was never proposed as a replacement for ultrasonic equipment but rather as a visual inspection enhancement tool to quickly eliminate large areas without any damage.

c) The USAF damage tolerance design guide includes damage assumptions: delaminations 5 inches in diameter are the maximum delamination size which may remain undetected in service and therefore the structure has to be built to withstand it. It is more realistic to attempt to tune *D SIGHT* to structurally significant inspections.

d) The apparent lack of success of current DAIS heads in locating delaminations during the

2 days at Tinker was related to one type of structure: convex glass fiber skins on paper (or possibly nomex) honeycomb or foam core. This type of structure was not tested for impact visibility in the past and was not included in the planned material selection for laboratory testing largely because this type of construction is not typically used for structurally significant components.

12.3 Kelly AFB (SA-ALC)

From Nov. 30 to Dec. 2, 1993, a USAF ALC NDI Manager's Meeting was held at Kelly Air Force Base in San Antonio, Texas. This meeting was used as an opportunity to introduce the DAIS system to ALC NDI managers. Frank Karpala, Charlie Buynak, and Jerzy Komorowski were the contract participants who attended.

The contract participants met with a number of ALC NDI managers. The meeting and tour was organized by the USAF NDI Program Office. During a series of ongoing presentations from other outside participants, Jerzy Komorowski gave an excellent overview of *D SIGHT* research from work on impact damage to cold worked holes. The presentation was well received by the managers.

During the second day, the DAIS-500 was demonstrated to the NDI managers. One major concern that developed prior to the demonstration was the use of Snoflake as a highlighter. After a large number of phone calls, use of WD-40 was permitted, but not Snoflake. Clearly a new highlighter must be found in order to perform *D SIGHT* inspections at military hangars and to improve the acceptability of DAIS as a viable inspection device.

Later, all managers and guests were given an excellent tour of C-5 aircraft maintenance and critical NDI inspection areas both inside and outside the aircraft. In particular, the C-5 engine pylon that has aluminum skin structural honeycomb takes 8 hours per side on one pylon to inspect. This inspection uses a portable ultrasonic instrument to inspect for disbonds.

One inspection carried out with the DAIS-500 was the inside surface of a large C-5 engine cowl. This cowl was checked for disbonds and delaminations; however, the surface curvature was concave and scarred badly from previous repairs.

An inspection performed on the pylon and cowl components with the DAIS-500 and WD-40 highlighter showed only impact damage that was not considered serious or important. The upper wing of a T-38, that looked delaminated from the physical bulge, was also inspected but coin tapping indicated it was not delaminated. It will be necessary to evaluate images with greater detail to reduce false calls produced by factors other than delaminations .

12.4 Hill AFB (OO-ALC)

A two day field trial to Hill AFB was arranged to obtain hands-on experience inspecting F-16 aircraft and to have USAF personnel become familiar with the use of the DAIS system for a future trip to Whiteman AFB. This field trial was the first to use the new DAIS-500 on a complete aircraft rather than simply on aircraft components in a lab setting.

The main participants were as follows:

Frank Karpala, Diffracto
Dave Willie, Diffracto
Jerzy Komorowski, NRC/IAR
Charlie Buynak, WPAFB
Mike Paulk, Kelly AFB

Equipment familiarization began in a lab environment using several pieces of aircraft components. The basic equipment setup and operation was described along with the steps required for inspection. These included the following:

a) setting up the hardware
b) creating an aircraft workfile
c) setting up for inspection
d) using the pendant
e) surface preparation
f) image acquisition
g) recall and image assessment

Because of the simplicity of the DAIS interface, participants became quite confident with the use of the system by the end of the first day to acquire images from a predefined inspection plan using the pendant. In addition, image interpretation for the presence of impact damage indications was easy, even for the most inexperienced observer.

During the second day, the equipment was taken to a hangar location to inspect one or more F-16's undergoing various repairs. The inspections concentrated on the horizontal stabilizers and the trailing flaperons. A number of aircraft were inspected. Only minor impact sites were found of no real significance.

The inspection procedure was not entirely worked out before hand so that some time was wasted attempting to position the sensor on the horizontal stabilizer. The size of the sensor felt too big for some of the participants requiring two people to manipulate the sensor for most of the placements. Because the horizontal stabilizers were not in a level position, the sensor was somewhat difficult to handle from the normal platforms. Charlie Buynak expressed the opinion that since the sensor was designed for large area inspection, such as might be found on the B-2, the problem of size should not cause major concern. Users of the pendant found it easy to use especially with the supplied monopod. However, the use of the monopod discourages helping the technician holding the sensor with highlighting or helping to hold the sensor. It was felt that two people holding the sensor made the task easier in addition to the person operating the pendant. Of course, the surfaces required highlighting and Electron was used exclusively on all surfaces.

Besides the F-16's, several Navy F-18's were also inspected on the horizontal stabilizers and trailing flaps. One delamination indication and other smaller impact damage indications were found on these aircraft; however, none were considered too serious (see **Figure 41** and **Figure 42**, respectively). The maintenance crews of the aircraft were shown the indications, in case they wished to consider further evaluation. Coin tapping did indicate the possibility of internal damage.

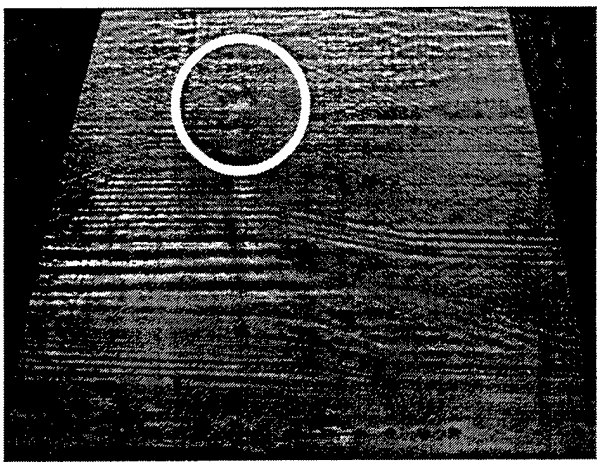

Figure 41: Delamination indication (circled)

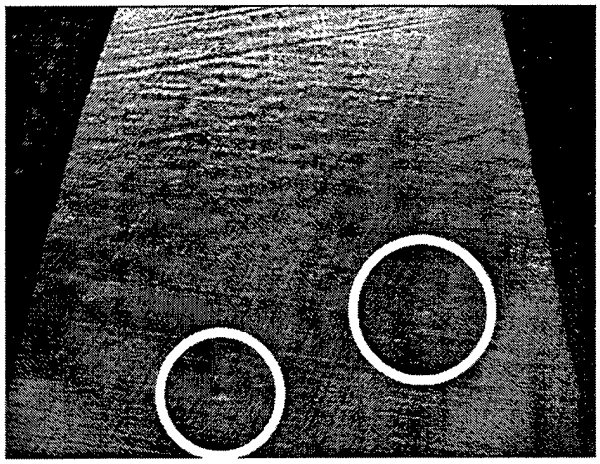

Figure 42: Small Impact Indications (circled)

12.5 Whiteman AFB

The purpose of this field trial was to allow Mike Paulk, an NDI engineer from the AF NDI Program Office who became familiar with the use of the DAIS system at Hill AFB, to inspect areas of a B-2 with an experimental "dry film highlighter" fixture. No contract participants were allowed to inspect the aircraft due for security reasons. CAD drawings of the DAIS-500 were provided to NRC/ IAR to allow for the design and construction of the components required to adapt the inspection head. The fixture was be fitted at the air force base by Ron Gould of IAR.

On the morning of May 16th, modifications were carried out to the inspection head at the NDI Laboratory in building T9. Modifications included the removal of the rubber skirt and integral frame. Two side rails and an air supply manifold were attached to the inspection head. The air supply manifold was configured to accept either air from a shop vacuum (operating as a blower) or from a shop compressed air supply. On the advice of TSgt Anderson, B-2 NDI Shop Chief, that their shop vacuum would not be permitted on the aircraft, the compressed air source was selected. Corrugated cardboard sheets were built-up from material on-site and attached at the manifold (inlet end) and also at the exit end to act as a flow regulator. The air supply into the manifold was controlled through the use of a trigger operated nozzle installed in the supply hose at the inspection head. It was found that the film highlighter materials, when used on the DAIS-500, did not conform to the surface in the same manner as when the DAIS-250C inspection head was used for material selection. Therefore, the placement technique was modified in that the inspection head was first charged with air before the film highlighter material was brought into contact with the surface.

The NDI Lab staff indicated that only lab specimens might be available for inspection. Most of the specimens available at the NDI Lab were smaller than the inspection area of the head and would have possibly punctured the film highlighter material. None of the specimens had the aircraft paint system. A limited number of trials, using the lab floor as the inspection surface, were carried out on the film highlighter materials which had been brought from Ottawa. Tests on a 0.003 inch (0.076 mm) thick clear vinyl film illustrated that the material had suffered from creasing during transportation. These creases remained as artifacts in the image even when the system was inflated and the film stretched. A 0.0015 inch (0.038 mm) thick latex film was tested but was known

to have noticeable lumps in the material and had been folded for many years. A thick 0.010 inch (0.254 mm) black vinyl material proved to provide the best results of the materials available at this time. It was realized that this thickness might mask subtle features of the surface to be inspected.

Drawings of the aircraft had been prepared at NRC/IAR. Diffracto had developed inspection plans for a number of areas on the lower side of the control surfaces, leading edges, and gear doors of the aircraft. One of the inspection plan pages is shown in **Figure 43**. Due to the experimental nature of the effort; however, the generic inspection plan available in the software package was used instead.

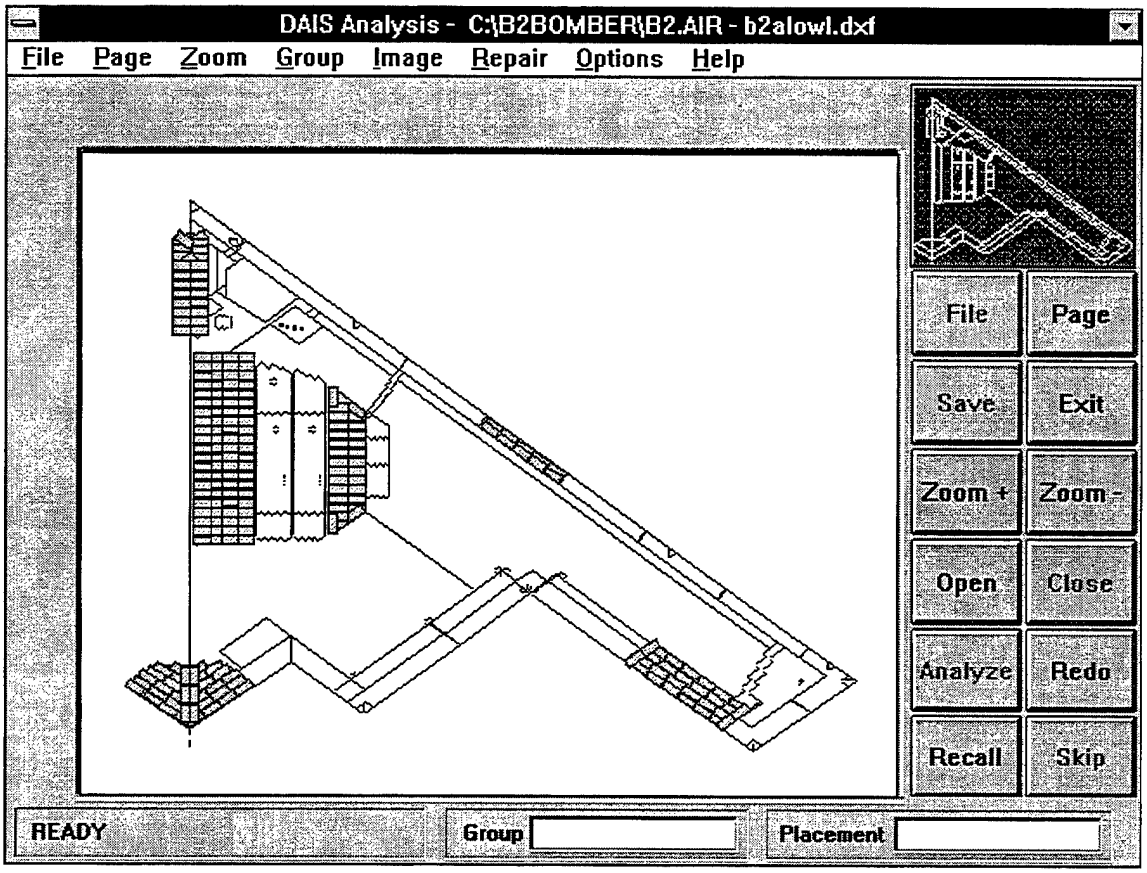

Figure 43: Example Inspection Plan for Lower Left Wing of B-2

Mr. Paulk was assisted by Capt. Jablunovsky, WL/MLLP, and Mr. Voeller, OC-ALC/LAPPI, to inspect a B-2 aircraft for security reasons. The DAIS was used on selected areas of the lower surface. The first images were with the system operated in a normal manner with the surface highlighted with a mixture of water and alcohol. This mixture proved to be very difficult to apply evenly and did not last long but was used as a baseline. Similar views were collected with three film highlighter materials and a compressed air source. The records from the morning inspections were reviewed. The thin latex film and a shrink-wrapping material proved to have too many integral flaws and artifacts which detracted from the information in the view. The heavy vinyl film was the

best material on hand but did mask subtle surface features as suspected. This was confirmed in comparisons with the liquid highlighter views. Working on lower surfaces created two factors which contributed to operator fatigue. As in the normal operation, head placement on lower surfaces is fatiguing. Secondly, compressing the inflated film highlighter added to the physical demands on the operator. The system could be configured to operate with a vacuum created directly from the compressed air supply allowing for the inspection head to be held in place as well as acting to conform the film to the surface or in a combination of vacuum assisted positioning and blown-film.

Due to the security constraints, it was difficult for the contract participants to easily evaluate the potential of the solid film highlighter. In principle, many of the health and safety concerns could be addressed with such an addition to the basic sensor.

12.6 McClellan AFB (SM-ALC)

The Sacramento air base visit was the third scheduled trip under the Large Area Composite Inspection System Program. A number of inspections were planned for the DAIS-500 system upon arrival to the air base but not all were performed. These included inspecting:

- sections of a SR-71 Blackbird
- fiberglass components of the T-3
- parts of the F-111
- sections of the E-3 or KC-135 rotodome
- the lower wing surface of the A-10A Thunderbolt II

The initial part of the field trial was disrupted by the late arrival of the DAIS-500 equipment to the air force base. When the DAIS equipment arrived, one technician was quickly trained. The DAIS trainee, Jim Ellison, was a very computer-literate technician, primarily involved with X-ray inspections. He picked up on the basics of the software quickly and asked the expected and intelligent questions. Mainly, Jim was concerned about how he could keep track of images and manipulate them *away from the DAIS host.* He was driving at the idea of using his very well-equipped X-ray computer hardware suite for looking at the images. Once he was assured that the images are saved as BMPs or TIFFs he felt he could use some of his usual tools to manage the images he'd be interested in.

The DAIS-500 was introduced to Ellison on the afternoon of the June 1. The opening discussion and demonstration of the equipment were also attended briefly by Don Bailey and Al Rogel - both staff members of the NDI department at McClellan. The hands-on at site demonstrations and trials were attended by Charles Buynak, Jim Ellison and Diffracto staffers Don Clarke and Dave Willie.

On-site, images from the lower wing surface of an A-10A Thunderbolt II were acquired. Specifically, the plane areas of a radome, suspected of delaminations, were looked at with DAIS. A cut up section of another radome was also inspected for impact sites.

12.6.1 A-10A Lower Wing Surface:

This was an inspection for corrosion in an aluminum skin structure. While the DAIS-500 is not set up for this type of inspection, the effort was made to see if we could detect anything resembling a typical corrosion signature. The size of the sensor head was an initial concern, but images from only the outer section of the lower wing allowed plenty of room for sensor manipulation (see **Figure 44**). The wing was secured to a dolly which denied access to the entire lower surface.

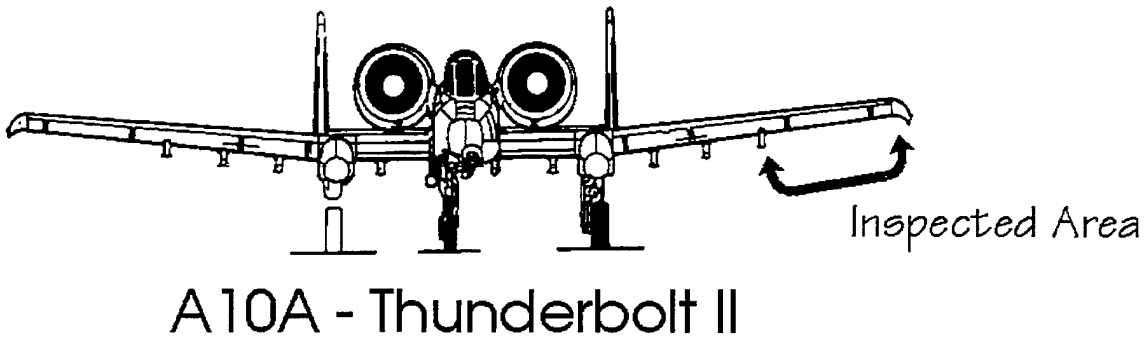

Figure 44: A-10A Inspection Area

A generic "box" plan file was used to acquire and archive the DAIS images. While initial attempts to understand the acquired image artifacts proved frustrating, there appeared to be sufficient definition to allow for future coding of signature distinctions. The DAIS-500's magnification and large-area field of view hampered the possibility of capturing detailed corrosion signatures. The resolutions of both the host monitor and the pendant screen proved to be too low to see the signature details. **Figure 45** shows the actual inspection of the under wing.

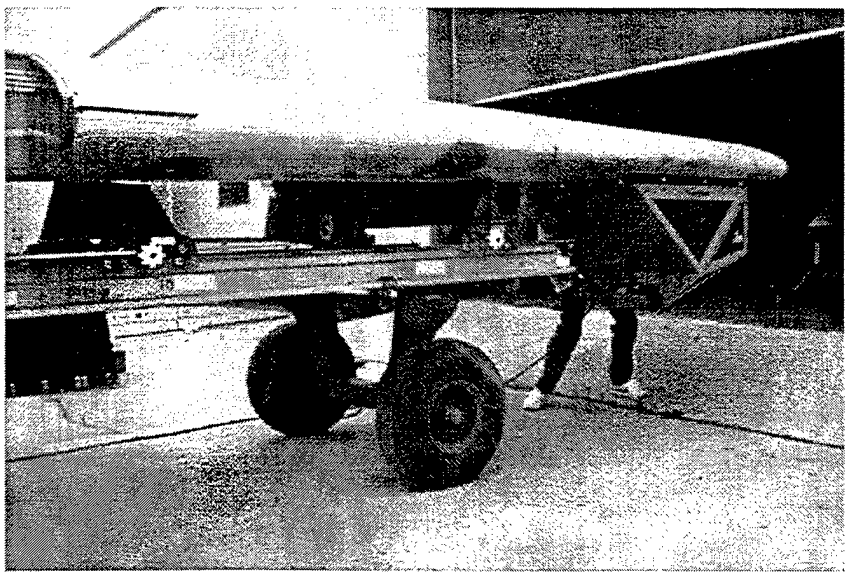

Figure 45: A-10A Inspection with DAIS-500

12.6.2 The Milstar Radome

The DAIS-500 was tried on two separate radome sections. Both parts were accessible on the shop floor (see **Figure 46**). The first specimen was constructed of an extremely textured, nonreflective material. As such, a great deal of highlighter fluid was used to acquire the DAIS images from this radome part.

The second radome was smoother and absorbed less light. However, the impact site introduced to the radome surface by Jim Ellison was of an extremely sharp and curt nature - negating the typical broad lipped impact site easily picked up by DAIS imaging.

Both radomes confirmed previous observations that porous, textured surfaces are difficult for the DAIS-500 to inspect.

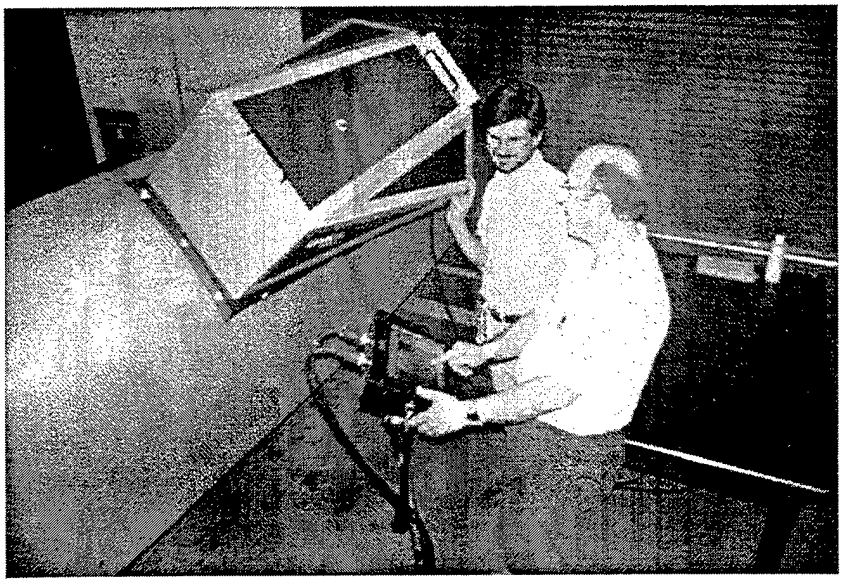

Figure 46: Radome Inspection with DAIS 500

12.6.3 Summary

The main lesson learned from the McClellan AFB field trial is again how simply the system can be assimilated by a technician experienced with the Windows operating environment. Experience has also been gained about how much harder it is to point out or even locate impact sites on "field monitors" as compared to a high resolution "work station-type" monitor. Ultimately, users will explore ways of using existing computer hardware to make analysis decisions. Or, they will source the equipment necessary to provide the image detail they request of the DAIS system.

While the McClellan trip dealt with NDI technicians in a basic laboratory situation, it should be pointed out that field technicians might not require the exacting resolution the NDI group at McClellan feels they require. In demonstration situations it would be advantageous to have access to a high resolution monitor to display the detail that is inherent in a *D SIGHT* image.